Effect of Hofmeister Salts on the Compressibility of Bovine Serum Albumin

by

Sultana Perven

A Thesis Submitted to the Faculty of Graduate Studies of

The University of Manitoba

in partial fulfillment of the requirements of the degree of

MASTER OF SCIENCE

Department of Food Science

University of Manitoba

Winnipeg

I hereby declare that I am the sole author of this thesis.

I authorize the University of Manitoba to lend this thesis to other institutions or individuals for the purpose of scholarly research.

Sultana Perven

I further authorize the University of Manitoba to reproduce this thesis by photocopying or by other means, in total or in part, at the request of other institutions or individuals for the purpose of scholarly research.

Sultana Perven

The University of Manitoba requires the signatures of all persons using or photocopying this thesis. Please sign below and give address and date.

Acknowledgements

I wish to express my sincere appreciation to my honorable research supervisor Dr. Martin G. Scanlon, Department of Food Science, University of Manitoba for his continuous active supervision, constructive suggestions and criticism in planning and executing the research work and in the written presentation of this thesis. I am also thankful to Dr. Martin G. Scanlon for the received financial assistance from his NSERC grant.

I would like to express gratefulness to Dr. Harry D. Sapirstein and Dr. J.H. Page for allowing the use of their laboratory facilities. I would like to thank to my committee members Dr. Susan Arntfield and Dr. Rotimi Aluko for their valuable suggestions in my research. Again, I wish to thank to all staffs especially to Patricia Kenyon and Michael Stringer, and to all graduate students especially to Zhuo Zhang of the Department of Food Science, and to Anatoliy Strubulevych, Research Associate, Department of Physics and Astronomy for their scientific and technical help during my research.

Finally, I feel deep and sincere gratitude to my parents, brothers and sisters and my husband for their best wishes and continuous inspiration.

Abstract

Determination of whether ion specific potassium halides binding with BSA occurred within the experimental conditions was the aim of the study. Ultrasound velocity measurements using a Resoscan system and density measurements using a DMA 5000M density meter were made to analyse BSA conformation in the presence of potassium salts of the Hofmeister series.

It was found that the density and the adiabatic compressibility of BSA-potassium halide mixed aqueous solutions cannot be predicted from the density and the adiabatic compressibility of potassium halide solutions and that of BSA solutions. Interaction occurs between BSA and Br-, I- and F- ions in mixed aqueous solutions of BSA-KBr, BSA-KI and BSA-KF, but there is no interaction between BSA and Cl^- ion in BSA-KCl mixed aqueous solution. The interaction of ion to BSA is ion non-specific to the Hofmeister series.

Used Physical Parameters

Symbol	Parameter	Unit
τ	Shear stress	Pa
τ_o	Yield stress	Pa
$\dot{\gamma}$	Shear rate	s^{-1}
η	Dynamic viscosity of liquid	Pa.s
η_s	Solution viscosity	Pa.s
η_o	Water viscosity	Pa.s
η_r	Relative viscosity	-
η_T	Viscosity of water at temperature T ^oC	Pa.s
η_{20}	Viscosity of water at 20 ^oC	Pa.s
$[\eta]$	Intrinsic viscosity	$cm^3.g^{-1}$
m	Consistency index	$Pa.s^n$
n	Flow behaviour index	-
Φ	Volume fraction of a solute	-
Φ_o	Volume fraction of solvent	-
ΔE_η	Arrhenius energy of activation	$J.mol^{-1}$
R	Gas constant	$J.K^{-1}.mol^{-1}$
T	Absolute temperature	K
ΔV_η	Volume of activation	$m^3.mol^{-1}$
P	Pressure	Pa
φ	Fluidity of the solution	$cm.s.g^{-1}$
φ_o	Fluidity of water	$cm.s.g^{-1}$
V_h	Hydrodynamic volume	$cm^3.mol^{-1}$

V	Volume	m^3
V^o	Partial molar volume	$m^3.mol^{-1}$
υ	Specific volume of spherical molecules	$cm^3.g^{-1}$
R	Axial ratio	-
K_S	Adiabatic compressibility of a solution	$cm^3.g^{-1}.bar^{-1}$
K_T	Isothermal compressibility of a solution	$cm^3.g^{-1}.bar^{-1}$
β_S	Adiabatic compressibility coefficient of a solution	bar^{-1}
β_o	Adiabatic compressibility coefficient of a solvent	bar^{-1}
β_T	Isothermal compressibility of a solution	bar^{-1}
C_V	Specific heat capacity at constant volume	$J.K^{-1}.g^{-1}$
C_P	Isobaric specific heat capacity	$J.K^{-1}.g^{-1}$
ρ	Density of a solution	$g.cm^{-3}$
ρ_o	Density of a solvent	$g.cm^{-3}$
E	Elasticity of a liquid	Pa
v	Ultrasound velocity	$m.s^{-1}$
α	Ultrasound attenuation coefficient	m^{-1}
d	Distance	m
λ	Wavelength	m
f	Ultrasound frequency	Hz
ω	Ultrasound angular frequency	$rad.s^{-1}$
v^o	Partial specific volume of a solute	$cm^3.g^{-1}$
k_S^o	Partial specific adiabatic compressibility of a solute	$cm^3.g^{-1}.bar^{-1}$
β_S^o	Partial specific adiabatic compressibility coefficient of a solute	bar^{-1}

Used Abbreviations

BSA	Bovine Serum Albumin
KCl	Potassium Chloride
KBr	Potassium Bromide
KI	Potassium Iodide
KF	Potassium Fluoride
KSCN	Potassium Thiocyanate
KCOOH	Potassium Formate
$KCOOCH_3$	Potassium Acetate

Table of Contents

List of Figures

List of Tables

List of Copyrighted Materials

1. Introduction

Compressibility is a thermodynamic property of a substance which is a measure of the elasticity of the substance. It is possible to calculate the compressibility of a solution by measuring the sound velocity in the solution and the density of the solution (Pfeiffer, Heremans, & Wevers, 2008). Millero, Ward and Chetirkin (1976) examined the compressibility of aqueous lysozyme solutions as a function of concentration (weight percentage), and the researchers observed a linear relationship between compressibility and concentration with the compressibility decreasing with the increase in concentration. Protein compressibility measurements give information about general thermodynamic properties of protein molecules such as characteristics of the protein interior, the protein's conformational state, and interatomic interactions such as disulfide bonds within the macromolecule (Gekko, Kimoto, & Kamiyama, 2003; Taulier, Beletskaya, & Chalikian, 2005). The compressibility of a globular protein molecule in aqueous solution is a characteristic feature of the protein's tertiary structure, and it is important to know about protein compressibility in order to understand the structure-function relationship of proteins. Highly compressible proteins are found to have good emulsifying activity, foaming capacity, and they are easily digested by proteases (Gekko & Yamagami, 1991). There are various factors which determine protein compressibility including partial specific volume, hydrophobicity and polarity parameter (the volume ratio of polar and nonpolar amino acids of a specific protein). Proteins with large partial specific volumes show large adiabatic compressibilities (Kauzmann, 1959). Highly hydrophobic proteins show a large compressibility relative to hydrophilic proteins (Gekko & Noguchi, 1979). A high value of the polarity parameter indicates low compressibility of

the protein molecule (Bigelow, 1967). Because of this relationship between compressibility and tertiary structure, the presence of salt has a role in altering protein compressibility. Strong denaturants such as guanidinium chloride are responsible for protein unfolding. Because of unfolding, the loss of internal imperfect packing volume and hydration of exposed amino acids occurs and these events ultimately decrease protein compressibility (Frye & Royer, 1998; Kamiyama & Gekko, 1997; Tanford 1968).

The ranking of cations and anions in terms of their ability to precipitate proteins or to stabilize proteins is known as the Hofmeister series. The series has importance in protein chemistry and also in colloid, surface, membrane and polymer chemistry (Shimizu & McLaren, 2006). The Hofmeister series effect arises from the impact of salts on solvent structure as well as the interactions of the salts themselves with proteins (Cacace, Landau, & Ramsden, 1997). Among the ions, kosmotropes are water structure makers, and the more ordered water structure is largely determined by the electrostatic interaction between water molecules and the kosmotropes. A water molecule interacts with kosmotropes more strongly than the water molecule binds to a neighboring water molecule. On the other hand, chaotropes are water structure breakers, and water molecules surrounding the chaotropes are more movable than bulk water molecules. (Hribar, Southall, Vlachy, & Dill, 2002). Neutral salts in the Hofmeister series have effects on protein solubility and protein conformational change. Kosmotropes increase the hydrophobicity of protein-water interfaces, and chaotropes increase the hydrophilicity of protein-water interfaces in an aqueous solution. These impacts of kosmotropes and chaotropes can be explained by the water structure making property of

anionic kosmotropes and water structure breaking property of anionic chaotropes (Der, 2008). According to Machado and coworkers (2007), salt addition alters both the water structure and the protein conformation in a protein aqueous solution, and causes either salting in or salting out of the protein. Salting out of protein is a phenomenon which can be defined as the precipitation of protein upon addition of neutral salts or ions. Following the ascending order of the Hofmeister series, ions exhibit their effectiveness in salting out (Curtis & Lue, 2006). The phenomenon of increasing protein solubility in the presence of salt is known as salting in. Salting in of protein occurs because of electrostatic interaction between salt ions and the dipole moment of the peptide group (Nandi & Robinson, 1972; von Hippel & Schleich, 1969). Ions exhibit their effectiveness in salting in proteins following the descending order of the Hofmeister series (Robinson & Jencks, 1965; Nandi & Robinson, 1972; Schrier & Schrier, 1967). Specificity of the interaction between a given ion and a dipolar molecule is a matter of controversy (Baldwin, 1996). For instance, according to Nandi and Robinson (1972), this interaction is ion specific whereas Hamabata & Hippel (1973) argue that this type of interaction is non-specific. Again, according to Heyda, Vincent, Tobias, Dzubiella and Jungwirth (2010), "weakly hydrated Hofmeister anions (such as bromide or iodide) probably do not destabilize proteins via direct interactions with the backbone amide groups" rather "this destabilizing activity may be partly due to the affinity of large soft ions for hydrophobic groups and residues, which makes them more accessible to the aqueous solvent". Lund, Va´cha and Jungwirth (2008) proposed that the binding of specific ions with macromolecules depends on the surface property of the macromolecules. For example, iodide ion, which is a poorly hydrated ion, binds to hydrophobic surfaces, and iodide ion binding is preferred if a positively charged group

resides under the macromolecular surface. Again, highly solvated fluoride ion binding occurs by specific anion-cation interactions. Fluoride ion preferably binds macromolecules with high surface charge density. The specificity of binding of ions of the Hofmeister series to the peptide group is the challenge of my research.

The protein bovine serum albumin (BSA) has been considered as a model protein for my research. There is some functional significance of BSA in the dairy industry since BSA has both gelation and emulsifying activity (Haque & Kinsella, 1989; Hirose, Nishizawa, & Lee, 1990). Although both casein and BSA are known as good emulsifiers, according to Haque and Kinsella (1989) BSA has better emulsifying activity than casein. The protein BSA is a highly studied water soluble globular and flexible protein that is present in bovine serum and milk, although bovine milk contains only 0.1-0.4 $g.dm^{-3}$ of BSA. BSA is a well sequenced single chain albumin protein having a molecular weight of ~66kDa and 582 amino acid residues, and the protein consists of 17 disulfide bonds and one sulfhydryl group (Fox & McSweeney, 2003; Lakshmanan, Dhathathreyan & Miller, 2008; Mohanty & Swain, 2010). Salts have been shown to have an impact on BSA conformation. Yamasaki, Yano and Aoki (1991) found that at pH 7, salts including NaCl, NaBr, NaI, NaSCN, $NaSO_4$, and $NaClO_4$ restrain the heat-promoted conformation transition and enhance thermostability at ionic strengths of 0.01 and 0.1, and the ranking of anions was $ClO_4^- \geq SCN^- > I^- > SO_4^{2-} > Br^- > Cl^-$ for an ionic strength of 0.01, but SO_4^{2-} was less effective at ionic strength of 0.1.

The objective of the study is to examine the impact of the Hofmeister salts on the compressibility of aqueous solutions of BSA by considering the following 3 concerns:

- Investigation of whether ion binding to BSA in the Hofmeister series is ion specific or non-specific.

- Can density and compressibility of each BSA-potassium halides mixed solutions be predicted from the sum of partial specific volume of BSA and that of potassium halides?

- Validity of the hard sphere model in analyzing the density and compressibility of aqueous solutions.

In order to accomplish the objective of the study, the following steps have been considered:

- Measurement of density of BSA solutions and of mixture solutions of the four potassium halide salts and the protein bovine serum albumin.

- Measurement of ultrasound velocity of mixture solutions of the four potassium halide salts and the protein bovine serum albumin as a function of concentration of both BSA and salts.

- Measurement of ultrasound velocity of salt solutions including the potassium halides, potassium acetate, potassium formate and potassium thiocyanate as a function of salt concentration.

2. Review of Literature

2.1. Liquid viscosity

2.1.1. Introduction

Viscosity is an inherent property of liquids which can be defined as the liquid's internal resistance to flow generated from friction of liquid molecules. Liquids are deformed producing a velocity gradient among the layers of liquid that are subjected to a shearing stress on the upper layer of liquid. The upper layer is deformed the most and moves at the highest velocity, with lower velocities in the liquid layers further away from the top layer. The shearing stress on the liquid surface can be defined as the shearing force per unit area ($N.m^{-2}$) while the rate of velocity gradient or rate of shear can be expressed as s^{-1}, and the liquid's viscosity determines the velocity gradient (Lewis, 1987).

Newton established a correlation between shear stress and shear rate in characterizing the viscous character of fluids. According to Newton, for a liquid, the ratio of shear stress (τ) and shear rate ($\dot{\gamma}$) has a constant value which is the viscosity of that liquid. There is another way to express liquid viscosity which is known as kinematic viscosity, that is the ratio of dynamic viscosity to the density of liquid. According to SI units and cgs unit systems the units of dynamic viscosity are $N.s.m^{-2}$ or pascal. second (Pa.s) and $dyn.s.cm^{-2}$ or poise (P), respectively. The commonly used unit of dynamic viscosity is mPa.s where 1 mPa.s = 10^{-3} Pa.s ($N.s.m^{-2}$) = 1cP. Viscosity is highly sensitive to temperature with almost all liquids showing lower viscosity at higher temperature; thus during viscosity measurement controlling temperature by ± 0.1 ^{o}C is a crucial factor (Jenkins & Marcus, 1995; Lewis, 1987).

2.1.2. Types of liquid viscosity

Liquids can be classified into two principal groups according to their viscous response with time; one is a time independent character of liquid viscosity and another is a time dependent character of liquid viscosity. The viscosity under a specified experimental circumstance is termed as apparent viscosity. The apparent viscosity of time-independent liquids does not alter with respect to time and shearing history; at a specific shear rate the liquid has a stable apparent viscosity. On the other hand, the apparent viscosity of time-dependent liquids alters with respect to time and shearing history; these liquids show variable apparent viscosity at a specific shear rate (Lewis, 1987).

2.1.2.1. Time independent character

Among liquids, two types of time independent characteristics have been observed; one is Newtonian liquid behaviour and another is non-Newtonian liquid behaviour. In the case of a Newtonian liquid, viscosity is ideal and can be determined from the slope of the linear relationship of shear stress and shear rate (Jenkins & Marcus, 1995). The viscosities of Newtonian liquids are dependent on temperature and pressure. In case of Newtonian liquids, with increasing temperature, the Brownian motion of liquid constituent molecules increases; therefore, viscosity decreases with increasing temperature. Usually for liquids having higher viscosity, reduction of viscosity with increasing temperature is higher compared to that of liquids having lower viscosity. **Table 2.1** represents the viscosity of some common Newtonian liquids at room temperature (20 ^{o}C) (Barnes, 2000). When temperature increases by 1 degree, water viscosity decreases by ~ 3%, the viscosity of motor oils decreases by ~ 5% and bitumen viscosity decreases ~ 15%.

Table 2.1. Viscosity of common Newtonian liquids at 20 ^{o}C (Barnes, 2000)

Liquid	Approx. viscosity in Pa.s
Petrol	3×10^{-4}
Water	10^{-3}
Lubricating oil	10^{-1}
Glycerol	10^{0}
Corn syrup	10^{3}
Bitumen	10^{9}

Considering pressure effects on Newtonian liquids, it has been observed that viscosity of most Newtonian liquids increases with increasing pressure from atmospheric pressure to 100 MPa, maintaining a linear relationship between viscosity increase and pressure increase. Above 100 MPa, the viscosity increase is more than linear with pressure increase. At 100 MPa viscosity is double compared to viscosity at atmospheric pressure, but at 200 MPa a 10 fold increase in viscosity is observed (Barnes, 2000).

Numerous liquids exhibit viscosity dependency on shear rate and either show shear thinning or shear thickening viscosity characteristics. The shear thinning viscosity behaviour can be defined as lower viscosity with increasing shear rate while the shear thickening behaviour can be characterized by higher viscosity with increasing shear rate (Strobl, 2007). These liquids are known as non-Newtonian liquids. Macromolecular solutions with high concentrations are typically non-Newtonian liquids. There are four kinds of non-Newtonian liquids, which are plastic, pseudo-plastic, dilatant, and non-ideal plastic. Plastic liquids need a certain stress greater than their yield stress to commence flow, as a result of breakage of intermolecular bonding of molecular solutes or entanglements. These liquids act like a solid at low shear stress and perform as a Newtonian liquid as soon as the shear stress reaches the yield value. For plastic liquids,

viscosity can be expressed according to the following equation where τ_o is the yield stress.

$$\tau = \tau_o + \eta\dot{\gamma} \quad (1)$$

In the case of pseudo-plastic liquids, the relationship between shear stress and shear rate is not linear, and these liquids show lesser apparent viscosity at elevated shear rate or strain rate. Thus, pseudo-plastic liquids exhibit a shear thinning character. Dilatant liquids show exactly the opposite character, shear thickening, as these liquids exhibit higher apparent viscosity at elevated shear rate. Non-ideal plastic liquids show either pseudo-plastic or dilatant character, but like plastic liquids their yield stress needs to be exceeded to commence flow (Franks, 1988; Lewis, 1987).

2.1.2.2. Time dependent character

Three kinds of time dependent character have been observed including thixotropic, rheopectic, and rheodestructive. At a certain shear rate and temperature thixotropic liquids exhibit a reversible decrease in shear stress and viscosity because of breakage of molecular bonds; when the shear is removed the molecular bonds reform at times and rates that vary for different liquids. On the other hand, rheopectic liquids show an increase in viscosity due to more structuring or molecular entanglement while they are undergoing strain; this change in structure is also reversible with time. On the contrary, rheodestructive liquids show a non-reversible decrease in shear stress and viscosity under strain (Franks, 1988; Lewis, 1987).

2.1.2.3. Model for liquid flow

Some mathematical models have been introduced to describe the time independent non-Newtonian liquids' flow behaviour, such as the power law equation for non-plastic liquids, and the power law plastic equation for plastic liquids. The power law equation evolves from the log-log plot of shear stress against shear rate which is as follows (Franks, 1988; Lewis, 1987):

$$\tau = m\dot{\gamma}^n \tag{2}$$

where m is known as the consistency index, which tells about the viscidness of the liquid and n is the flow behaviour index which tells about the closeness or deviation of the liquid from Newtonian behaviour. Again, the power law plastic equation includes the yield stress value with the power law equation which is as follows (Franks, 1988; Lewis, 1987):

$$\tau = \tau_o + m\dot{\gamma}^n \tag{3}$$

where τ_o is yield stress. According to the power law equation, if n = 1 then the liquid is Newtonian, if $0<n<1$ then the liquid is pseudoplastic, and if $1<n<\infty$ the liquid is dilatant (Lewis, 1987).

2.1.3. Molecular basis for viscosity

There are numerous aspects which determine the viscosity of liquids including characteristics of continuous and dispersed phase, interactions between solute-solute and solute-solvent molecules, concentration, shape, size and chemical composition of solute molecules (Lewis, 1987). In the case of a disperse system, viscosity is largely

determined by the continuous phase which could be either Newtonian or non-Newtonian, and it is expected that viscosity is proportional to the viscosity of the continuous phase. The viscosity of the continuous phase can be altered by changing temperature and soluble additive concentration.

Water is a typical continuous phase whose viscosity can be increased or decreased by adding salts. The impact of soluble additives on the properties of the continuous phase depends on molecular weight and shape. Solutes of high molecular weight, such as dextran, enhance water viscosity (almost double) at low concentration (~2.75%), whereas solutes of low molecular weight, such as glucose, enhance viscosity to a similar extent at high concentration (~22%) (Barnes, 2000). For dilute solutions where solute particles are considered as non-interacting, viscosity can be presented as relative viscosity which is the viscosity of the solution relative to the viscosity of water. Relative viscosity (η_r) can be expressed as follows:

$$\eta_r = \eta_s/\eta_o = 1 + k\Phi \quad (4)$$

where η_s is solution viscosity, η_o is water viscosity, Φ is the volume fraction of solute particles, and k is a constant which is 2.5 for spherical solutes and greater than 2.5 for other shaped solutes. Since for dilute solutions, volume fraction is proportional to concentration (c), the above equation can be written as follows:

$$\eta_r = 1 + kc;\ \eta_r - 1 = kc$$

where η_r -1 is known as specific viscosity or viscosity increase because of solute inclusion. For concentrated solutions, solute-solute interactions can be considered by using the following equation (Franks, 1988):

$$\eta_r = \eta_s/\eta_o = 1 + k\Phi + k'\Phi^2 + \cdots \quad (5)$$

2.1.4. Viscosities of aqueous salt solutions

2.1.4.1. Water viscosity

Water is a well-studied liquid whose properties have been analysed at various temperatures and pressures. At 25 ^{o}C and 1 atm pressure the viscosity of water is $0.8903*10^{-3}$ Pa.s (Jenkins & Marcus, 1995). Again, water viscosity is constant at $1.002*10^{-3}$ Pa.s at 20 ^{o}C and at atmospheric pressure and this water viscosity has been taken as reference to calculate water viscosities at temperatures up to 100 ^{o}C using the following relationship (Weast, 1988-1989):

$$\log_{10}(\eta_T/\eta_{20}) = \{1.3272(20 - T) - 0.001053(T - 20)^2\}/(T + 105) \quad (6)$$

where η_T is the viscosity of water at temperature T ^{o}C, η_{20} is the viscosity of water at 20 ^{o}C.

In the case of liquids there is an exponential relationship between viscosity reduction and an increase in temperature at constant pressure as follows (Franks, 1972):

$$\eta = \eta_0 exp(-\Delta E_\eta/RT) \quad (7)$$

where η is the viscosity of liquid at a certain temperature, η_0 is the pre-exponential factor, R is the gas constant, T is absolute temperature and ΔE_η is the Arrhenius energy of activation which is higher for water with increment in temperature compared to the majority of liquids (Franks, 1972).

While temperature is constant, liquid viscosity as pressure changes can be expressed as follows (Franks, 1972):

$$\eta = A' exp\left(P.\Delta V_\eta / RT\right) \quad (8)$$

where A' is a constant, P is pressure, and ΔV_η is the volume of activation. The sign of volume of activation is positive when viscosity is enhanced with pressure increment, and it has a negative sign when viscosity is reduced with pressure increment. In the case of water, the positive and negative value of volume activation is observed at high and low temperature, respectively. At temperatures less than 30 ^{o}C the viscosity decreases up to a certain pressure and then increases with pressure, while at higher temperature viscosity shows a linear increment with pressure. On the other hand, viscosity of other liquids does not decrease with increasing pressure at less than 30 ^{o}C. Thus, the anomalous behaviour of water in comparison with other liquids is also obvious in the viscosity and pressure relationship (Franks, 1972).

2.1.4.2. Change in water viscosity by salt addition

When salts are added to water in order to make an aqueous electrolyte solution, the viscosity of water alters according to the nature of the soluble salt ions. The mobility or entropy of surrounding water molecules remains unchanged when cations of size 1.06 Angstrom and anions of size 1.78 Angstrom dissolve in water. Above and below these

sizes cations and anions cause change in the mobility of water molecules surrounding the ions, and taking these sizes as reference, ions are considered as large or small. Small ions, which have large charge density, bind water molecules strongly; as a result, the mobility of surrounding water molecules is reduced (ions known as kosmotropes). In contrast, large monovalent ions, which have small charge density, bind water molecules weakly and enhance the mobility of surrounding water (ions known as chaotropes) (Collins, 1997). **Table 2.2** represents a list of kosmotropes and chaotropes with crystal ionic radii (Haynes, 2010). For instance, lithium and sodium ions are small kosmotropes which cause water immobilization whereas cesium, chloride, bromide, and iodide ions are considered as chaotropes which enhance water mobility (Collins, 1997).

Table 2.2. Ionic radius of kosmotropes and chaotropes (Haynes, 2010)

Kosmotropes	Crystal ionic radii in Angstrom	Chaotropes	Crystal ionic radii in Angstrom
Li^+	0.59	K^+	1.37
Na^+	0.99	Cs^+	1.67
F^-	1.33	Cl^-	1.81
		Br^-	1.96
		I^-	2.20

In 1847 Poiseulle first observed that some salts are able to enhance water viscosity and some salts are responsible for a reduction of water viscosity (Jenkins & Marcus, 1995). Again, Jones and Dole identified that in the case of electrolyte solutions, the electrostatic forces have a role in determining solution viscosity, and the electrostatic forces are proportionally related to the square root of the concentration. Therefore, Jones and Dole proposed a relation between relative fluidity, which is the reciprocal of relative

viscosity, and concentration for dilute electrolyte solutions (0.005 to 1.0 mol.dm^{-3}) which is as follows:

$$\varphi/\varphi_o = 1 + A'c^{1/2} + B'c \quad (9)$$

here φ/φ_o is the relative fluidity of the solution, c is molar concentration of electrolytes or ions in mol dm^{-3}, A' and B' are coefficients. The fluidity and viscosity of liquid are inversely related. Later, Jones and Dole modified the equation for relative fluidity to relative viscosity according to the following equation:

$$\eta_r = \eta_s/\eta_o = 1 + Ac^{1/2} + Bc \quad (10)$$

where η_r or η_s/η_o is relative viscosity, and A and B are coefficients. The A coefficient relates to ion-ion interactions and can be estimated theoretically, and the B coefficient relates to ion size and interactions between ion and solvent that depends on ionic volume. This equation is known as the Jones-Dole equation. The two coefficients are variable depending on the salt (Jenkins & Marcus, 1995).

Ions can be categorized as kosmotropes and chaotropes considering the Jones-Dole viscosity B coefficient as this coefficient is related to charge density. The viscosity B coefficient is positive for kosmotropes and negative for chaotropes. For example, it is observed that $CH_3COO_2^-$ > F^- > HCO_2^- in terms of viscosity B coefficient positivity and SCN^- > I^- >Br^-> Cl^- in terms of viscosity B coefficient negativity. **Table 2.3** represents the viscosity B coefficient of some anions and cations (Collins, 1997). As the Jones and Dole expression above (10) is appropriate for dilute solutions of <0.1 M, the viscosity of concentrated solutions must be expressed by including another factor with the square of the concentration (Desnoyers & Perron, 1972).

$$\eta_r = 1 + Ac^{1/2} + Bc + Dc^2 \quad (11)$$

Table 2.3. Jones-Dole viscosity B coefficients ($dm^3.mol^{-1}$) for cations and anions (Collins, 1997)

Cations	B coefficient	Anions	B coefficient
Mg^{2+}	0.385	PO_4^{3-}	0.590
Ca^{2+}	0.285	$CH_3CO_2^-$	0.250
Ba^{2+}	0.22	SO_4^{2-}	0.208
Li^+	0.150	F^-	0.10
Na^+	0.086	HCO_2^-	0.052
K^+	-0.007	Cl^-	-0.007
NH_4^+	-0.007	Br^-	-0.032
Rb^+	-0.030	NO_3^-	-0.046
Cs^+	-0.045	ClO_4^-	-0.061
		I^-	-0.068
		SCN^-	-0.103

It is possible to estimate $Ac^{1/2}$ using conductivity data, and the B and D coefficient can be determined from the intercept and slope respectively of the plot of $(\eta_r - 1 - Ac^{1/2})/c$ against c. The viscosity D coefficient depends on all the solute-solvent and solute-solute interactions which occur in concentrated solutions and which are not estimated by the A and B coefficients (Desnoyers & Perron, 1972).

Marcus (2009a) mentioned in his review paper that there is an importance of the temperature coefficient, dB/dT, along with the viscosity B coefficient in order to define ions as water structure maker or structure breaker. Usually $B > 0$ and $dB/dT < 0$ was observed for structure making ions, and $B < 0$ and $dB/dT > 0$ was observed for structure breaking ions.

Desnoyers and Perron (1972) plotted B against partial molal volume V^o, which is the change in volume when one mole of substance is added to the solution, for several ions to recognize the mechanism of the effect of the ions on water structure. The Einstein

equation for determining the hydrodynamic impact of non-hydrated spherical colloidal suspensions is as follows (Desnoyers & Perron, 1972):

$$\eta_r = 1 + 2.5\Phi \tag{12}$$

where Φ is volume fraction; the above equation can be written according to the following equation:

$$\eta_r = 1 + 0.0025 V_h c \tag{13}$$

where V_h is the hydrodynamic volume in $cm^3.mol^{-1}$, c is the concentration in moles per liter. In the case of a suspension of non-hydrated ions and ideal solvent (the solvent which is dimensionless and structure less) V_h is equal to the partial molal volume of the ions, and the relationship between the B coefficient and partial molal volume V^o is supposed to be linear with slope 0.0025. Both structure maker and structure breaker ions deviate from the Einstein expression. Tetra-alkyl ammonium ion, Li^+, Na^+, and F^- are known as water structure makers, and they showed positive deviation from the Einstein expression as the slope dB/dV^o is more positive. On the other hand, the ions known as structure breakers, such as Rb^+, Cs^+, Br^-, and I^-, showed negative deviation from Einstein equation as the slope dB/dV^o is more negative (Desnoyers & Perron, 1972).

Banipal et al. (2008) measured the viscosity of some acetates including lithium, sodium, potassium, magnesium and calcium acetates over a temperature range (288.15K-318.15K) and found a positive viscosity B coefficient for all metal acetates. The viscosity B coefficients were found to be reduced with temperature increment; as a result dB/dT showed negative values. Thus, metal acetates can be considered as water

structure maker salts. Again, Saeed, Uddin, Masood and Asif (2009) studied the viscosity of ammonium chloride and ammonium bromide within a concentration range from $1x10^{-2}$ to $9x10^{-2}$ $mol.dm^{-3}$ and also evaluated their viscosity A and B coefficient with temperature from 298K to 323K to recognize ion-ion interactions and ion-solvent interactions, respectively. The viscosity of aqueous solutions of these two salts rose with concentration increase at a specific temperature. As an explanation, they mentioned the loss of kinetic energy of salt and solvent molecules which favours attachment of molecules to each other. The viscosity of these salt solutions reduces at higher temperature because of enhanced flow behaviour of the solution. The value of the A coefficient varied depending on ion size and degree of hydration. Reduced A coefficient specifies a greater degree of hydration compared to ion-ion interactions. The value of A coefficient reduced with temperature increase which indicates reduction of ion-ion interaction because of kinetic energy enhancement. Moreover the positive values of viscosity B coefficients for ammonium chloride and ammonium bromide signifies their structure making property (Saeed, Uddin, Masood & Asif, 2009).

2.1.5. Viscosity of protein solutions

The viscosity of a protein solution is determined by the protein concentration. In the case of a dilute protein solution, apparent viscosity depends on the size, shape and rigidity of the protein molecule. Since protein molecules are polyelectrolytes, the viscosity of an aqueous solution of protein is dominated by the solution pH and ionic strength (Franks, 1988). The kinetic energy of protein molecules depends on solution temperature and higher kinetic energy can split intermolecular interactions. Thus, at higher temperature,

the kinetic energy of protein molecules increases and protein solution viscosity decreases (Sikorski, 2001).

Einstein proposed an equation to interpret the viscosity of non-electrolyte suspensions of spherical particles which is as follows (Jenkins & Marcus, 1995):

$$\eta = \eta_o(1 + 2.5\upsilon) \tag{14}$$

where υ refers to the specific volume of spherical molecules. For spherical solutes the coefficient of υ is 2.5 whereas for solutes of different shapes the coefficient is considered as 'α' which is related to the axial ratio *R* of the molecules. Stokes and Mills (1965) proposed a relationship between α and *R*:

$$\alpha = 2.5 + 0.59(R - 1) + 2.40(R - 1)^2 \tag{15}$$

When $\alpha\upsilon$ is considered for a molecular size solute, then $\alpha\upsilon$ can be written as the product of coefficient α times the molar volume of hydrated solute times molar concentration. This product of 'α' times the molar volume of hydrated solute times the molar concentration' is comparable to Bc (c is molar concentration) in the Jones-Dole equation $B = \left[(\eta/\eta_o) - 1 - Ac^{1/2}\right]/c$ (Jenkins & Marcus, 1995). At low concentration, the viscosity of the protein solution follows the Einstein equation, but at higher concentration, where interaction between protein molecules occurs, viscosity of the solution does not follow equation (14) (Franks, 1988).

2.1.5.1. Protein solution viscosity determining feature

The viscosity of a protein solution depends on numerous causes which can be subdivided into two groups: intrinsic causes and environmental causes. Within intrinsic causes, protein shape and conformation, molecular weight, hydration, and electric charge play a role in determining the viscosity of protein solutions. The shape and conformation are inherent features of the protein. The viscosity of a protein solution largely depends on the molecule's axial ratio which is the ratio of the protein's length to diameter. It has been observed that globular proteins with spherical shape exhibit reduced viscosity because of lower axial ratio whereas ellipsoid shaped protein, fibrous protein, and denatured protein show higher viscosity due to a higher axial ratio. The reason behind this viscosity difference is difference in entanglement; the entanglement enhances for protein with high axial ratio. **Table 2.4** represents the intrinsic viscosity and axial ratio relationship of some proteins. The intrinsic viscosity [η] can be defined as the limit of η_{sp}/c where $c \rightarrow 0$ (η_{sp} is specific viscosity and c is concentration) and the unit of intrinsic viscosity is $ml.g^{-1}$. The properties of isolated protein molecules, such as shape and volume, determine the value of intrinsic viscosity (Franks, 1988; Hill, Ledward & Mitchell, 1998). Again, molecular weight as an intrinsic property has less impact on globular protein solution's viscosity, but solutions of fibrous or denatured protein with higher molecular weight exhibit higher viscosity (Malkin & Isayev, 2006).

Table 2.4. Axial ratio and intrinsic viscosity of some proteins (Franks, 1988)

Protein	Intrinsic viscosity [η] ($ml.g^{-1}$)	Axial ratio
Ovalbumin	3.49	1.5
Bovine serum albumin	3.9	2.3
β –Lactoglobulin B {dimer}	2.86	1.0
Collagen (374 kDa)	1250	>100

Net electrical charge, which is determined by ionic strength and pH of the solution, also has a significant role. Elevated electric charges are responsible for increased viscosity due to charge repulsion. This phenomenon is evident in the case of very small spherical proteins (Hill, Ledward & Mitchell, 1998).

As environmental causes, factors such as concentration, shear rate, pH, and temperature can be mentioned. Usually less concentrated protein solutions behave like Newtonian liquids, and as the concentration is increased, the viscosity is enhanced. It has been observed that at a certain concentration, the viscosity of protein solutions increases drastically because of attachment of hydrated protein molecules (Malkin & Isayev, 2006). Moreover, the effect of shear rate on protein solution viscosity can vary according to the nature of the protein and interactions between the protein molecules; a concentrated protein solution may act either as a pseudoplastic or a dilatant liquid. Protein solution viscosity is also affected by the solution pH. Near the isoelectric point, the viscosity of a protein solution is high due to protein aggregation; viscosity is also found to be enhanced at extreme alkaline and acidic pH because of protein denaturation. Furthermore, if temperature continues to increase to denature protein molecules, the aggregated denatured protein molecules (due to hydrophobic effect) lead to an increase in axial ratio which increases the viscosity of the protein solution. The impact of temperature is found to be highly predominant in the case of protein solution viscosity (Franks, 1988; Photchanachai & Kitabatake, 2001).

2.1.5.2. Studies on protein solution viscosity

Bull (1940) measured the viscosity of egg albumin solutions of native, heat denatured, and urea denatured conformation at various concentrations which were less than 1%.

The temperature and pH were maintained at 35 ^{o}C and 8, respectively. Under this experimental condition, the specific viscosity was found to be enhanced with concentration increase. The specific viscosities of denatured egg albumin solutions were higher than the specific viscosity of native egg albumin solution in the concentration range from 0.2% to 0.8%, and urea denatured egg albumin solutions had higher specific viscosity than heat denatured protein solutions. In the case of native egg albumin solution, a linear relationship was observed between the specific viscosity and protein concentration whereas with increasing albumin concentration, both of the denatured protein solutions deviated from the linear relationship between the specific viscosity and protein concentration. Pradipasena & Rha (1977) studied the impact of concentration on viscosity of a β-lactoglobulin solution at pH 7 and ionic strength 0.04. The range of β-lactoglobulin concentrations 3-40% were analysed at shear rates from 800-1700 s^{-1}. They observed a linear relationship between the apparent viscosity (viscosity at certain conditions) and concentration up to a concentration of 10% which followed the Einstein equation $\eta_s = \eta_o (1 + 0.8C)$ where C is concentration in % and 0.8 is the Einstein constant for % of β-lactoglobulin solution which comes from multiplying 2.5 (shape factor) by the volume fraction. Above 10% concentration of the β-lactoglobulin solution, the apparent viscosity does not follow the Einstein equation, and positively deviates from the linear relationship between the apparent viscosity and protein concentration. The apparent viscosity of a 20% solution was double that of a 10% solution; for a 30% solution it was three times higher than that of a 20% solution, and the apparent viscosity of a 40% solution was around thirteen times higher than a 30% solution. For the range of protein concentrations, a linear relationship between the shear stress and the shear rate started at relatively high shear rates.

The impact of temperature on viscosity of β-lactoglobulin A solutions (10 $mg.ml^{-1}$) was examined measuring viscosity in the range of temperature 20 – 150 ^{o}C at pH 6.4. It was found that protein solution viscosity increased up to a temperature of 100 ^{o}C; the reason was interpreted as due to protein denaturation, aggregation, and polymerization of the unfolded structure. Above 113 ^{o}C the viscosity was found to be reduced due to protein structure destruction (Photchanachai & Kitabatake, 2001).

A group of researchers showed the hydration of three proteins, including hemoglobin, trypsin and gelatin, can be estimated with the aid of viscosity measurements, and they also compared the values with the hydration of these proteins obtained from osmotic pressure measurement and diffusion methods that produced similar values (Kunitz, Anson & Northrop, 1934).

2.2. Compressibility

2.2.1. Fundamental compressibility

Compressibility is a thermodynamic property of a fluid (liquid and gas) or solid which can be defined as a measure of the relative volume change of a fluid or solid with a change in surrounding pressure. There are two kinds of compressibility, adiabatic compressibility and isothermal compressibility, which have been widely studied (Chalikian & Breslauer, 1996).

2.2.1.1. Adiabatic compressibility and isothermal compressibility

Adiabatic compressibility of fluids can be defined as the relative change in volume because of a change in pressure at constant entropy. The adiabatic compressibility, K_S,

can be expressed in term of the following equation where V is volume, P is pressure, and β_S is the adiabatic compressibility coefficient and the subscript 'S' denotes constant entropy (Sarvazyan, 1991):

$$K_S = -(\delta V/\delta P)_S = \beta_S \mathrm{V} \quad (16)$$

where $\beta_S = -1/V(\delta V/\delta P)_S$.

Isothermal compressibility of fluids can be defined as the relative change in volume because of a change in pressure at constant temperature (Dadarlat & Post, 2001). The isothermal compressibility, K_T, can be expressed in term of the following equation where β_T is the isothermal compressibility coefficient (Sarvazyan, 1991):

$$K_T = -(\delta V/\delta P)_T = \beta_T \mathrm{V} \quad (17)$$

where $\beta_T = -1/V(\delta V/\delta P)_T$.

2.2.1.2. Relationship between adiabatic and isothermal compressibility

The adiabatic compressibility and isothermal compressibility of fluids are related to each other. The isothermal compressibility coefficient β_T can be determined from the following equation (Gekko & Noguchi, 1979):

$$\beta_S = \beta_T(C_V/C_P) \quad (18)$$

where β_S is the adiabatic compressibility coefficient, C_V is the specific heat capacity at constant volume, and C_P is the isobaric specific heat capacity (Gekko & Noguchi, 1979). The isothermal compressibility coefficient can also be determined from the adiabatic compressibility coefficient if the isobaric specific heat capacity, C_P, density, ρ,

and the volume coefficient of thermal expansion, k, are known using the following equation (Sarvazyan, 1991):

$$\beta_T = \beta_S + k^2 T/\rho C_P \quad (19)$$

where $k = V^{-1}(\delta V/\delta T)_P$. The parameter isobaric specific heat capacity, C_P, can be determined using calorimetric methods such as differential scanning calorimetry, and the density of the solution can be easily measured using a density meter (Blandamer, Davis, Douheret & Reis, 2001).

2.2.2. Compressibility of liquids

The compressibility of a liquid can be defined as the alteration of liquid volume when there is a variation of pressure upon the liquid. The concept of bulk modulus of elasticity determines the compressibility property of a substance. The bulk modulus of elasticity (E) can be expressed as (Mott, 1990):

$$E = dP/(dV/V) \quad (20)$$

Since the units of dV and V are the same, the unit of E is that of the unit of pressure.

As the density of a material is associated with the volume of material, this equation can also be written as (Mott, 1990):

$$E = dP/(d\rho/\rho) \quad (21)$$

In terms of compressibility, liquids and gases are very different. The gases are extremely compressible whereas liquids are incompressible to a large extent, with pressure altering volume only a small amount. Therefore, for liquids the values of bulk modulus are high.

The magnitude of bulk modulus of elasticity for water and some liquids are listed in **Table 2.5** (Mott, 1990):

Table 2.5. Bulk modulus of some liquids (Mott, 1990)

Liquids	Bulk modulus (MPa)
Ethyl alcohol	896
Benzene	1062
Water	2179
Glycerine	4509
Mercury	24750

Water exhibits an anomalous adiabatic and isothermal compressibility coefficient compared to other liquids. The β_S and β_T of water are controlled by temperature and minimum values are observed at 60 ^{o}C and 46.5 ^{o}C respectively. The β_S and β_T of water below these temperatures are found to be reduced with increase of temperature while above these temperatures the compressibility coefficients of water increase with increase in temperature similar to other liquids. This abnormality of water is attributed to a change in the structural and dynamic property of the hydrogen bonding network of water as temperature changes. Moreover, the anomalous temperature effect on water compressibility is only observed at atmospheric pressure whereas at higher pressure (2-4 kbar) the compressibility linearly increases with increase in temperature (Chalikian, Sarvazyan & Breslauer, 1994). According to Bridgman (1970) and Isaacs (1981), for liquids, compressibility is higher at lower pressure because of the void volume between molecules whereas in the case of higher pressure compressibility of liquids is attributed to liquid molecules internal compressibility and compressibility due to intermolecular interaction because with increased pressure the void volume decreases.

2.2.3. Measuring compressibility

Since pure homogenous liquid does not attenuate ultrasound to a large extent, the ultrasound wave velocity in a pure liquid is related to the adiabatic compressibility and density of the liquid according to the following equation (McClements, 1991):

$$v^2 = 1/\rho.\beta_S \quad (22)$$

where v is ultrasound velocity, ρ is density, and β_S is adiabatic compressibility coefficient. In the case of an emulsion or a suspension (another substance mixed to a pure liquid), attenuation, density, and adiabatic compressibility are altered. The altered adiabatic compressibility coefficient and density can be written as follows (McClements, 1991):

$$\beta_S = \beta_o = (1 - \Phi)\beta_1 + \Phi\beta_2 \text{ and } \rho = \rho_o = (1 - \Phi)\rho_1 + \Phi\rho_2 \quad (23)$$

where Φ is the volume fraction of the dispersed phase and subscripts 1 and 2 denote properties of the continuous phase and disperse phase, respectively.

2.2.3.1. Principles of ultrasonic velocimetry

The ultrasonic velocity is the velocity of an ultrasonic wave which travels through a medium depending on the medium's physical properties including the density (Equation 22). The sound velocity which is presented in the Newton-Laplace equation is phase velocity. The phase velocity can be defined as the velocity at which the phase of any single frequency component of the sound signal transmits. The phase velocity can be expressed in term of the equation v = ω/ɳ where ω is angular frequency and ɳ is wave number, and the frequency and the wavelength of a plane sound wave are related to the

angular frequency and wave number according to the relations, $f = \omega/2\pi$ and $\lambda = 2\pi/\eta$, respectively (Kaatze, Eggers & Lautscham, 2008). Thus, through measuring the ultrasound velocity and density of a liquid, the adiabatic compressibility coefficient of the liquid can be estimated directly (Pfeiffer, Heremans & Wevers, 2008).

2.2.3.2. Technologies of ultrasonic velocimetry

2.2.3.2.1. Pulse methods

Pulse methods can be subdivided into two categories according to signal shape and sample excitation including narrow-band pulse techniques and broad-band sharp pulse techniques. Narrow-band pulse techniques are simple and widely used to measure sound velocities in liquids. The narrow-band pulse techniques use plane wave sound propagation at one well defined frequency or carrier frequency (Hosoda, Takagi, Ogawa, Nomura & Sakai, 2005). Usually for narrow-band pulse methods, the pulse duration time is between 1 and 20 μs, and carrier frequency is near 10 MHz. The broad band sharp pulse techniques utilize sharp pulses with duration time less than 1 μs and the broad band sharp pulse techniques use a wide range of frequencies (0 to 20 MHz). Among the pulse methods, the transmission method and the pulse-echo methods are widely used (Kaatze, Eggers & Lautscham, 2008).

2.2.3.2.1.1. Transmission or sing-around method

The sing around method is a pulse technique. Now, this method is considered as one of the simplest methods for the measurement of ultrasound velocity. This method is also known as the transmission method. Two transducers are involved in this method; one transducer is known as the transmitter and the other transducer is the receiver. The signal

generator forms the pulse-modulated signal or sharp pulse which is converted by a piezoelectric transmitter to an acoustic signal. This signal passes through the liquid in the measuring cell to a piezoelectric receiver transducer and the received ultrasonic pulse is then used to retrigger the transmitter. The received signal is amplified by an amplifier which is then transferred to the computer system for analysis and to calculate the sound velocity (Kaatze, Eggers & Lautscham, 2008; Povey, 1997).

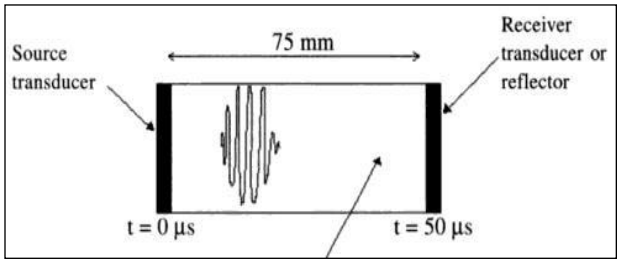

Figure 2.1. Block diagram of an acoustic pulse-echo apparatus. (Adapted from Ultrasonic techniques for fluids characterization, M. J. Povey, p. 12 , Copyright (1997), with permission from Academic Press)

With the aid of **Figure 2.1** the transmission method can be explained easily. For single transmission, when the acoustic signal transmitted from a transmitter transducer travels 75 mm within 50 µs to reach a receiver transducer then the velocity of sound would be 1500 $m.s^{-1}$. It is essential to maintain a stable temperature to obtain an accurate velocity measurement (Papadakis, 1973; Sarvazyan, 1991).

2.2.3.2.1.2. Pulse-echo method

The pulse-echo method utilizes only one transducer and a sound reflector for the measurement of the ultrasound velocity of a liquid. The transducer acts as both pulse transmitter and receiver. The pulse propagates through the sample and reflects back as echoes. Both narrow-band pulse modulated signals and broad-band sharp pulse signals can be utilized for the pulse-echo methods (Papadakis, 1967). The measurement of

sound velocity by the pulse-echo method is simple and easy. According to the definition of velocity, sound velocity can be measured from the distance travelled by a sound wave in a certain time. In the case of a single reflection, the acoustic signal transmitting from the transmitter transducer travels 75 mm within 50 μs to reach a reflector, instead of a receiver transducer (**Figure 2.1)**, and then reflects back to the transmitter again. The acoustic signal travels double distance (150 mm) in double time (100 μs) and the sound velocity would be 1500 $m.s^{-1}$ (Povey, 1997). The pulse-echo apparatus can measure the sound velocity of a relatively concentrated protein solution (10 $mg.ml^{-1}$ or more) with an accuracy of 1 $m.s^{-1}$ and a precision of 0.1 $m.s^{-1}$ (Apenten, Buttner, Mignot, Pascal & Povey, 2000).

2.2.3.2.2. Resonator method

In the ultrasonic resonator method, there are two transducers (Eggers & Funck, 1973). One transducer or oscillating wall generates the sound waves which are reflected by another transducer or reflector. Acoustic resonance results because of reflected sound waves and sample interference, and a field of standing waves form at a distinct resonance frequency. When the transducer and reflector are parallel and are separated by a certain distance, then a series of acoustic resonances can be created within the distance by changing the frequency (Eggers & Funck, 1973). For an ideal system, the resonance conditions are related to the ultrasonic velocity according to the relation $d = n \lambda/2 = nv/2f$ where d is the distance between transducer and reflector, λ is wavelength, f is frequency and n is an integer or order number of the resonances. The relation between ultrasound velocity and resonance can also be written as follows (Coupland, 2004; Eggers & Funck, 1973):

$$v = 2d(f_n - f_{n-1}) \quad (24)$$

where f_n is the sequence of the resonance frequencies. There are two principal criteria which make the resonator method popular for biomolecular studies: small sample volume and comparatively higher precision. Less than 1 ml sample volume is sufficient for the resonator method with five fold better precision compared to pulse methods. The bulk water compressibility and hydration shell water compressibility differ from each other. When there is any change in polymer conformation then a change also occurs in the hydration shell water of the polymer. Therefore, changes in polymer conformation can be detected by measuring the compressibility of polymer solutions using the resonator method (Coupland, 2004; Sarvazyan, 1991).

2.2.4. Bulk viscosity

In a homogenous liquid ultrasound does not scatter and the attenuation of an ultrasonic wave is due to absorption which results from thermodynamic relaxation processes (McClements, 1991). The bulk viscosity is a hydrodynamic property for compressible Newtonian liquids that assesses the liquids' compressional resistance (Dukhin & Goetz, 2009; Guo & Zhang, 2001). The difference between dynamic viscosity or shear viscosity and bulk viscosity is the dynamic viscosity of a liquid only considers translational molecular movement whereas bulk viscosity considers relaxation of rotational and vibrational molecular movement of liquids. The sound attenuation in liquids is determined by both the bulk viscosity and the dynamic viscosity of liquids (Dukhin & Goetz, 2009). Bulk viscosity is related to ultrasonic wave absorption and dispersion in liquids; the ultrasonic wave amplitude reduces with distance due to an absorption

coefficient, α, or attenuation, and dispersion, dv/dω, where ν is wave velocity and ω is angular frequency.

The compressional relaxation and bulk viscosity of liquid arises due to a compressional relaxation time which can be defined as the time between the introduced stress wave on a liquid and the reaction of the liquid. The compressional relaxation time, which depends on temperature and pressure, is associated with the liquid's intermolecular forces. Thus, intermolecular forces can be predicted from the bulk viscosity (Guo & Zhang, 2001; Narasimham, 1993). This kind of viscosity is also known as volume viscosity, second viscosity coefficient, expansion coefficient of viscosity, and coefficient of bulk viscosity in various research areas (Dukhin & Goetz, 2009). Bulk viscosity is introduced in the Navier-Stokes equation for compressible Newtonian liquids as follows (Dukhin & Goetz, 2009):

$$\rho\left[\frac{\delta v}{\delta t} + (v\nabla)v\right] = -grad\ P + \eta\Delta v + \left(\eta^b + \frac{4}{3}\eta\right) grad\ div\ v \qquad (25)$$

where the symbols ρ, t, v , P, η, η^b are for density, time, liquid velocity, pressure, shear viscosity, and bulk viscosity, respectively. Little experimental data on the bulk viscosity of Newtonian liquids is available; for example, bulk viscosity of water is 3.09 mPa.s at 15 ^{o}C and that of methanol is 2.1 mPa.s at 2 ^{o}C, as stated in a review by Litovitz and Davis (1964). Thus, it is necessary to have more experimental data on bulk viscosity to understand compressible Newtonian liquid properties.

It is considered that measurement of the bulk viscosity of liquids is only possible by measuring ultrasound attenuation as ultrasound attenuation is the result of viscosity (bulk viscosity and dynamic viscosity) and thermal conduction (Dukhin & Goetz, 2009). For liquids, the thermal conduction impact on ultrasound attenuation is insignificant, and viscosity plays the significant role in ultrasound attenuation. Thus, bulk viscosity of compressible Newtonian liquids can be calculated from ultrasound attenuation, ultrasonic velocity, and dynamic viscosity utilizing the following equation (Dukhin & Goetz, 2009):

$$\alpha_{long} = \frac{\omega^2}{2\rho v^3}\left[\frac{4}{3}\eta + \eta^b\right] \quad (26)$$

where α_{long} is the ultrasound attenuation coefficient, ω is ultrasound angular frequency, and ν is sound velocity. Again, longitudinal viscosity (viscosity arising from longitudinal stress) $\eta_{long} = \eta^b + \frac{4}{3}\eta$ (for Newtonian liquid) and

$\eta_{long} = 2\alpha_{long}\rho v^3/\omega^2$ (for non-Newtonian liquid). In the case of Newtonian liquids the bulk viscosity is ultrasound frequency independent and dynamic viscosity is shear rate independent, whereas for non-Newtonian liquids bulk viscosity is dependent on ultrasound frequency and dynamic viscosity is shear rate dependent (Dukhin & Goetz, 2009; Franks, 1972).

2.2.5. Compressibility of salt solutions

2.2.5.1. Alteration of liquid compressibility by salts

Freyer (1931) measured the velocity of sound in aqueous salt solutions including KCl, KBr, KI, NaCl, NaBr and NaI over a wide range of concentrations (~1% - ~45%) and temperatures (10 – 60 ^{o}C) in order to examine the impact of these salts on water compressibility. At 20 ^{o}C the velocities of sound were found to be elevated with increasing salt concentration for KCl, NaCl, KBr, and NaBr solutions. In the case of KI solution the sound velocities were found to be reduced with concentration increment at temperatures of 25, 35, 45 ^{o}C and the minimum velocity was observed at approximately 37%; but the velocity was increased at 45% concentration at temperatures of 15-35 ^{o}C. All the halides showed increased velocity with increasing temperature. Usually the sound velocity of a solution increases if the solution has a lower adiabatic compressibility and density. The researcher also observed the fractional change in adiabatic compressibility and change in density for a 10% solution. From the observation he concluded that in the case of NaCl, KCl, NaBr and KBr, the dominating factor is altered compressibility which is responsible for the increased sound velocity and the order of reduction in dominance is NaCl> KCl> NaBr> KBr. In the case of KI and NaI, the dominating factor is density change and the sound velocity was found to decrease with increment in concentration. Depending on the nature of the salts all of these halides were found to reduce the compressibility of the solvent water, and the order of the halides in decreasing compressibility was NaCl> KCl> NaBr > KBr> NaI> KI.

2.2.5.2. Factors associated with altered compressibility

Compressibility of electrolyte solutions is largely determined by ion solvation and electrostriction. Hydration of ions is correlated with the alteration of solvent compressibility. The ion which is very hydrated can reduce the compressibility of water to a large extent. When a salt dissolves in water it dissociates into its composing ions which reorganize the solvent molecules around them. The change in compressibility is related to ionic radii; small ionic radii have large charge density and attract the water dipole more strongly. As a result, contraction of solvent molecules occurs in surrounding ions of small ionic radii and an ultimate result of this contraction is a lowering of the compressibility of the solution (Freyer, 1931). Moreover, comparison between alkali metal chlorides and potassium halides were done by plotting the partial molal compressibility of individual ions as a function of Pauling ionic radius. Again it was observed that partial molal compressibility was negative for both the alkali metal chlorides and the potassium halides series, and the negative partial molal compressibility increased for ions with reduced ionic radii, with halide anions having more impact on compressibility changes than alkali metal cations. Furthermore, large R_4N^+ ions reduced partial molal compressibility but the reason was attributed to a hydrophobic effect on structure of solvent water. Partial molar compressibility of ionic solutions is dependent on structure determining features such as interaction between solute and solvent rather than other features such as volume, entropy, and activity coefficient (Mathieson & Conway, 1974).

2.2.6. Compressibility of protein solutions

Study of compressibility or volume fluctuation of biomolecules is of growing interest in the biological research field. Compressibility of a protein is a measure of protein softness. General thermodynamic properties of protein molecules such as characteristics of the protein interior, its conformational state, and molecular interactions can be obtained from protein compressibility measurements (Gekko, Kimoto & Kamiyama, 2003; Taulier, Beletskaya & Chalikian, 2005). Many techniques have been used to measure the compressibility of biomolecules and analysis thereafter. Using hydrogen-exchange experiments, it was found that a protein molecule fluctuates with respect to the relative positions of its constitutive amino acids and X-ray analysis of protein molecules shows imperfect packing or cavities inside the protein molecules (Frauenfelder et al., 1987). Using ultrasound velocimetry, the compressibility of the protein can be resolved from the ultrasonic wave velocity measurement for both the solution and solvent. The compressibility measured using this technique is the partial adiabatic compressibility (Mori, Seki, Yamada & Matsumoto, 2006). This is the only direct method to measure protein compressibility in aqueous solution. In addition, fluorescence spectroscopy and nuclear magnetic resonance spectroscopy are able to measure the local compressibility of a protein molecule with respect to the atomic distances within a protein molecule (Li, Yamada & Akasaka,1999; Mori, Seki, Yamada & Matsumoto, 2006).

Because of the presence of imperfect packing, when mechanical force is applied to protein molecules, internal motion occurs. The value for the compressibility of a globular protein molecule in aqueous solution is a characteristic feature of its tertiary structure (Gekko & Yamagami, 1991). Globular proteins show lower compressibility

than liquids such as ethanol and water, and solid polymers such as polyethylene, and higher compressibility than metals and covalent solids. Again, globular proteins are more compressible as compared to the compressibility of fibrous proteins such as gelatin (Gavish, Gratton & Hardy, 1983).

To clarify the physical mechanisms which are responsible for the structure-function relationship of proteins, it is necessary to have information about protein compressibility (Gekko & Yamagami, 1991). Although some proteins are similar with respect to primary and tertiary structures, they show different functional properties. For example, α-lactalbumin and lysozyme are highly similar with respect to their primary and tertiary structures but α-lactalbumin shows good emulsifying and foaming properties as compared to lysozyme. The dynamic structural property of protein is closely related to its functional characteristics and the compressibility of protein is linked to the flexibility or dynamic structural property of protein. Highly compressible proteins are easily digested by proteases whereas proteases themselves are less compressible. It is also observed that transport proteins, including bovine serum albumin, myoglobin and haemoglobin, which bind with other molecules to transport them from one organ to another, have a large compressibility. Again, proteins with high compressibility show good foaming capacity as well as emulsifying activity (Gekko & Yamagami, 1991). Thus, compressibility measurements of an aqueous protein solution give valuable information about the protein with respect to its thermodynamic properties and its functionality.

2.2.6.1. Compressibility contribution factors

According to Dadarlat and Post (2003), variation in compressibility of different protein solutions occurs due to the competition between protein-solvent attractive forces and the preferable intramolecular interactions within the protein interior. The adiabatic compressibility of a protein is closely related to the partial specific volume (v^o), hydrophobicity and polarity of the protein molecule. The partial specific volume of a protein in solution is comprised of the constitutive volume (sum of constitutive atomic or group volumes), the void volume of the molecule (the cause of intrinsic compressibility), and the volume change due to any structural change of water, i.e., degree of hydration.

Proteins with large partial specific volumes show large adiabatic compressibilities (Kauzmann, 1959). Adiabatic compressibility of protein molecules in aqueous solution is dependent on the intrinsic compressibility of protein molecules and the difference in the compressibility of the hydration shell relative to bulk water (Gekko & Hasegawa, 1986). Intrinsic compressibility of protein molecules arises from the void volume created due to the imperfect packing of polypeptide chains into the protein interior. A protein molecule having a rigid interior shows smaller intrinsic compressibility. Thus, intrinsic compressibility of protein molecules has a role in increasing the overall compressibility (Sarvazyan, 1991). Hydration has a negative contribution to the overall protein compressibility as an increase in the hydration contribution tends to lower the overall compressibility of a protein. The compressibility of the protein in a hydration shell depends on the chemical nature of the protein-water interface. The compressibility of water hydrating charged atoms, nonpolar atoms, and polar atoms are lower, higher,

and about the same, respectively, as compared to bulk water compressibility (Dadarlat & Post, 2006).

Highly hydrophobic proteins show very large compressibility relative to hydrophilic proteins. Most of the polar amino acids reside on the surface of protein molecules and play a role in hydration, and residing in the protein interior, most of the hydrophobic amino acids play a role in the imperfect packing of polypeptide chains (Gekko & Noguchi, 1979). The polarity parameter (P) proposed by Bigelow can be defined as the volume ratio of polar and nonpolar amino acids. This parameter considers both the contributions of polarity and hydrophobicity of a protein. So, from the values of the polarity parameter of a specific protein molecule, the compressibility of that protein molecule can be predicted. High values of the polarity parameter indicate low compressibility of the protein molecule and low values of the polarity parameter indicate high compressibility of the protein molecules (Bigelow, 1967). When unfolding of a protein molecule occurs, more atomic groups of the protein come in contact with the aqueous solvent relative to the folded protein, and the unfolded protein exhibits lower compressibility (Gotto & Isemura, 1964).

According to Cooper (1976), the isothermal compressibility coefficient is directly related to the volume fluctuation of a protein molecule following the equation:

$$\delta\bar{V}^2 = \text{ə}T\beta_T V \tag{27}$$

where $\delta\bar{V}^2$ is the volume fluctuation and ə is the Boltzmann constant. The intrinsic isothermal compressibility of globular proteins varies because of the variation of excess surface charge. The excess surface charge can be defined as the difference between the

fraction of charged atoms on the surface and the overall fraction of charged atoms. The increase in the intrinsic isothermal compressibility of globular proteins with excess surface charged atoms is observed due to competition between the attractive solvation forces and the intra-protein attractive forces (Dadarlat & Post, 2003). Since adiabatic compressibility and isothermal compressibility are related, and the bulk adiabatic compressibility is three-fourths of the bulk isothermal compressibility in the case of organic liquids and solids (Eden, Matthew, Rosa & Richards, 1982), it can be said that the impact of the excess surface charge of a globular protein on the adiabatic compressibility of the protein would be similar as on the isothermal compressibility of a globular protein.

2.2.6.2. Relationship between compressibility of protein and molecular interactions of specific amino acid structures

The compressibility property of a protein reflects the interior structure as well as the functional characteristics of the protein molecule. It is predicted that secondary structure elements likely contribute to protein compressibility. Helix rich proteins such as myoglobin and hemoglobin show large compressibility whereas helix-deficient proteins such as trypsin and trypsinogen show low compressibility (Gavish, Gratton & Hardy, 1983). The compressibility of globular proteins also depends on many other structural contributors including disulfide bonds, prosthetic groups (metal, carbohydrate, and lipid), coenzymes, and the number and shape of protein domains. Moreover, compressibility of proteins also depends on the amino acid composition since it is seen that Leu, Glu, Phe and His amino acids are responsible for large compressibility, and Asn, Gly, Ser and Thr amino acids are responsible for lower compressibility.

Compressibility of proteins does not only depend on the polar or nonpolar nature of proteins but also depends on the structure element such as helix element of proteins. Helix element has a role in volume fluctuation, and Glu and His amino acids are helix structure former. Therefore, although Glu and His are polar amino acids, they have a role in raising protein compressibility (Gekko & Hasegawa, 1986).

Comparing residue specific nonbonding energies of a set of globular proteins which vary in their compressibilities, Dadarlat and Post (2003) found that residue specific electrostatic energy varies greatly among the protein molecules whereas the residue specific van der Waals energy did not show significant variation. In addition, they found that compressibility of globular protein molecules depends on the excess charge on the surface of the native protein. The intrinsic compressibility of protein arises from the competition between the attractive protein-water interactions (related to the fraction of charged atoms on the surface) and the intra-protein attractive forces (related to the overall fraction of charged atoms). A higher percentage of surface charge versus interior charge lowers the protein-water surface tension which leads to a higher protein-water attractive force (causing volume expansion) than intra-protein attractive force (causing volume compaction) and gives protein a larger compressibility than proteins with balanced charge distribution in surface and interior positions. Thus, it can be concluded that electrostatic interactions have a noticeable function in protein compressibility (Dadarlat & Post, 2003).

2.2.6.3. Compressibility of protein in the presence of salts

Tanford (1968) reported that in the presence of a strong denaturant, such as guanidinium chloride, extensive unfolding of protein takes place. Gekko and co-workers found that

upon addition of guanidinium chloride to the solutions of ribonuclease A and hen egg white lysozyme, unfolding occurs in association with a large decrease in compressibility (Kamiyama & Gekko, 1997; Tamura & Gekko, 1995) and they hypothesized that the reduction in compressibility is due to the loss of imperfect packing volume and hydration of exposed internal amino acids, an idea that was later experimentally supported by Frye & Royer (1998).

2.2.6.4. Partial specific adiabatic compressibity entailing compression of protein in liquid

When the principal interest is in solute solvent interactions or hydration, compressibility of the whole solution is not informative enough. It is necessary to know about apparent molar or specific compressibility of a solute which arises from three types of interactions: one type of interaction is between the atoms of a molecule (interatomic interactions) which contributes to the intrinsic compressibility of the solute, the second one is the interaction between solute molecules and solvent molecules, and the third type of interaction is between solute molecules which depends on experimental criteria (Chalikian, Sarvazyan & Breslauer, 1994). The solute-solute interaction can be reduced by diluting the solution and at infinite dilution the apparent molar or specific compressibility of the solute molecule is equivalent to the partial molar or specific compressibility of the solute (k_S^o) (Chalikian, Sarvazyan & Breslauer, 1994). The apparent molar volumetric fraction of solvent in solution (Φ_o) and the partial molar volume of solute can be measured from density values using the following equations:

$$\Phi_o = [(\rho - c)/\rho_o] \quad (28)$$

$$v^o = \lim_{c \to 0}[(1 - \Phi_o)/c]$$

or

$$v^o = \lim_{c \to 0}[\{1 - (\rho - c)/\rho_o\}/c] \quad (29)$$

where ρ is the density of solution, ρ_o is the density of solvent, and c is the concentration of solution.

Again, the partial specific adiabatic compressibility coefficient can be expressed according to the following equation:

$$\beta_s^o = -\left(\frac{1}{v^o}\right)\frac{\delta v^o}{\delta P} = \left(\frac{\beta_o}{v^o}\right)\lim_{c \to 0}\left[\frac{(\beta/\beta_o - \Phi_o)}{c}\right] \quad (30)$$

here β and β_o are adiabatic compressibility coefficient of the solution and the solvent, respectively (Gekko & Hasegawa, 1986).

Partial specific compressibility of a protein solution entails the intrinsic compressibility of the protein molecule and the hydration contribution to overall compressibility. Partial specific adiabatic compressibility also gives information about protein conformational status such as tertiary structure. If the surface accessible groups (charged, polar and nonpolar) of a solute or protein molecule are known, then the hydration contribution to the partial molar or specific compressibility can be determined (Andrews, Moses, Sendhil, Rakkappan & Jayakumar, 2002; Chalikian, Sarvazyan & Breslauer, 1994).

Partial specific adiabatic compressibility measurement is a powerful tool which is able to differentiate between protein conformational transitions (Chalikian & Breslauer,

1996). There are four potential thermodynamic states of conformation for globular proteins including native (N) state, compact intermediate (CI), partially unfolded (PU), and fully unfolded (FU). The native state of a globular protein is defined as a specific tertiary conformation with a closely packed hydrophobic core inside the protein. Compact intermediate or molten globule is characterized as a floppy tertiary structure which is rich in secondary conformation with a loosely packed hydrophobic core compared to the native state. The hydrophobic inside packing of the PU state is looser than the CI state together with no existence of tertiary or secondary structure. Finally, the FU state can be characterized as a fully solvated amino acid sequence with a random coil structure. The partial specific adiabatic compressibility k_S^o of compact intermediate conformations of single domain globular proteins increased by $+(1 - 4)\times10^{-6}$ $cm^3.g^{-1}.bar^{-1}$ compared to the native conformation whereas the partial specific adiabatic compressibility k^0s of partially unfolded conformations of the proteins decreased by $-(3 - 7)\times10^{-6}$ $cm^3.g^{-1}.bar^{-1}$. In the case of a fully unfolded protein, a large decrease in partial specific adiabatic compressibility was observed: $-(18 - 20)\times10^{-6}$ $cm^3.g^{-1}.bar^{-1}$ (Chalikian & Breslauer, 1996). The range of partial specific adiabatic compressibility for native globular proteins varies from -1×10^{-6} to 10×10^{-6} $cm^3.g^{-1}.bar^{-1}$ whereas the partial specific volume varies only from 0.70 to 0.75 $cm^3.g^{-1}$, therefore it is more advantageous to consider partial specific adiabatic compressibility to examine native globular protein conformational characteristics (Chalikian, Totrov, Abagyan & Breslauer, 1996). Chalikian and coworkers (1996) measured the partial specific volume and the partial specific adiabatic compressibility of 15 globular proteins at temperatures of 18, 25, 35, 45 and 55 ^oC and found both parameters increased with increasing temperature. It is possible to define partial molar volume using the following equation:

$$V^o = V_M + V_T + V_I + \beta_{To}RT \quad (31)$$

where V_M is the intrinsic molar volume of solute, V_T (thermal volume) is the volume surrounding the solute molecule that arises due to thermal motions of the solute, V_I is known as the interaction volume that arises from interactions of protein with water, β_{To} is the isothermal compressibility coefficient of the solvent, R is the gas constant. As the value of $\beta_{To}RT$ for aqueous solutions is very low, approximately 1 $cm^3.mol^{-1}$, and the partial molar volume for macromolecules is around 10^4 $cm^3.mol^{-1}$, $\beta_{To}RT$ can be ignored from the partial molar expression. Now, considering the molecular weight of a protein M, the partial specific volume of the protein can be expressed as follows (Chalikian, Totrov, Abagyan & Breslauer, 1996):

$$v^o = v_M + v_T + v_I \quad (32)$$

where $v_M = V_M/M$, $v_T = V_T/M$, and $v_I = V_I/M$. The parameter V_I can be represented as $n_h(V_h^o - V_o^o)$ where n_h is hydration number, V_h^o represents the partial molar volume of water in the hydration shell, and V_o^o is the partial molar volume of bulk water. Thus, the above equation (32) can be rewritten as:

$$v^o = v_M + v_T + n_h(V_h^o - V_o^o)/M \quad (33)$$

2.3. Hofmeister salts and their effect on water structure

2.3.1. Water structure

Two hydrogen atoms interact covalently with one oxygen atom to form a molecule of water. The water molecule is a polar molecule because there is a net negative charge toward the oxygen end and a net positive charge toward the hydrogen end. Thus, the

oxygen atom in a water molecule can interact with two hydrogen atoms of two other water molecules through hydrogen bonding and the three dimensional structure of water forms. The liquid water has a surface tension property since surface tension is a property of liquids resulting from intermolecular attraction. Due to surface tension, molecules close to the surface of a liquid experience a net attraction to the rest of the liquid whereas molecules far from the surface experience no net attraction (Franks, 1972).

2.3.2. What is the Hofmeister series?

The Hofmeister series can be defined as a rank ordering of neutral salts according to their impact on the hydrophobic interactions of protein or the first and second vicinity hydration shells (Dill, Trusket, Vlachy & Lee 2005). When neutral salts in the Hofmeister series are added to aqueous protein solutions, the conformation and solubility property of the protein is altered showing Homeister effects. The Hofmeister effects are the ability of certain salts or ions to cause stabilization or destabilization of protein conformation, and the salts are ranked according to their effectiveness in salting out of the protein or causing protein precipitation (Curtis & Lue, 2006). Anions in the Hofmeister series are more effective compared to cations. **Figure 2.2** represents the order of some anions in the Hofmeister series together with some relevant properties. Anions residing on the left of the Cl^- ion are kosmotropes while anions residing on the right of the Cl^- are chaotropes (Zhang & Cremer, 2006).

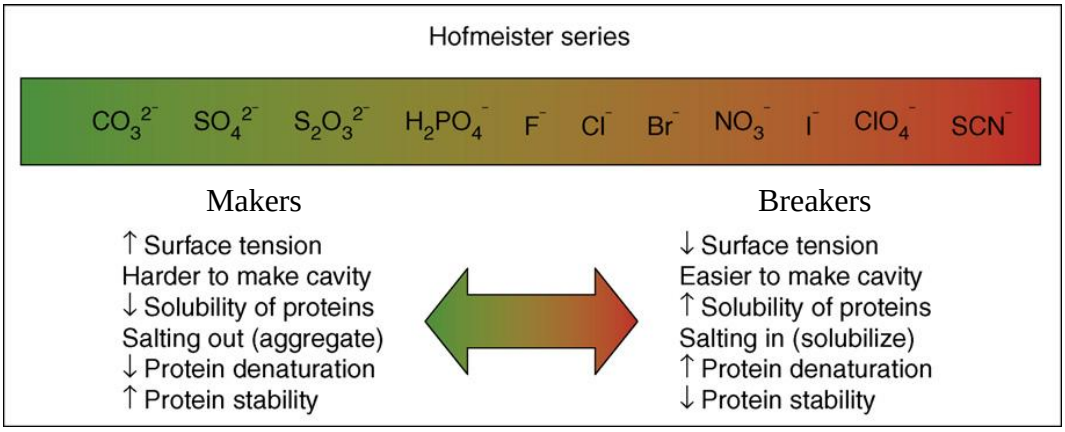

Figure 2.2. Anions in the Hofmeister series (Adapted from Current Opinion in Chemical Biology, v. 10, Y. Zhang and P.S. Cremer, Interactions between macromolecules and ions: the Hofmeister series, p. 659, Copyright (2006), with permission from ELSEVIER)

2.3.3. Interaction of neutral salts with water

The water structure is affected by ions according to their nature. For example, small ions (kosmotropes) with high charge density break down the hydrogen bonds among water molecules and interact with water molecules through strong electrostatic interactions which give a more ordered water structure. Kosmotropes are known as structure makers. On the other hand, for large ions (chaotropes) with low charge density, the electrostatic interactions are smaller, and water structure in the vicinity of the ion is largely determined by water-water hydrogen bonding in the first shell around the ion. Chaotropes are known as structure breakers (Hribar, Southall, Vlachy & Dill, 2002). Furthermore, neutral salts alter the surface tension of water by changing the hydrogen bonding among water molecules. Structure making ions are responsible for increasing the surface tension of the solution (Nakai & Li-Chan, 1988). On the other hand, structure breaking ions are responsible for lowering the surface tension of the solution (Lewin, 1974).

2.4. Hofmeister effects on proteins

2.4.1. Protein in aqueous solution

2.4.1.1. Types of interaction

Protein unfolding occurs due to conformational entropy which is an important component of the free energy of protein association, while proteins are stabilized by numerous molecular interactions including hydrogen bonding, hydrophobic interactions, van der Waals interactions, and electrostatic interactions. Thus, stabilization of protein in an aqueous solution is a delicate balance between conformational entropy and molecular interactions. The native protein conformation is affected in the presence of stabilizer or denaturant (neutral salts in the Hofmeister series) as the stabilizer and denaturant alter molecular interactions (Frederick, Marlow, Valentine & Wand, 2007; Ghelis & Yon, 1982).

2.4.1.2. Protein conformation

Hydrophobic interactions between the nonpolar amino acids of a protein and water molecules have a dominant role in determining protein conformation (Engel, Drobney & Reid, 2008). In protein aqueous solution, the water structure is subject to change and the entropy decreases. So, the nonpolar groups of a protein tend to combine together to reduce the water contacting surface area which ultimately solves the problem of unfavourable entropy change. Therefore, the protein chain is folded in such a manner that the nonpolar or hydrophobic groups remain inside and the polar or hydrophilic groups remain outside giving protein a stable structure (Gunton, Shiryayev & Pagan, 2007; Tanford, 1980).

Hydrogen bonding and van der Waals interactions contribute to protein conformation (Dill, 1990). The secondary structure of protein is a consequence of hydrogen bonding. As polypeptide chains consist of numerous hydrogen donors and oxygen and nitrogen receptors, they have the ability to interact with water surroundings through hydrogen bonding (Gunton, Shiryayev & Pagan, 2007). In addition, electrostatic interactions contribute to protein conformation as the fully charged amino acid residues, side chains, and partially charged atoms can interact with each other and any free ions in the solvent as well. The energy of electrostatic interactions, which is dependent on the quantity of charges and their distribution, can be defined through Coulomb's law (Ghelis & Yon, 1982).

2.4.2. Effect of neutral salts on the solubility of protein

Protein-solvent interactions determine the stability of a protein in a solution. The solubility of a protein in solution increases when protein molecules interact with the surrounding solvent molecules. On the other hand, the solubility of proteins decreases when protein molecules interact with each other instead of interacting with the solvent molecules (Curtis & Lue, 2006). So, protein solubility is dependent on the nature of the surrounding environment.

2.4.2.1. Hydrophobic and hydrophilic properties of protein-water interface

Neutral salts in the Hofmeister series have effects on protein solubility and protein conformational change as a function of protein-water interfacial tension. Kosmotropes increase the hydrophobicity of protein-water interfaces, and chaotropes increase the hydrophilicity of protein-water interfaces in an aqueous solution (Der, 2008). At high

concentrations, anionic kosmotropes are excluded from interfaces causing an increase in the interfacial tension. In contrast, at high concentrations, anionic chaotropes are accumulated at the interfaces causing a decrease in the interfacial tension (Der, 2008; Manciu & Ruckenstein, 2003). These impacts of kosmotropes and chaotropes can be explained by the water structure making property of anionic kosmotropes and water structure breaking properties of anionic chaotropes (Cacace, Landau & Ramsden, 1997, Der, 2008). In addition, salts can also alter the existing electrostatic interactions among macromolecules such as proteins (Fennema, 1993). According to Machado and coworkers (2007), salt addition alters both the water structure and the protein conformation in a protein aqueous solution to cause either salting in or salting out of the protein.

2.4.2.2. Salting in of protein

The phenomenon of increasing protein solubility in the presence of salt is known as salting in. Salting in of protein occurs because of electrostatic interaction between salt ions and the dipole moment of the peptide group (Nandi & Robinson, 1972; von Hippel & Schleich, 1969). At its isoelectric point, a protein molecule has no net charge, and the solubility of the protein is minimal in the absence of additional ions. Salting in of the protein happens if the net charge of protein increases because of binding of ions to the protein. Therefore, the overall solubility of the protein is increased (Collins, 2004). Following the descending order of the Hofmeister series, ions exhibit their effectiveness in salting in (Nandi & Robinson, 1972; Robinson & Jencks, 1965; Schrier & Schrier, 1967). The specificity of the interaction between ion and dipolar molecule is a matter of controversy (Baldwin, 1996). For instance, according to Nandi and Robinson (1972),

this interaction is ion specific whereas Hamabata & Hippel (1973) argue that this type of interaction is non-specific. According to Lund, Va´cha and Jungwirth (2008), the binding of specific ions with macromolecules depends on the surface property of the macromolecules. For example, iodide ion, which is a poorly hydrated ion, interacts with hydrophobic surfaces, and iodide ion binding is preferred if a positively charged group resides under the macromolecular surface. Again, highly solvated fluoride ion binding occurs by specific anion-cation interactions. Fluoride ion preferably binds with macromolecules with high surface charge density. Lund, Va´cha and Jungwirth (2008) have proposed that the specific ion binding is the result of hydrophilic and hydrophobic interactions.

2.4.2.3. Salting out of protein

Salting out of a protein can be defined as the precipitation of protein upon addition of neutral salts or ions. The nature of the ion and its position in the Hofmeister series determines the effectiveness of ions in salting out. Anions are more effective in the Hofmeister series following the decreasing order such as SO_4^{2-}> HPO_4^{2-}> CH_3COO^-> Cl^-> Br^-> I^-> SCN^- than cations in the Hofmeister series such as Li^+> Na^+> ~ K^+> NH_4^+> Mg^{2+} (Curtis & Lue, 2006). According to Collins and Washabaugh (1985), divalent ions and ions with small hydrated radii are typically more effective than monovalent ions and large ions. The effectiveness of ions in salting out also depends on the pH of the solution and the pI of the respective protein. When the pH of the solution is above the pI of the protein, salting out efficacy of ions rises according to the ion's position in the ascending Hofmeister series. Ions interact with water molecules, and this inhibits the formation of hydrogen bonds between water molecules and the protein

exterior, therefore, protein-protein interactions occur which leads to protein precipitation (Collins, 2004). In contrast, when the pH of the solution is below the pI of the protein, salting out by anions occurs according to the reverse Hofmeister series. In the presence of SCN^-, the protein lysozyme was highly precipitated while it was scarcely precipitated in the presence of SO_4^{2-} (Finet, Skouri-Panet, Casselyn, Bonnete & Tardieu, 2004; Pan & Glatz, 2003; Rieskautt & Ducruix, 1989). It is considered that salting out of protein is "correlated with the surface tension increment of the salt" in a positive manner (Curtis & Lue, 2006).

2.4.3. Effect of neutral salts on the heat capacity of aqueous protein solutions

The heat capacity is a thermodynamic property which describes the response of a system in terms of temperature to heat flow. Heat capacity can be measured by differential scanning calorimetry (DSC) (Engel, Drobney & Reid, 2008). The heat capacity increases when protein denaturation occurs. One possible reason is the exposure of originally buried hydrophobic groups to water and this condition is energetically unfavourable, therefore energetically favourable cluster formation occurs; as a result, additional heat is necessary for destruction of these clusters (Sochava & Smirnova, 1993). Ions in the Hofmeister series which are responsible for salting in, such as I^- and SCN^-, are known as denaturants as they preferably interact with the peptide group of an unfolded protein (Hippel & Wong, 1964; Jencks, 1987). Oppositely, ions responsible for salting out are known as stabilizers. According to Penkova and coworkers (1996), at intermediate concentrations (20-500 mM), neutral salts in the Hofmeister series either stabilize or destabilize protein calf skin collagen to some extent. So, it can be assumed

that neutral salts in the Hofmeister series have an impact on the change in heat capacity of protein on unfolding.

The heat capacity of a protein depends on the distribution of different atoms in the protein interior. Hydration of nonpolar groups has a positive contribution (responsible for an increase in heat capacity), and hydration of polar or charged groups has a negative contribution (responsible for a decrease in heat capacity) to the change in heat capacity on protein unfolding. Therefore, a large number of nonpolar groups in the protein interior is responsible for a large heat capacity change on protein unfolding. On the other hand, hydration of polar and charged groups is responsible for reduction of the heat capacity change (Dadarlat & Post, 2003; Lladze, Ermolenko & Makhayadze, 2001). Recently, Lee and coworkers (2005) experimentally proved that electrostatic interactions have a negative role in the change in heat capacity. They showed that mutation of charged amino acids Glu6, Lys9 and Agr 92 to neutral amino acids in the thermophilic ribosomal protein of Thermococcus celer (L30e) significantly decreased its thermostability and increased the change in heat capacity of unfolding. There is evidence that hydrophobic interactions which arise due to water properties contribute to the large heat capacity change (Dill, 1990). In addition, hydrogen bonding, which is affected by temperature or denaturant, also contributes to the change in heat capacity on protein unfolding. At high temperature, the number of protein-water hydrogen bonds decreases and concomitantly the change in heat capacity on protein unfolding is increased (Cooper, 2000).

2.4.4 Studies on salt impact on bovine serum albumin conformation

Yamasaki and co-researchers (1991) studied the impact of neutral salts in the Hofmeister series on the conformational transition of BSA (bovine serum albumin) with respect to pH and ionic strength using the differential scanning calorimetric method. Observing the enthalpy of thermal denaturation (ΔH) and temperature of denaturation (T_d), they noticed that at pH range 3.5 – 8 and at a concentration 0.01 M, NaSCN has higher BSA stabilizing potential than that of NaCl. The major anion binding site in BSA is attributable to arginine residues, and among 23 arginyl residues of BSA one-fourth is present in the Arg 184 – Arg 216 fragment which contains Trp 212. After binding with anions, electrostatic repulsive forces on BSA were reduced and the denaturation temperature and the enthalpy of thermal denaturation were increased. Again, at pH 7, Yamasaki and co-researchers (1991) compared the efficacy of several salts including NaCl, NaBr, NaI, NaSCN, $NaSO_4$ and $NaClO_4$ on restraining the heat-promoted conformation transition and in enhancing thermostability at ionic strengths of 0.01 and 0.1, and the ranking of anions were $ClO_4^- \geq SCN^- > I^- > SO_4^{2-} > Br^- > Cl^-$ and $ClO_4^- \geq SCN^- > I^- > Br^- > Cl^- > SO_4^{2-}$ for ionic strengths of 0.01 and 0.1, respectively. Therefore, at low and moderate concentrations, chaotropic salts behave as stronger thermo-stabilizers than kosmotropic salts. On the basis of T_d measurements, at high salt concentrations (1 - 3 M), chaotropes act as a BSA thermo-destabilizer and kosmotropes act as a BSA thermo-stabilizer (Damodaran, 1989).

3. Materials and Methods

3.1. Introduction

The principle of a scientific study is accuracy. In order to ensure that samples were prepared accurately and precisely, viscosity measurement of samples was performed. When experimental viscosity data were similar to those of the literature, it was confirmed that the sample preparation procedure was acceptable. Afterwards ultrasound velocity and attenuation measurement of aqueous salt solutions, bovine serum albumin solutions, and mixtures of salt and bovine serum albumin solutions were measured to analyse protein conformation in the presence of potassium salts of the Hofmeister series. For the purpose of this study the specific materials and methods considered are discussed in the following sections.

3.2. Materials

3.2.1. Chemicals and reagents

The chemicals and reagents utilized for experiments are described in the **Table 3.1.** The purity of KCl, KBr, KI, KSCN, KCOOH, $KCOOCH_3$ salts were ≥ 99.0%, the purity of KF was ≥99.5%, and the purity of Bovine serum albumin was ≥96%.

3.2.2. Equipments

The equipments utilized for the research are presented in **Table 3.2.**

Table 3.1. Chemicals and reagents

Chemicals and Reagents	Molecular Weight	Providers
Bovine Serum Albumin (BSA)	~66 kDa	Sigma-Aldrich, Oakville, ON
Potassium Chloride	74.55	Sigma-Aldrich, Oakville, ON
Potassium Bromide	119.01	Sigma-Aldrich, Oakville, ON
Potassium Fluoride	58.10	Sigma-Aldrich, Oakville, ON
Potassium Iodide	166.01	Sigma-Aldrich, Oakville, ON
Potassium Thiocyanate	97.18	Sigma-Aldrich, Oakville, ON
Potassium Formate	84.12	Sigma-Aldrich, Oakville, ON
Potassium Acetate	98.14	Sigma-Aldrich, Oakville, ON
Chromerge solution		Fisher Scientific
Milli Q water		Department of Food Science, University of Manitoba

Table 3.2. Equipments

Equipment	Providers or Manufacturers
Ubbelohde viscometer	Fisher Scientific, Whitby, ON
Pipette filler or bulb	Fisher Scientific, Whitby, ON
0.45 μm PTFE filer units	Fisher Scientific, Edmonton, AB
3 mL Syringes	Fisher Scientific, Edmonton, AB
Stop watch or timer clock	Fisher Scientific, Whitby, ON
Volumetric flasks	Fisher Scientific
20 mL glass pipette	Fisher Scientific
100 and 1000 μL Micropipette	Eppendorf
Mettler AE 200 Balance	Mettler Instrument, Switzerland
Mettler PM 4600 DeltaRange Balance	Department of Food Science, University of Manitoba
Weighing balance S-234	Denver Instrument
Vacuum pump Edwards 8	Czech Republic by Edwards Manor Royal
Hamilton gastight syringe	Hamilton company, Switzerland
Resoscan system	TF Instruments Inc., Germany
Anton-Paar DMA 5000 M Density Meter	Anton-Paar High Precision Instruments, USA
Milli-Q^{TM} water system	Fisher Scientific
Water bath with precision temperature controller PTC-41	Tronac Inc., Orem, Utah
TJ style thermistor probe	Omega
Hot plate or magnetic rotator	Fisher Scientific

3.3. Methods

3.3.1. Viscosity measurement

The relative viscosities of KCl and KBr solutions were measured for eight different concentrations (1mM, 2.5 mM, 5.0 mM, 10 mM, 25 mM, 50 mM, 100 mM, and 250 mM) at 25 ^{o}C and were compared with the relative viscosity calculated from the Jones-Dole empirical expression of relative viscosity (Jenkins & Marcus, 1995). The relative viscosity of aqueous electrolyte solution at a certain concentration can be determined using the Jones-Dole empirical expression (Jenkins & Marcus, 1995):

$$\eta/\eta_o = 1 + Ac^{1/2} + Bc + Dc^2 \quad (34)$$

where η is solution viscosity, η_o is water viscosity, c is concentration in mol.dm^{-3}, and A, B, and D are coefficients which depend on the solute, solvent and temperature.

3.3.1.1. Solution preparation

The weight of KCl and KBr salts from Sigma-Aldrich was measured in a balance whose precision (d) was 0.1 mg. For concentrations of 1mM, 2.5 mM, 5.0 mM, 10 mM, 25 mM, 50 mM, 100 mM, and 250 mM, salt solutions were prepared using 500 ml, 500 ml, 250 ml, 100 ml, 100 ml, 50 ml, 50 ml, 50 ml volumetric flasks with glass stoppers respectively, in order to get maximum accuracy. Millipore water (deionized distilled water through a milli Q system with resistivity less than 10 mega-ohms per centimeter) was used for up making all solutions. Before solution making, the viscosities of the Millipore water from one laboratory and the Millipore water from another laboratory were measured and the viscosities were compared with each other.

For the purpose of making an accurate solution, salts were weighed on weighing paper, and then the weighed salts were transferred directly to the respective volumetric flasks. A small amount of water was added to dissolve the salts. Then, more water was added, approximately up to the middle of the volumetric flask, and the volumetric flask was shaken up and down 25 times or more to ensure dissolution. Then more water was added up to the volumetric flask mark, and again the flask was shaken 50 times or more to ensure a homogeneous solution. As viscosity is highly sensitive to dust particles and bubbles (Cannon Instrument Company; Heintz, Klasen, and Lehmann, 2002), dust and bubbles were removed from the solution. To remove dust particles from solution, solutions were filtered using 0.45 μm PTFE filter units from Fisher Scientific under a laminar flowhood. To get rid of bubbles, the beaker containing the solution was placed in a vacuum chamber attached to a vacuum pump, with pumping speed 8.0 $m^{3}{\cdot}hr^{-1}$, which was run until all the bubbles had been removed, and no bubble nucleation was observed.

3.3.1.2. Measurement

Liquid viscosity is highly sensitive to temperature (Franks, 1988). Thus, viscosity of the solutions was measured in a water bath with a precision temperature controller PTC-41 which can control temperature to within 0.001 ^{o}C. For viscosity measurement of KCl and KBr salt solutions, an Ubbelohde viscometer from Fisher Scientific with size 0C and with an uncertainty of 0.16% was used. For the purpose of attaining an accurate result, the reading for the lowest concentrated solution was taken first. The viscometer was filled and washed with the solution of a specific concentration two times, and then the

sample solution to be analysed was poured into the viscometer to fill between the recommended two lines ‘G’ and ‘H’.

Then, the solution in the viscometer was kept in the water bath whose temperature was very close to 25 ^{o}C for 25 to 30 minutes to attain an equilibrium temperature. The average temperature of the water bath holding the viscometer was 25.09 ^{o}C ± 0.022 and 25.09 ^{o}C ± 0.011 while measuring the viscosity of KCl and KBr aqueous solutions, respectively. Then, by placing a finger on the ‘M’ tube, the solution was sucked through the ‘N’ tube using a pipette bulb up to the center of bulb D of the viscometer. Then, the solution was left to flow down freely, and the efflux time was measured by starting the stopwatch as soon as the meniscus of the solution came to the E line which is above the ‘C’ bulb and by stopping the stopwatch as soon as the solution meniscus came to the ‘F’ line which is below the ‘C’ bulb. The kinematic viscosity was calculated by multiplying the efflux time in seconds by the viscometer constant.

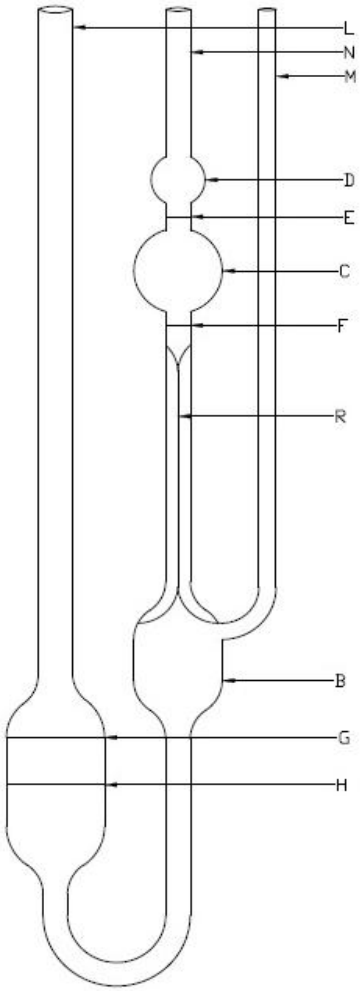

Figure 3.1. Ubbelohde viscometer used in viscosity measurement

The dynamic viscosity was calculated by multiplying the kinematic viscosity with the solution density in $g.cm^{-3}$. Density for each concentration was taken from the literature (Kirino, Yokoyama, Hirono, Nakajima, and Nakashima, 2009; Nikam and Sawant, 1997; Out and Los, 1980). Then, the relative viscosity of the solution was calculated by dividing the dynamic viscosity of the solution by the dynamic viscosity of water at the measured temperature. The dynamic viscosity of water for corresponding temperature was determined using an equation taken from the CRC Handbook of Chemistry and Physics (Weast, 1988-1989):

$$\log_{10} \eta_T/\eta_{20} = [1.3272\ (20 - T) - 0.001053\ (T - 20)^2] \div (T + 105) \quad (35)$$

where η_T is the viscosity of water at temperature T ^{o}C, η_{20} is the viscosity of water at 20 ^{o}C which is 1.002 mPa.s, T is temperature in degree Celcius (Weast, 1988-1989). The temperature was monitored using a TJ style thermistor probe (model no.TJ36.44033-1/8-12). One metal end of the probe was inserted into the water bath, and the resistance, which is corresponding to a specific temperature of the water bath, was shown on the thermistor probe reading screen.

The viscometer was cleaned periodically with Chromerge solution and was washed with distilled water. After each day's analyses, the viscometer was washed with distilled water and was filled with Millipore water until the analyses of the next day.

3.3.2. Ultrasound velocity and attenuation measurement

3.3.2.1. Salt solution preparations

For preparation of KCl and KBr solutions a similar procedure was followed as solution preparation for viscosity measurements and the prepared solutions were kept overnight to ensure homogeneity. One additional change was performed for ultrasound velocity measurements. The prepared solutions were weighed before and after degassing or bubble removing, and from the difference between the weights the amount of water loss from solutions was calculated. Afterwards, an equivalent amount of degassed water was added slowly to the solutions using both 100 and 1000 µL micropipettes by touching the edge of beaker. The solutions were then mixed gently and kept for one to one and half hours on the bench to ensure homogeneity.

Since some salts were hygroscopic, to weigh accurately a beaker was used instead of weighing paper for the rest of the salts including HCOOK, KI, KF, KSCN, and CH_3COOK. Moreover, for KF, 100 mM and 250 mM solutions were made in a 100 mL volumetric flask and for KSCN and CH_3COOK salts 50 mM, 100 mM and 250 mM solutions were prepared in a 100 mL volumetric flask. All the changes were done in order to get accurate and repeatable values of measurement. Three replicates were prepared for every concentration.

3.3.2.2. Preparation of solutions containing salts and BSA

For the purpose of preparation of solutions containing salts and bovine serum albumin protein, salt solutions and BSA solutions were prepared separately. For salt solutions, potassium halides (KCl, KBr, KI, and KF) were chosen. Potassium halide solutions of concentrations of 400 mM, 200 mM, 100 mM, and 50 mM were prepared for mixing with BSA solutions of 2.4 mM, 1.2 mM, 0.6 mM, and 0.3 mM, respectively. All the solutions were prepared in 100 mL volumetric flasks. For preparation of BSA solutions, bovine serum albumin was weighed into a beaker using a Mettler AE 200 Balance with a precision of 0.1 mg. After that a small amount of milli Q water was added to the BSA and a magnetic stirrer bar was placed in the beaker. The beaker containing protein, water and magnetic stirrer bar was placed on a magnetic rotator and stirring was maintained until all the BSA was dissolved. Next the dissolved BSA was transferred to a 100 mL volumetric flask with the aid of a glass rod. The beaker was washed repeatedly with milli Q water and poured into the volumetric flask, and then water was added up to the volumetric flask mark. The volumetric flask was shaken more than 50 times to prepare a homogeneous solution and the protein solution was kept at 4 ^{o}C overnight. The

following day the protein solutions were left on the bench for 1-2 hours to reach room temperature-around 22 ^{o}C. During this period of time, the salt solutions, which were made up on the previous day, were filtered through 0.45 μm filter units into beakers under a laminar flowhood. The beakers were covered with paraffin paper. At that point, 40 mL of the BSA solution was mixed with 40 mL of potassium halide solution and the mixture was stirred up and down more than 70 times. For the purpose of adding salt solutions to protein solutions 20 mL glass pipettes were used. Then, water was added up to the mark to reach 100 mL volume and again stirred up and down more than 50 times. Following preparation of protein- salt solutions, the solutions and filtered milli Q water were degassed using a vacuum pump. The protein-salt solutions were weighed before and after degassing, and from the difference of weight, the loss of water during degassing was calculated. Then the equivalent volume of degassed water was added and left on the bench for one and half hours to attain homogeneity. Thus, the final concentrations of (salts + BSA) solutions were (160 mM + 0.96 mM), (80 mM + 0.48 mM), (40 mM + 0.24 mM), and (20 mM + 0.12 mM). Two replicates of these solutions for four potassium halides were prepared and these 32 solutions were prepared randomly on different days. The random series for ordering of the experimental treatments was generated using a random sequence generator.

3.3.2.3. Ultrasound velocity measurement using Resoscan system

The Resoscan system measures the velocity of ultrasound propagating through the solution by a resonator method. The system has a Peltier metal block thermostat which can maintain constant temperature within the samples with a precision of ± 0.003K and the resonator system has two cells made of titanium and gold for samples of volume 200

μL. Using this resonator system, the velocity of sound in water can be measured with precision of ± 1cm.s^{-1} and at room temperature, the sound velocity in water differs by approximately 3m.s^{-1}.K^{-1}(TF Instruments, Inc.). The operating frequency for this system is 7.5 to 9.5 MHz. The system is also capable of measuring ultrasonic attenuation, which is a measure of the reduction in the amplitude of the sound waves or the loss of energy of sound waves (TF Instruments, Inc.). The losses of energy occur at two levels: absorption or losses at a molecular level which comprises viscosity, thermal conductivity, relaxation processes, and transfer of mechanical energy to molecular levels, and attenuation or energy losses because of geometric wave effects comprised of reflection, scattering, and diffraction (TF Instruments, Inc.; McClements, 1991). The range of ultrasonic velocity and attenuation that can be quantified by this very precise system is 1100 to1900 ms^{-1} and 10^{-14} to 10^{-13} s^2.m^{-1} (TF Instruments, Inc.).

At the beginning of a series of experiments it is necessary to check whether the cells are clean enough to perform experiments. In order to wash the cells properly, the milli Q water from the reference cell was aspirated with Reso Pump I (the pump provided with the Resoscan system) and milli Q water was reinserted. These steps were repeated for several times. Then following the same procedure on the reference cell, both cells (the reference cell and the sample cell) were filled with degassed milli Q water. To check cleanliness of the cells, measurement of ultrasound velocity in degassed milli Q water in both cells was performed regularly before each set of experiments. For the purpose, a 250 μL Hamilton syringe was rinsed with distilled water several times and then with degassed milli Q water three times. After that, the syringe was carefully filled with degassed milli Q water up to 200 μL to avoid any bubble inside which might give an

erroneous result and the degassed milli Q water was inserted into the reference cell. Then following the same procedure on the reference cell, the sample cell was also filled with degassed milli Q water and both cells were capped properly. The temperature of cells was selected to be 25 ^{o}C. After waiting for some time until the screen, Peltier Thermostat Control Unit (PTC) and Cell Temperature Measurement Unit (CMT) showed that the temperature was stable, the ultrasound velocity measurement was performed by choosing automatic peak selection. When the difference in velocity in degassed milli Q water between the two cells (the reference cell and the sample cell) was less than 0.05 m.s^{-1}, the cells were considered clean enough to proceed to further experiments. The reference cell was filled with degassed milli Q water as the blank (same water filled in from calibration) and the sample cell was filled with sample solution choosing the lowest concentrated solutions first followed successively by the higher concentrations. Before filling the sample cell with sample the syringe as well as the cell were filled and washed with the sample solution three times. The ultrasound velocity and attenuation of the sample was then measured.

When the velocity difference between the reference cell and the sample cell was more than 10 m.s^{-1}, then active initialization was performed. Doing active initialization, the correct resonance peak and its frequency were selected automatically. All the measurements were performed at 25 ^{o}C. At the end of the measurements on a given day, measurement of ultrasound velocity in milli Q water within the two cells was again performed to check cleanliness of the cells.

In the case of salt solutions, the syringe and the sample cell were washed three times, and the syringe filled for the fourth time with salt solution was considered as the sample.

Moreover, in case of solutions of the salt and BSA mixture, the syringe and the sample cell were washed with respective solution seven times and the eighth one was considered as the sample. For each solution, three samples were considered which were termed as subsamples and between subsample readings the sample cell was washed three times. Active initialization was performed in the case of (salt + BSA) solutions of concentrations (160 mM + 0.96 mM) and (80 mM + 0.48 mM) compositions.

3.3.3. Density measurement

3.3.3.1. Preparation of solutions containing salts and BSA

This was conducted exactly as described in section *3.3.2.2.*

3.3.3.2 Density measurement using DMA 5000 M density meter

The density of solutions containing salts and BSA at 25 ^{o}C were measured using a DMA 5000 M density meter (Anton-Paar High Precision Instruments, USA) which uses a small volume sample of 1 mL and gives fast, consistent results with an accuracy up to 0.000005 g.cm^{-3}. The density meter has a well-controlled thermobalance, thus accurate density measurements are possible at a range of temperatures.

At the beginning of a series of experiments, a water check was performed by filling the U-tube with deionized water to check the cleanliness of the measuring U-tube. If water check was passed, it infers that the measuring tube is clean enough to start experimental measurements. Then, the tube was filled with ethanol and was allowed to air-dry by pressing the dry symbol on the density meter screen. In order to check the dryness of the tube, an air check was performed. When the air check was passed, the measuring tube

was filled with the first sample solution of the lowest concentration after slowly (to avoid bubbles) withdrawing an aliquot of the sample solution using a 3 mL syringe. As soon as the temperature was stable, the density measurement was commenced by pressing the start option on the screen. Three subsamples were considered for each solution, and between each subsample readings, the measuring U-tube was washed twice with the sample, considering the third one as the subsample of sample solution. After each sample solution measurements the U-tube was washed thoroughly with deionized water followed by performing a water check and an air check similarly to the treatments conducted at the beginning of an experimental set.

4. Results and Discussion

4.1. Analysis of viscosity measurements

4.1.1. Measurement of water viscosity

Viscosity of Millipore water from two sources was determined in order to check the reliability of water. One source of Millipore water was from the department of Food Science, and another source of Millipore water was the department of Biosystems Engineering, University of Manitoba. The dynamic viscosity of water was calculated from the kinematic viscosity considering the density of water to be 0.997 $g.cm^{-3}$ at 25 ^{o}C (James, Mulcahy, and Steel, 1984; Kirino, Yokoyama, Hirono, Nakajima and Nakashima, 2009). From each water source two subsamples were tested, and four readings were taken for each subsample. The standard deviations for both temperature and dynamic viscosity were calculated taking account of these four readings of the two subsamples. The temperature of measurement and the dynamic viscosity for both water sources together with standard deviations are given in **Table 4.1**. From the table it is evident that water from both sources gave similar results.

Table 4.1. Dynamic viscosities of water from two different sources. Errors represent standard deviations

Water source	Average temperature in (^{o}C)	Average dynamic viscosity (mPa.s)
1	25.109 ± 0.0084	0.886 ± 0.00029
2	25.104 ± 0.0053	0.886 ± 0.00041

Therefore, Millipore water from source 1 was chosen for the rest of the experiment.

4.1.2. Measurement of viscosity of KCl and KBr solutions

Accurate measurement of relative viscosity of electrolyte solutions demands precision from the experimentalist in term of sample solution preparation (Jenkins and Marcus, 1995). Therefore, the experimental relative viscosities of KCl and KBr aqueous solutions were compared with the theoretical relative viscosity to guide development of good procedures of sample preparation and to have confidence in the experimental results. The kinematic viscosity of KCl and KBr solutions from a concentration range of 1 mmolar to 250 mmolar was measured using an Ubbelohohe 0C type viscometer. Then the dynamic viscosity of the solutions was calculated by multiplying kinematic viscosity by the density in $g.cm^{-3}$. For KCl and KBr solutions, density values were taken from the literature (Kirino, Yokoyama, Hirono, Nakajima and Nakashima, 2009; Nikam and Sawant, 1997; Out and Los, 1980). The relative viscosities for each solution were calculated by dividing the dynamic viscosity of the solution by the dynamic viscosity of water. Thereafter, a graph for the relative viscosity against concentration was plotted which was compared with the relative viscosities derived from the Jones-Dole empirical equation; A, B, D coefficients at 25 ^{o}C for KCl and KBr were taken from the literature (Out and Los, 1980). **Figure 4.1** and **Figure 4.2** represent the change in relative viscosities with concentration for KCl and KBr aqueous solutions, respectively. In both graphs, the points with error bars for experimental relative viscosity were calculated as the mean value of eight readings where the error bars are the standard deviation of the readings. Among these eight readings, four readings were from one replicate and another four readings were from another replicate of the sample solution.

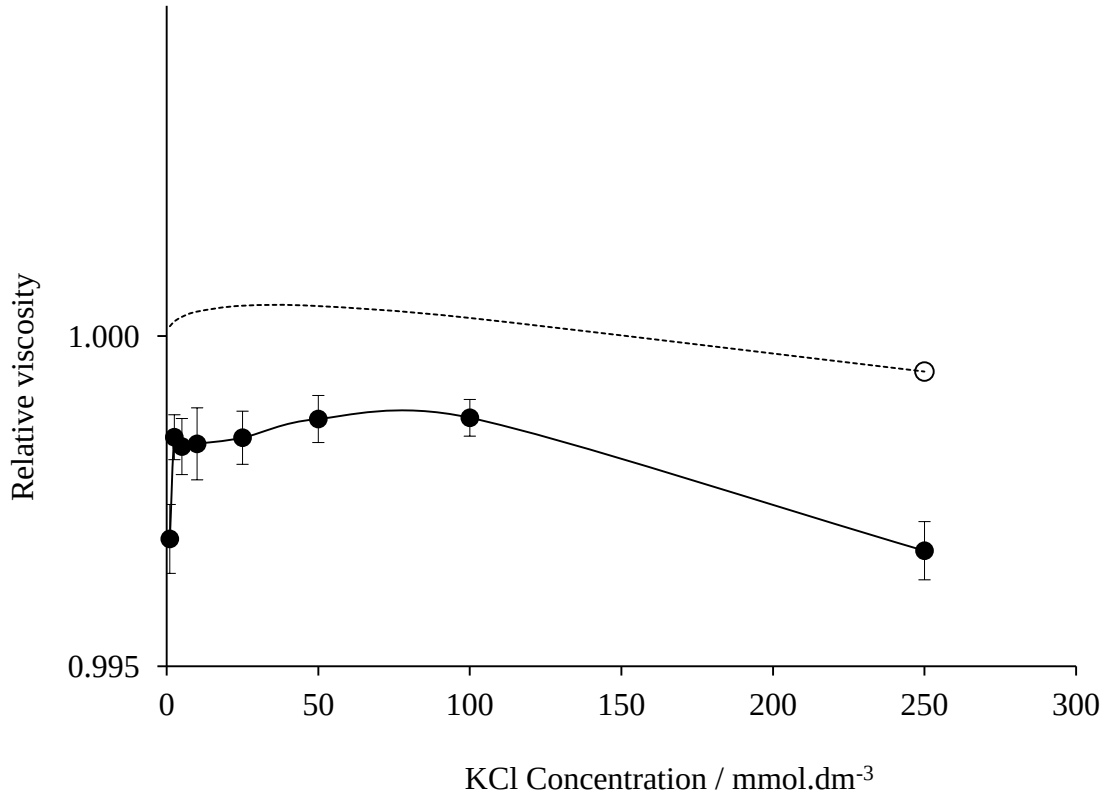

Figure 4.1. Relative viscosity of KCl against concentration. Solid line represents experimental relative viscosity and dotted line is for the Jones-Dole equation derived relative viscosity

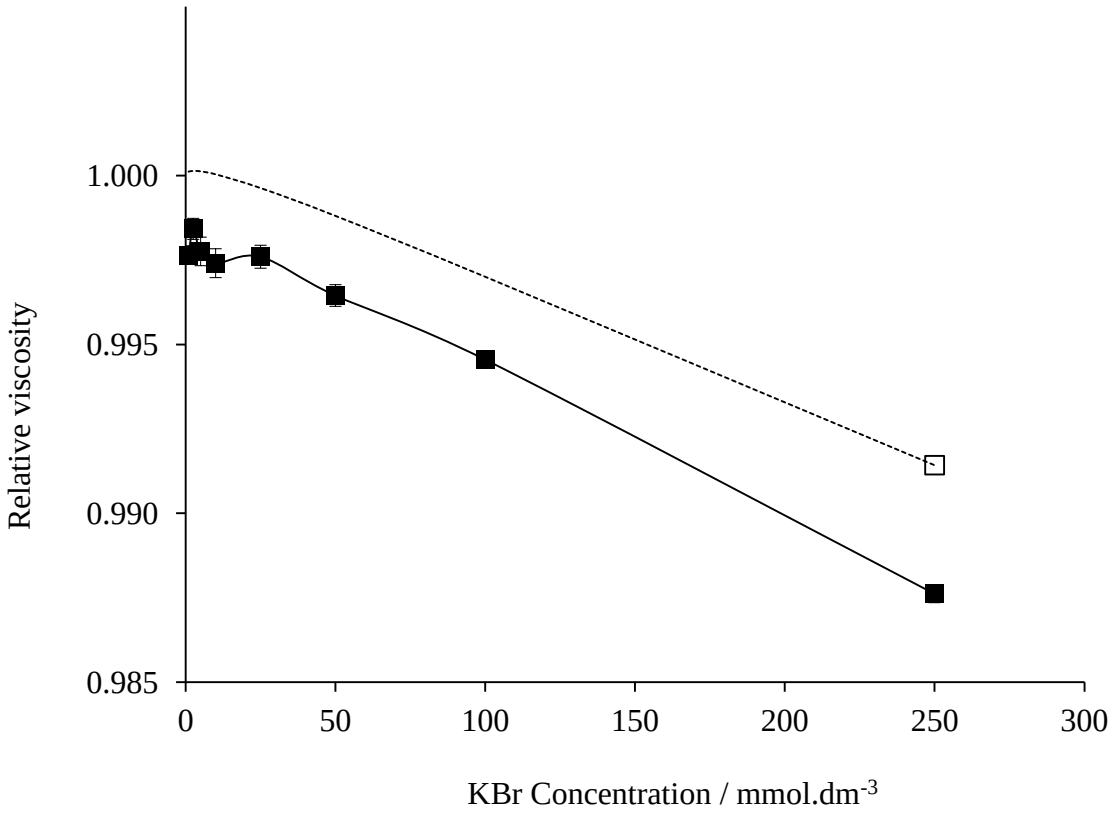

Figure 4.2. Relative viscosity of KBr against concentration. Solid line represents experimental relative viscosity and dotted line is for the Jones-Dole equation derived relative viscosity

The average temperature of the water bath holding the viscometer was 25.09 ^{o}C ± 0.022 and 25.09 ^{o}C ± 0.011 while measuring the viscosity of KCl and KBr aqueous solutions, respectively. From both **Figure 4.1** and **Figure 4.2**, it is evident that the experimental relative viscosity of KCl and KBr aqueous solutions have similar curve patterns as the curves of theoretical Jones-Dole equation derived relative viscosity. Within the used concentration range for both the KCl and KBr aqueous solutions, relative viscosity increased slightly with concentration increase. This was followed by a decrease in relative viscosity with further increase in concentration. The phenomenon of decreasing relative viscosity with increase in concentration might be due to the ability of ions from KCl and KBr to increase the mobility of water.

The curve for experimental relative viscosity resides in a slightly lower position than the curve for theoretical relative viscosity in the case of both the KCl and KBr aqueous solutions. One possible reason might be the temperature of the water bath was very slightly higher than the temperature measured by the thermistor probe. The relative viscosity of a solution depends on the dynamic viscosity of water (the dynamic viscosity of water at the temperature measured by the thermistor probe was used to calculate the relative viscosity of a solution). If the temperature was higher, the dynamic viscosity of water would be lower; as a result, the relative viscosity of the solution would be higher (Jenkins and Marcus, 1995).

Specific viscosity provides information about a solute's ability to increment the viscosity of a solution. Therefore, the specific viscosity of solutions of a number of potassium salts gives a comparative explanation among the salts in terms of their viscosity increment to the solution. The specific viscosity for six potassium salts, including potassium halides, potassium acetate, and potassium formate, was calculated using the following equation (Collins, 1997):

$$\eta/\eta_o - 1 = Ac^{1/2} + Bc \tag{36}$$

$$\eta_{sp} = Ac^{1/2} + Bc \tag{37}$$

where $\eta_{sp} = \eta_r - 1$, and refers to specific viscosity. The A and B coefficients were taken from the literature (Banipal et al., 2008; Chmielewska, Stasiewicz and Bald, 2005; Desnoyers and Perron, 1972). **Figure 4.3** presents the specific viscosities of six potassium salts against concentration.

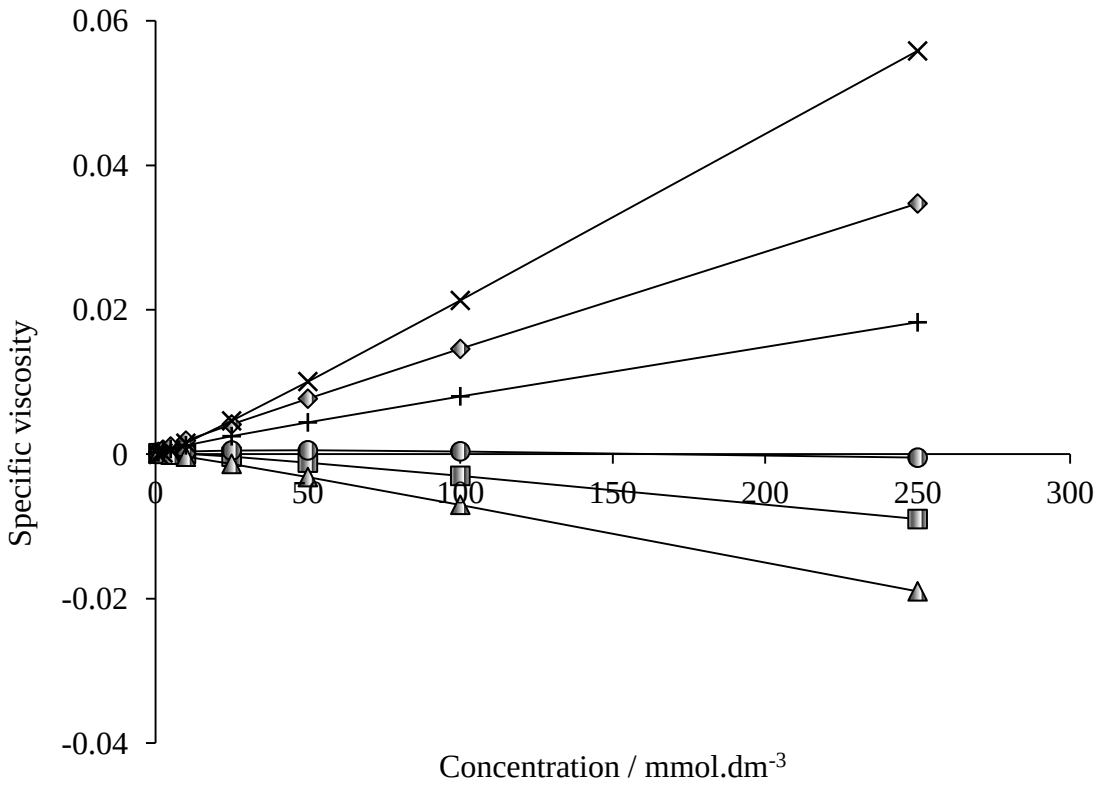

Figure 4.3. Specific viscosities of six potassium salts against concentration. Potassium acetate (cross sign), potassium fluoride (gradient diamond), potassium formate (plus sign), potassium chloride (gradient circle), potassium bromide (gradient square) and potassium iodide (gradient triangle)

Considering **Figure 4.3**, it can be said that potassium acetate has the highest capacity to increase the viscosity of a solution with increase in concentration. Potassium fluoride has the next highest ability to increase solution viscosity, and potassium formate has a lower ability to raise solution viscosity than potassium fluoride. In the case of potassium chloride, specific viscosity slightly increases up to a concentration of 100 $mmol.dm^{-3}$ followed by a slight decrease in specific viscosity with solution concentration increase (as seen in more detail in **Figure 4.1**). Potassium bromide decreases specific viscosity with increase in solution concentration while among the six potassium salts, potassium iodide shows the highest decrease in the specific viscosity. Since potassium acetate,

potassium fluoride and potassium formate cause viscosity to increase, this provides agreement with the statement that ions with large charge density bind water molecules tightly and reduce the mobility of surrounding water molecules. Thus, the kosmotropic nature of potassium acetate, potassium fluoride and potassium formate is obvious. In contrast, potassium iodide, potassium bromide and potassium chloride cause a reduction in solution viscosity because ions with small charge density bind water molecules loosely and enhance the mobility of surrounding water molecules. Therefore, the chaotropic nature of potassium iodide, potassium bromide and potassium chloride is also evident (Collins, 1997).

4.2. Analysis of ultrasound velocity and attenuation measurement

4.2.1. Precision of measurement in terms of velocity and attenuation

At the beginning of each day's measurements, sound velocity and attenuation in Milli Q water was measured after filling both cells of the Resoscan system to give separate velocity and attenuation readings from the two different cells. **Table 4.2** presents the ultrasound velocity and attenuation values with standard deviation in Milli Q water on different days. The table also represents the average temperature with standard deviation while measuring the ultrasound velocity and attenuation.

Table 4.2. Ultrasound velocity and attenuation in Milli Q water while measuring potassium chloride aqueous solutions

Day	Average temperature (^oC)	Average velocity in cell 1 (m s^{-1})	Average velocity in cell 2 (m s^{-1})	Average attenuation in cell 1 (s^2 m^{-1})	Average attenuation in cell 2 (s^2 m^{-1})
1	24.98 ± 0.0004	1496.57 ± 0.00076	1496.58 ± 0.00063	1.23×10^{-14} ± 4.69×10^{-17}	1.45×10^{-14} ± 3.68×10^{-17}
2	24.99 ± 0.0006	1496.60 ± 0.00031	1496.62 ± 0.00045	1.27×10^{-14} ± 4.16×10^{-17}	1.48×10^{-14} ± 4.36×10^{-17}
3	25.02 ± 0.0003	1496.68 ± 0.00064	1496.69 ± 0.00052	1.26×10^{-14} ± 4.05×10^{-17}	1.56×10^{-14} ± 5.09×10^{-17}
4	25.00 ± 0.0005	1496.63 ± 0.00057	1496.64 ± 0.00068	1.25×10^{-14} ± 5.28×10^{-17}	1.47×10^{-14} ± 4.80×10^{-17}
5	25.01 ± 0.0000	1496.64 ± 0.00031	1496.64 ± 0.00033	1.24×10^{-14} ± 5.72×10^{-17}	1.50×10^{-14} ± 3.11×10^{-17}
6	25.01 ± 0.0000	1496.64 ± 0.00036	1496.64 ± 0.00031	1.21×10^{-14} ± 3.51×10^{-17}	1.44×10^{-14} ± 3.16×10^{-17}

The standard deviation of ultrasound velocity, attenuation and temperature were calculated from each day's readings. The ultrasound velocity in liquid water depends on the temperature. Observing **Table 4.2**, it can be said that the ultrasound velocity increases slightly with slight increase in temperature in both cell 1 and cell 2. The average difference of ultrasound velocity between cell 2 and cell 1 was 0.0062 ± 0.009 $m.s^{-1}$ which is very small. There was no noticeable correlation observed between temperature and ultrasound attenuation. The average difference of ultrasound attenuation between cell 2 and cell 1 was $2.41 \times 10^{-15} \pm 3.23 \times 10^{-16}$ $s^2.m^{-1}$. Thus, there appears to be a consistent discrepancy in attenuation between cell 1 and cell 2 with attenuation being higher in cell 2. As the standard deviations for temperature, ultrasound velocity and attenuation were very small, it can be mentioned that the ultrasound resonator was extremely precise in measuring those formerly mentioned parameters. **Table 4.3** denotes the literature value of sound velocity and attenuation in water at 25 ^oC. The sound

velocity in water found from the experimental ultrasound resonator method is identical to the sound velocity in water values taken from the literature, but the experimental values in this study have lower standard deviation in comparison with the literature values. The ultrasound attenuation in pure water at 25 ^{o}C that is included in **Table 4.3** was calculated using equation (38) (Fisher and Simmons, 1977). The value at 25 ^{o}C derived from the equation is about 40% higher than the average attenuation of 1.36 x 10^{-14} s^2.m^{-1} experimentally determined from both cells.

Attenuation at temperature T (^{o}C) = $(55.9 - 2.37T + 4.77 \times 10^{-2} T^2 - 3.48 \times 10^{-4} T^3)10^{-15}\ s^2\ m^{-1}$ (38)

Table 4.3. Comparison of literature values for velocity and attenuation of sound in water

Reference	Temperature (^oC)	Experimental method	Sound velocity ($m.s^{-1}$)	Sound Attenuation ($s^2.m^{-1}$)
Barlow and Yazgan (1966)	25	Phase change method	1496.58 ± 0.04	-
Brooks (1960)	25	Time delay, variable path 1-2 m	1496.52 ± 0.34	-
McSkimin (1965)	25	Modulated pulse cancellation	1496.65 ± 0.10	-
Williamson (1969)	25	Standard Phase-Comparison Technique	1496.65 ± 0.20	-
Fisher and Simmons (1977); Pinkerton (1947)	25	Pulse method	-	2.10×10^{-14}

Using the ultrasound resonator method, ultrasound velocity and attenuation of seven potassium salts were measured. For each salt, eight concentrations were considered, and for each concentration, readings were taken for three replicates, with three subsamples taken into account for each replicate. The coefficient of variation of subsamples was calculated for each concentration and then the average coefficient of variation for each salt was estimated. **Table 4.4** represents the average coefficients of variation for ultrasound velocity and attenuation for seven experimental aqueous salt solutions.

Table 4.4. Average coefficient of variation of ultrasound velocity and attenuation of aqueous salt solutions based on precision of subsample measurements

Aqueous salt solutions	Average coefficient of variation for ultrasound velocity (%)	Average coefficient of variation for attenuation (%)
KCl	0.0007	2.14
KBr	0.0003	1.63
KI	0.0003	1.79
KF	0.0003	1.51
HCOOK	0.0004	1.34
CH_3COOK	0.0004	1.36
KSCN	0.0004	1.51

From **Table 4.4,** it is evident that the ultrasonic resonator technique is very precise in measuring ultrasound velocity as the highest average coefficient of variation based on subsample measurement was 0.0007% for KCl aqueous solutions while the lowest average coefficient of variation based on subsample measurement was 0.0003% (3 ppm). In the case of ultrasound attenuation measurements, the ultrasonic resonator technique was less precise than for velocity measurement. The highest average coefficient of variation for ultrasound attenuation was 2.14% which was observed for KCl, and the lowest average coefficient of variation was 1.34% for potassium formate. Using the resonator method, many researchers attained an accuracy of relative measurements of ultrasonic velocity of about ± 10^{-4}%, and an accuracy of the relative measurements of ultrasonic attenuation of about ± 2% (Gekko and Hasegawa, 1986; Lee, Tikhomirova, Shalvardjian and Chalikian, 2008; Sarvazyan, 1982; Sarvazyan, 1991; Sarvazyan and Chalikian, 1991). The accuracy in terms of velocity and

attenuation from other researchers is similar to the experimental accuracy I have obtained in my measurements of the acoustic properties of salt solutions.

4.2.2. Ultrasound velocity and attenuation analysis for seven potassium salts

Figure 4.4 and **Figure 4.5** depict the change in ultrasound velocity and attenuation as a function of concentration for KCl aqueous solutions, respectively. The points in the figures are the mean value of three replicates with respective error bars. The error bars represent standard deviations. From **Figure 4.4,** it is obvious that the ultrasound velocity of aqueous KCl salt solutions increases with increasing concentration. Attenuation of aqueous KCl salt solutions increases with increasing concentration up to a concentration of 100 mmol dm^{-3}, and then the sound attenuation decreases with concentration. A second order polynomial curve has been drawn through the data of **Figure 4.5**. As such, the pattern of change in attenuation with increase in KCl concentration is similar to that of viscosity, as seen in **Figure 4.1**.

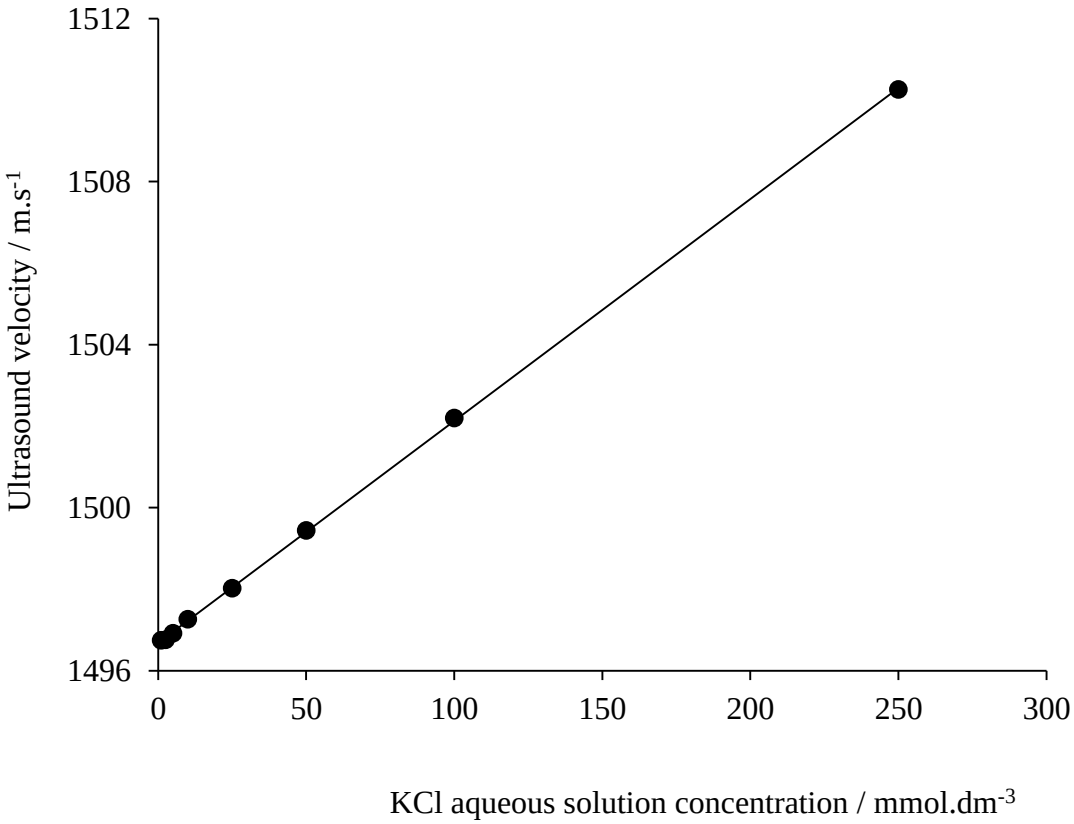

Figure 4.4. Ultrasound velocities of KCl aqueous solutions against concentration

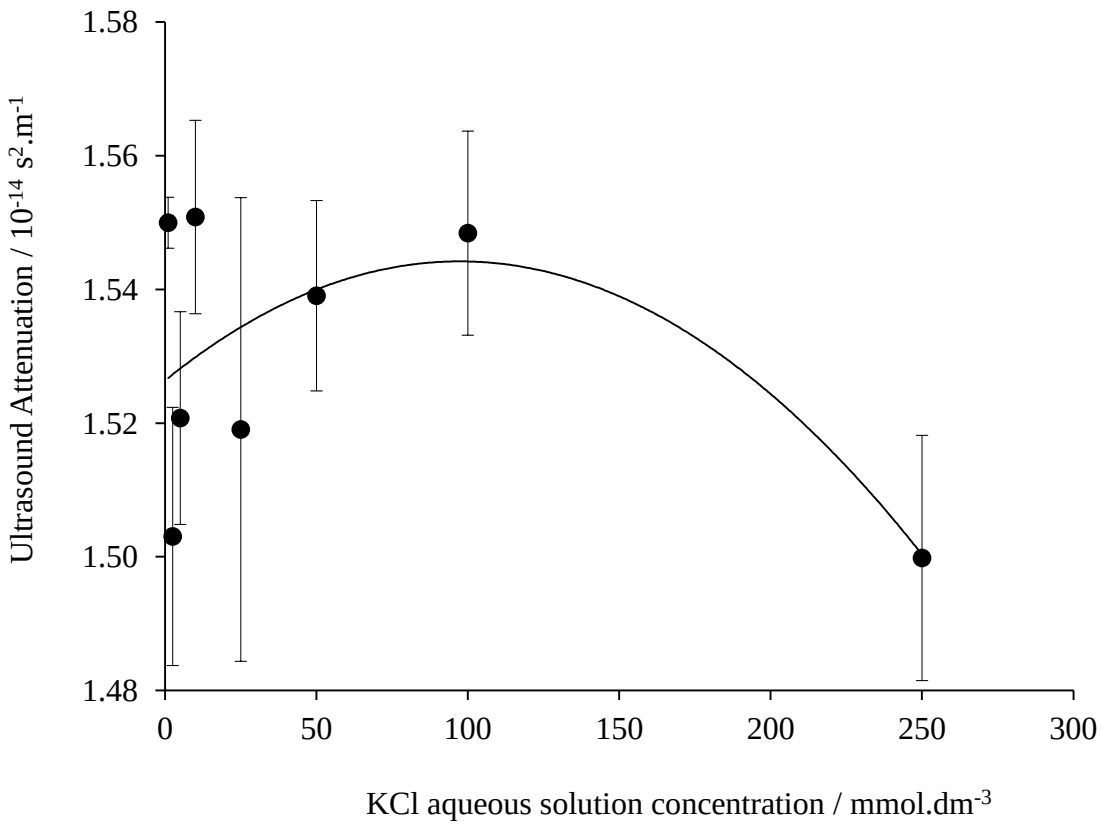

Figure 4.5. Attenuation of KCl aqueous solutions against concentration

Figure 4.6 represents a comparison of ultrasound velocity change with concentration for seven potassium salts including the potassium halides, potassium acetate, potassium formate and potassium thiocyanate. All data points were created similarly as the points of **Figure 4.4**. In all cases, error bars are much smaller than symbols.

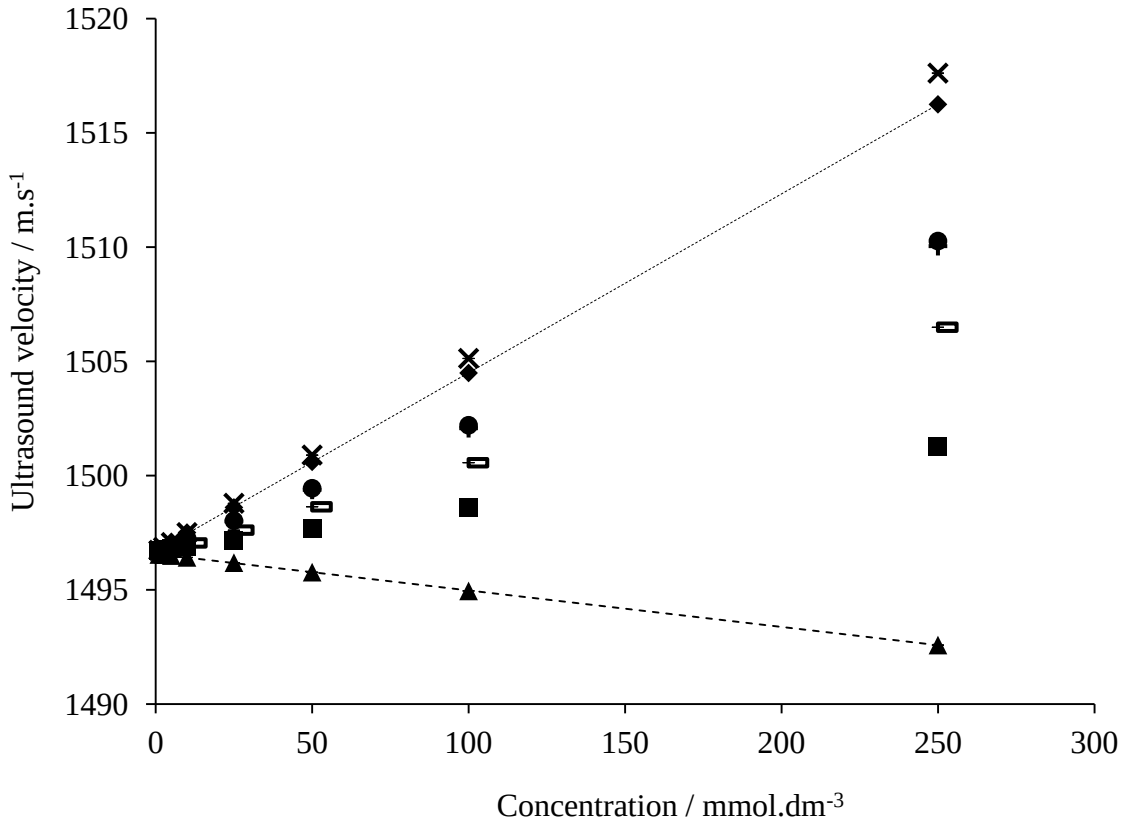

Figure 4.6. Comparison of average ultrasound velocity of seven potassium salt aqueous solutions against concentration. Potassium acetate (dark cross sign), potassium fluoride (solid diamond), potassium formate (dark plus sign), potassium chloride (solid circle), potassium bromide (solid square), potassium iodide (solid triangle) and potassium thiocyanate (rectangle sign)

The sound velocity increases with the increase in concentration for potassium acetate, potassium fluoride, potassium chloride, potassium formate, potassium thiocyanate and potassium bromide, but sound velocity decreases with increasing concentration for potassium iodide solution. The order of salt in increasing sound velocity was CH_3COOK > KF > KCl > KCOOH > KSCN > KBr where potassium chloride and potassium formate increase sound velocity with concentration similarly with a slope of 0.05 $m^4.s^{-1}.mol^{-1}$. The sound velocity of liquids depends on the density and the adiabatic compressibility of the liquids. Usually, the sound velocity of a solution increases with concentration if adiabatic compressibility of the solution decreases, and the sound

velocity of a solution also increases with concentration if the density of a liquid decreases. The increase or decrease of sound velocity of a solution is controlled by the dominating impact of either the density or the adiabatic compressibility of the solution (Freyer, 1931). Similar trends of sound velocity change were observed in the case of KCl, KBr and KI solutions from other research (Freyer, 1931).

Figure 4.7 represents a comparison of ultrasound attenuation changes with concentration for the seven potassium salts. The data points in **Figure 4.7** for the seven salts were created similarly to the data of **Figure 4.5**. The polynomial second order curves of attenuation as a function of concentration for KBr, KI andCH_3COOK were similar to the curve of KCl. In the case of KF, the sound attenuation decreases with concentration increase up to a concentration of 175 $mmol.dm^{-3}$, then again the attenuation tends to increase with concentration. For KSCN, attenuation decreased with concentration up to a concentration of 200 $mmol.dm^{-3}$, and then attenuation increased slowly with concentration. The sound attenuation was found to decrease gradually with concentration increase for KCOOH.

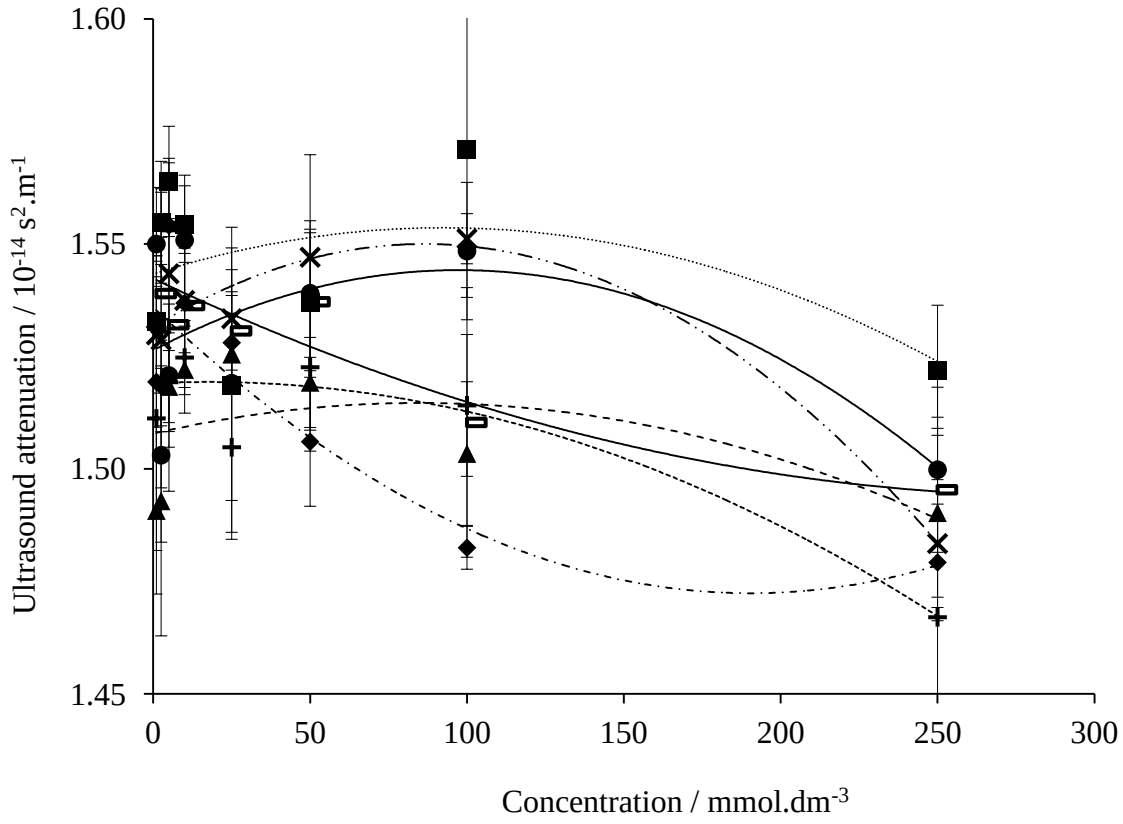

Figure 4.7. Comparison of average ultrasound attenuation of seven potassium salt aqueous solutions against concentration. Potassium acetate (dark cross sign), potassium fluoride (solid diamond), potassium formate (dark plus sign), potassium chloride (solid circle), potassium bromide (solid square), potassium iodide (solid triangle) and potassium thiocyanate (rectangle sign)

At a concentration of zero the solution is equal to pure water. The sound velocity at zero concentration for all seven salts was calculated from the zero concentration extrapolation of a linear line of velocity against concentration. The attenuation at zero concentration was calculated from the zero concentration extrapolation of a second order polynomial curve of attenuation against concentration. Both results are presented in **Table 4.5**. Sound velocity in Milli Q water and sound velocity at salt concentration zero were found to be similar by comparing the values in **Table 4.5** to the reported values for pure water

in **Table 4.2**. However, sound attenuation values were slightly higher at salt concentration zero than sound attenuation in Milli Q water of cell 2.

Table 4.5. Ultrasound velocity and attenuation of salt solutions extrapolated to zero concentration

Aqueous salt solutions	Sound velocity at zero concentration ($m.s^{-1}$)	Attenuation at zero concentration ($s^2.m^{-1}$)
KCl	1496.68	1.53×10^{-14}
KBr	1496.71	1.54×10^{-14}
KI	1496.57	1.51×10^{-14}
KF	1496.67	1.54×10^{-14}
HCOOK	1496.65	1.52×10^{-14}
CH_3COOK	1496.67	1.53×10^{-14}
KSCN	1496.64	1.54×10^{-14}

4.3. Analysis of potassium halide solutions

4.3.1. Comparison between experimental and literature densities

The experimentally derived density of KCl aqueous solution was compared with the literature derived density (Hai-Lang and Shi-Jun, 1996), and it was observed that the experimental points nicely overlaid the literature values (**Figure 4.8)**. Thus, I can have confidence that the use of literature derived values of density in the later analysis is appropriate for my experiments.

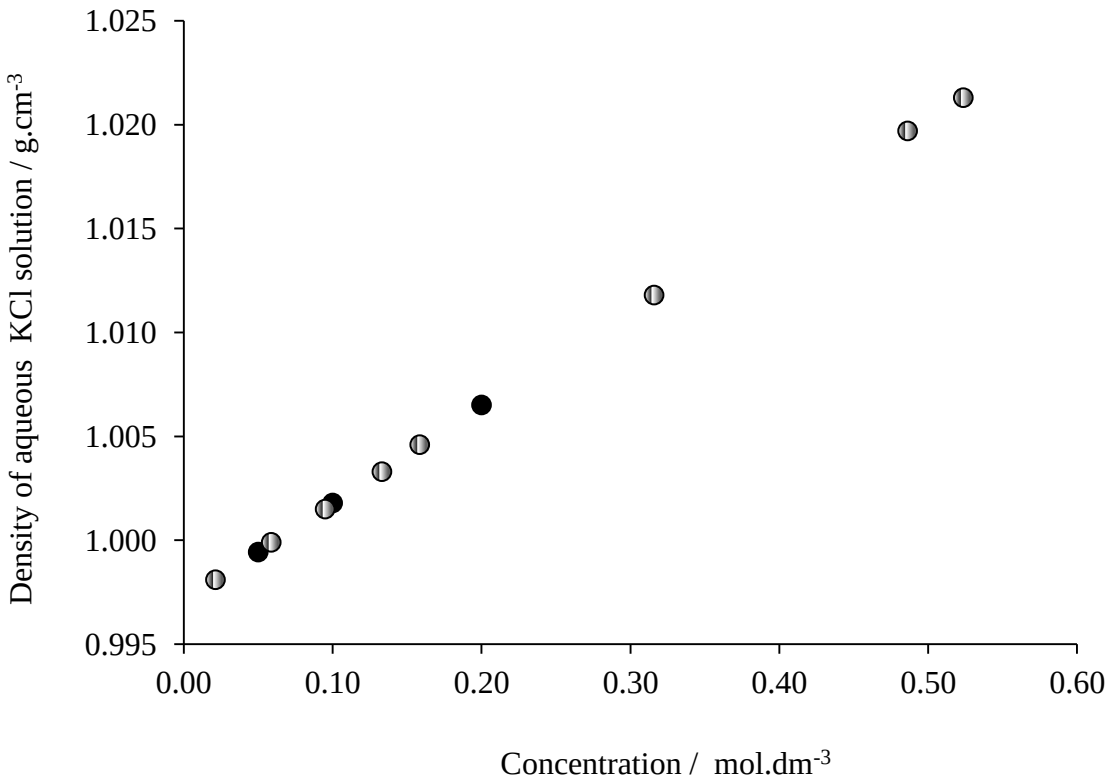

Figure 4.8. Density of potassium chloride aqueous solution against concentration. Experimental value (solid circle) and literature value (gradient circle)

4.3.2. Study of density and adiabatic compressibility of solutions

In order to limit the scope of the research, potassium halides had been chosen for further experiment and analysis because the physical properties of these salts are well studied. The analysis of potassium halide solutions has been done to see whether the ions have impact on the structuring of water in terms of density and adiabatic compressibility. For this purpose, comparison was made between the hard sphere model (Fredriksson and Åkerlind, 2008) and the experimental result. If structuring of water by the ions does not occur, then the hard sphere analysis should mimic the experimental values in terms of density and adiabatic compressibility. Graphs have been plotted in terms of change in density (ρ) and adiabatic compressibility (K_S) against volume fraction for the four

potassium halide aqueous solutions. The experimental values are represented by the solid symbol, the literature values are presented by the gradient symbol and the theoretically calculated values are depicted by empty symbols in the following figures.

Calculation of theoretical value of density:

The theoretical value of volume was calculated using equation (39) considering ions to be non-hydrated incompressible hard spheres. Therefore, the theoretical density ignores any structuring of water brought about by the ions.

$$V_T = V_K + V_{halide} + V_{free\ water} \quad (39)$$

Where V_T is total solution volume, V_K is volume occupied by potassium ion, V_{halide} is volume occupied by halide ion and $V_{free\ water}$ is volume occupied by free water. The molar volume of each ion was calculated from the non-hydrated ionic radius which was taken from the literature (Haynes, 2010; Nostrand, 2005). For the theoretical density calculation, non-hydrated ionic radius was considered instead of the hydrated ionic radius because significant differences were observed in the hydration number of ions and partial molar volume of ions in different sources of the literature (Bockris and Saluja, 1972; Heyrovska, 2007; Hinton and Amis, 1971; Hribar, Southall, Vlachy and Dill, 2001; Imai, Nomura, Kinoshita and Hirata, 2002; Koneshan, Rasaiah, Lynden-Bell and Lee, 1998; Marcus, 2009b; Ohtaki, 2001; Weight, 2007). The calculation of the theoretical value of the density of 1 molar KCl solution can be presented as an example:

$V_T = V_{free\ water} + V_K + V_{Cl}$

$V_{free\ water}$ = 1000 – (5.93 + 14.95), where V_T = 1000 cm^3, V_K = 5.93 cm^3 and V_{Cl} = 14.95 cm^3

V_{free} water = (1000 – 20.88) cm^3

= 979.12 cm^3

Density (ρ) of H_2O = 0.997 $g.cm^{-3}$ at 25 ^oC

Thus, mass of H_2O = (979.12 x 0.997) $cm^3.g.cm^{-3}$

= 976.18 g

Thus, theoretical mass of 1 molar KCl solution = (976.18 + 74.55) g, as the molecular weight of KCl is 74.55 g

= 1050.73 g

Now ρ of 1 molar KCl solution =1050.73 g /1000 cm^3

= 1.05 $g.cm^{-3}$

Calculation of adiabatic compressibility of potassium halide aqueous solution:

The hard sphere theoretical value of the adiabatic compressibility of the potassium halide solutions was calculated using the following equation (Rao and Verrall, 1987; Reis, 1998):

$$K_T = K_K \times \Phi_K + K_{halide} \times \Phi_{halide} + K_o \times (1 - \Phi_{K\ halide}) \quad (40)$$

Where K_T is the total adiabatic compressibility of the solution, K_K is the adiabatic compressibility of the potassium ion, Φ_K is the volume fraction of the potassium ions, K_{halide} is the adiabatic compressibility of the halide ion, Φ_{halide} is the volume fraction of the halide ions, K_o is the adiabatic compressibility of water and $\Phi_{K\ halide}$ is the volume fraction of potassium halide. The adiabatic compressibility of water was calculated from the sound velocity in water at 25 ^oC (Barlow and Yazgan, 1966) and the density of water at 25 ^oC (Kirino, Yokoyama, Hirono, Nakajima and Nakashima, 2009). First the adiabatic compressibility coefficient was determined using the Newton-Laplace equation,

$$\beta_S = (1/v^2\rho) \tag{41}$$

The determined compressibility coefficient of water was 4.48 x 10^{-5} bar^{-1} which is exactly similar to values of the literature (Bermúdez-Salguero and Gracia-Fadrique, 2011). The adiabatic compressibility coefficient was then multiplied by the specific volume of water (specific volume is inverse of density) in order to get the adiabatic compressibility of water.

The experimental adiabatic compressibilities of the potassium halide aqueous solutions were estimated following a similar calculation used to derive adiabatic compressibility of water. The density values of potassium halide solutions were taken from the literature (Hai-Lang and Shi-Jun, 1996; Nikam and Sawant, 1997; Out and Los, 1980; Sohnel and Novotny, 1985; Zaytsev and Aseyev, 1992) and the velocity values were taken from my experiments.

Calculation of volume fraction:

The theoretical values for the volume fraction of ions in the potassium halide aqueous solutions were calculated by dividing the non-hydrated volume of the potassium and halide ions of a certain concentration by the total solution volume using the notation of equation 2. The literature values of volume fraction of potassium halides were calculated from literature values of density as a function of concentration (Hai-Lang and Shi-Jun, 1996; Nikam and Sawant, 1997; Out and Los, 1980; Sohnel and Novotny, 1985; Zaytsev and Aseyev, 1992), and using the equations:

$$\Phi_{K\ halide} = (1 - \Phi_o) \text{ and} \quad (42)$$

$$\Phi_o = [(\rho - c)/\rho_o] \quad (43)$$

where Φ_o is the volume fraction of water, ρ is the density of the solution, c is the concentration in g cm^{-3} and ρ_o is the density of water (Gekko and Hasegawa, 1986).

Figure 4.9 is a comparison of change in density against volume fraction for four potassium halides considering the theoretically calculated hard sphere model and literature values of density. The literature derived values of density of KCl, KBr and KI were experimentally found by other researchers (Hai-Lang and Shi-Jun, 1996; Nikam and Sawant, 1997; Out and Los, 1980) and the values used were those within the range of 0 to 350 mmol.dm^{-3}. However, the literature derived density values of the KF solutions are average values (with standard deviations as error bars which are very small) of density from two sources (Sohnel and Novotny, 1985; Zaytsev and Aseyev, 1992). Both these two literatures report density values at higher concentration (more than 340 mmol dm^{-3}). Thus, in the case of KF solutions, I have less confidence in the

density values at very low concentrations such as 1 $mmol.dm^{-3}$. Because of the erroneous density values of KF at lower concentrations, the volume fraction calculated from densities shows negative values in **Figure 4.9**.

The density of four potassium halide solutions was found to increase with the increase in volume fraction in the case of both the theoretically derived and the literature derived values. However, the theoretically derived densities show discrepancy from the literature derived density values for all the potassium halides. The density of potassium fluoride solutions from the literature was higher than the theoretical density of the solutions, while the literature derived densities of potassium chloride, potassium bromide and potassium iodide solution were lower than the theoretical density of the respective solutions.

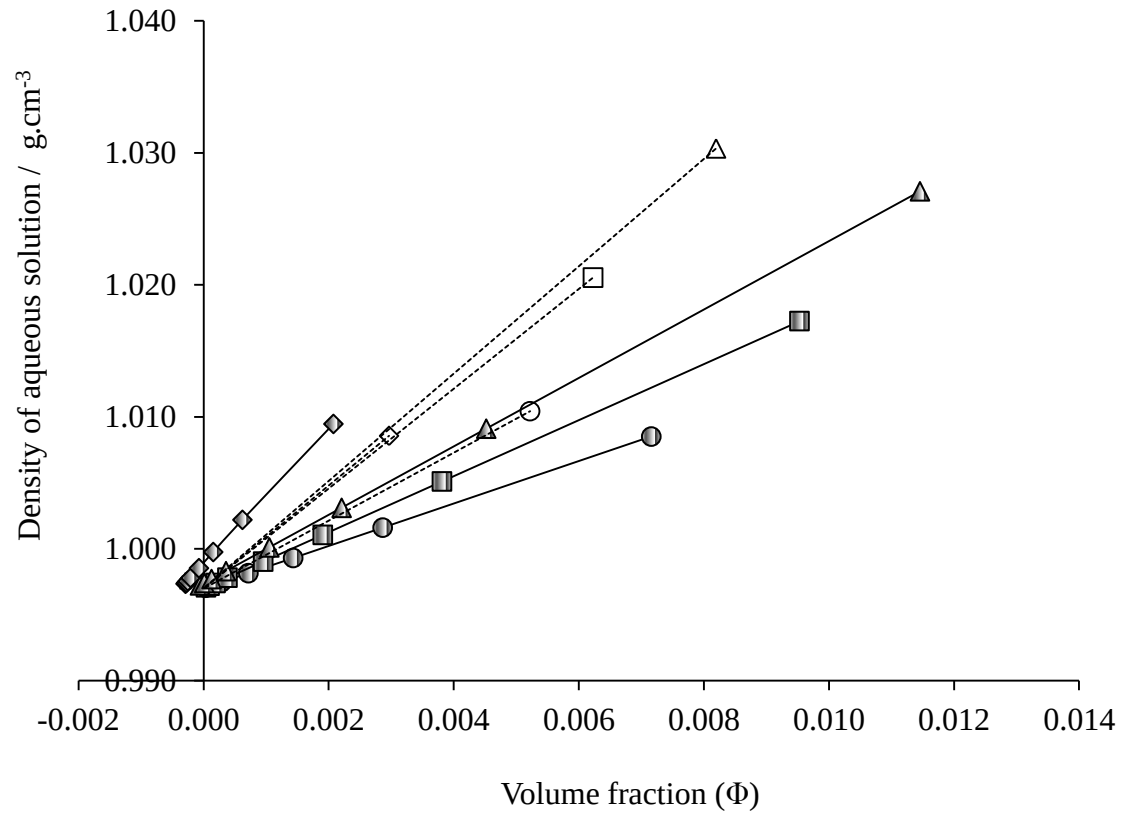

Figure 4.9. Theoretical and literature values of change in density of four potassium halide aqueous solutions against their volume fraction. Solid line with gradient symbols represents literature values whereas dotted line with empty symbols represents calculated values. Potassium fluoride (diamond), potassium chloride (circle), potassium bromide (square), and potassium iodide (triangle)

The change in density with volume fraction for the hard sphere potassium halides can be attributed to only the presence of ions in solution. On the other hand, the change in density with volume fraction for the literature values can be attributed to the structuring of water molecules around the ions (Kaun, Baena, Newnham and Lendl, 2005; Soper and Weckström, 2006), and the degree of structuring of water varies according to the ions. The packing density of water and the average hydrogen bond length in the surrounding water are subject to change in the presence of ions (Dougherty, 2001). The three dimensional structure of water forms due to hydrogen bonding between hydrogen and oxygen atoms (Franks, 1972). In the presence of a salt, the hydrogen bond strength

in water is disturbed. The change in hydrogen bond strength differs with concentration depending on the salt, and the strength of the hydrogen bond depends on electron polarizability between the ions and water molecule (Dougherty, 2001).

Figure 4.10 is a comparison of change in adiabatic compressibility against volume fraction for four potassium halide solutions considering theoretically calculated and experimental values of adiabatic compressibility. The experimental adiabatic compressibility was obtained from the ultrasound velocity of three replicate solutions and from the literature derived density. Experimental points are the average value of three replicates, presented with standard deviation as error bar, and the error bars are smaller than the symbols. The experimentally derived adiabatic compressibility of all the four potassium halide solutions was substantially different from the theoretically calculated adiabatic compressibility considering that the ions are hard spheres in solution.

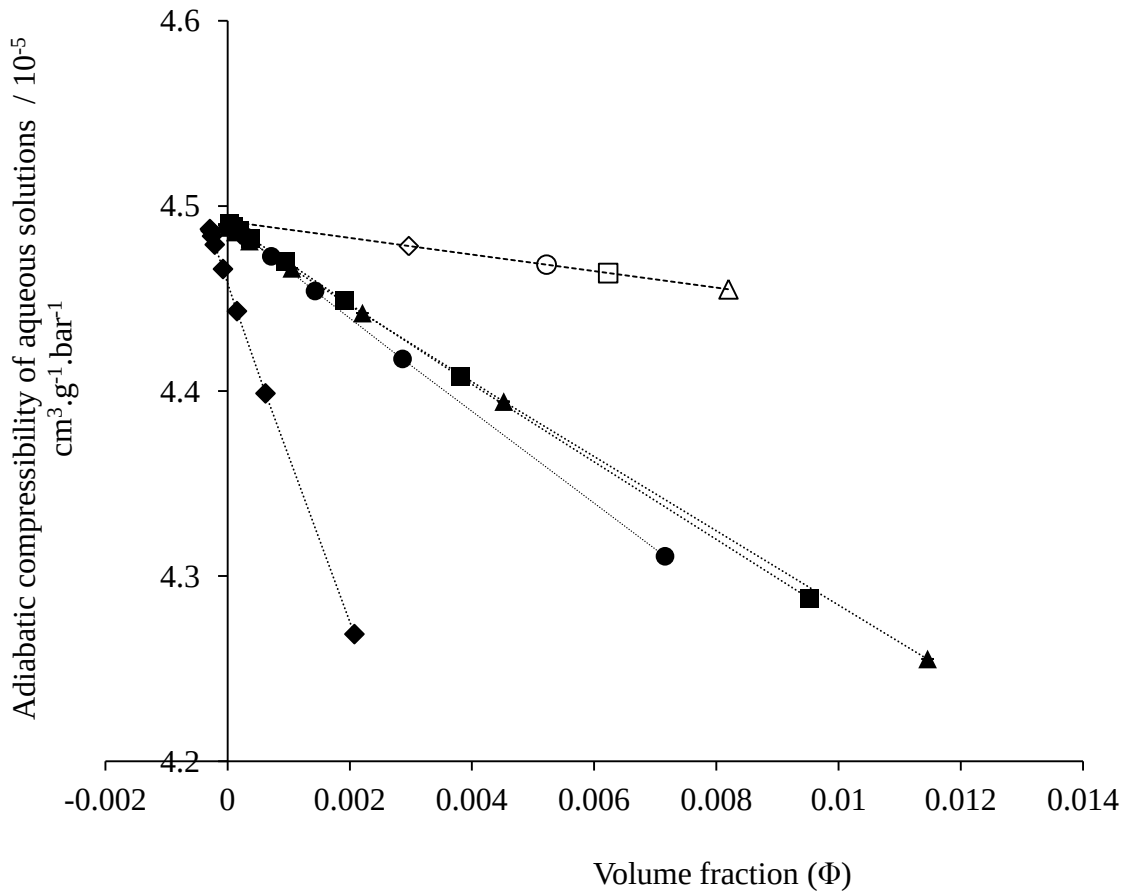

Figure 4.10. Comparison of the theoretical adiabatic compressibility and experimental adiabatic compressibility against volume fraction for four potassium halides. Solid and empty symbols are for experimental adiabatic compressibility and theoretical adiabatic compressibility, respectively. Potassium fluoride (diamond), potassium chloride (circle), potassium bromide (square), and potassium iodide (triangle)

The adiabatic compressibility of four potassium halide solutions was found to decrease with increase in volume fraction. In the case of the hard sphere model (theoretical value), the slope of adiabatic compressibility against volume fraction does not vary for the four halides, and the slope is -4.49 x 10^{-5} $cm^3.g^{-1}.bar^{-1}$. On the contrary, variation in the slope among the potassium halides was observed in the case of experimental estimated adiabatic compressibility with a slope of -9.27 x 10^{-4} $cm^3.g^{-1}.bar^{-1}$ for KF, -2.52 x 10^{-4} $cm^3.g^{-1}.bar^{-1}$ for KCl, -2.13 x 10^{-4} $cm^3.g^{-1}.bar^{-1}$ for KBr and -2.04 x 10^{-4} $cm^3.g^{-1}.bar^{-1}$ for KI. The order of the capacity of potassium halides in

reducing adiabatic compressibility of aqueous solution is KF > KCl > KBr > KI. According to **Figure 4.6,** the order of potassium fluoride, potassium chloride and potassium bromide in increasing ultrasound velocity against concentration is KF > KCl > KBr; however, potassium iodide decreases ultrasound velocity with increasing concentration. By observing the fractional change in adiabatic compressibility and change in percentage density, Freyer (1931) mentioned that the dominating factor for increasing ultrasound velocity with concentration increase of KCl and KBr is reduced compressibility, and in the case of KI, the dominating factor for decreasing ultrasound velocity with concentration increase is increased density. The researcher emphasised the effect of the degree of hydration of different ions on the extent of compressibility reduction with concentration increase. Highly hydrated ions are responsible for a large reduction in compressibility. Observing **Figure 4.6**, **Figure 4.9** and **Figure 4.10**, it can be assumed that for KF aqueous solution, the dominating factor is compressibility in determining the ultrasound velocity. Moreover, according to Matheison and Conway (1974), the negative partial molal compressibility of halide ions was found to increase with reduced ionic radii. Thus, from the density and adiabatic compressibility analysis of potassium halide solutions, it can be concluded that the presence of ions in the aqueous solution is not as hard spheres but rather the ions are responsible for the restructuring of water.

4.4. Analysis of Bovine Serum Albumin (BSA) aqueous solutions

The ultrasound velocity and attenuation values at five concentrations (0.076, 0.152, 0.379, 0.758 and 1.515 $mmol.dm^{-3}$) of aqueous BSA solution were taken from another research work (Beneddif, 2010). Each point generated in **Figure 4.11** and **Figure 4.12**

was the mean value of three replicates, with error bars the standard deviation. The sound velocity of aqueous BSA solutions at 25 ^{o}C was found to increase linearly with the increase in concentration (**Figure 4.11**). The ultrasound attenuation also increased linearly with concentration increase of the aqueous BSA solutions (**Figure 4.12**). The linear behaviour of ultrasound velocity and attenuation change over the concentration range (low concentration range up to ~10%) is due to water and BSA interaction, and it can be assumed that no intermolecular interaction between BSA molecules occurs within the used concentration range (Goss and Dunn, 1974); indeed a linear relationship between ultrasound velocity and concentration up to a concentration range of ~25% (~3.79 mmol.dm^{-3}) was reported.

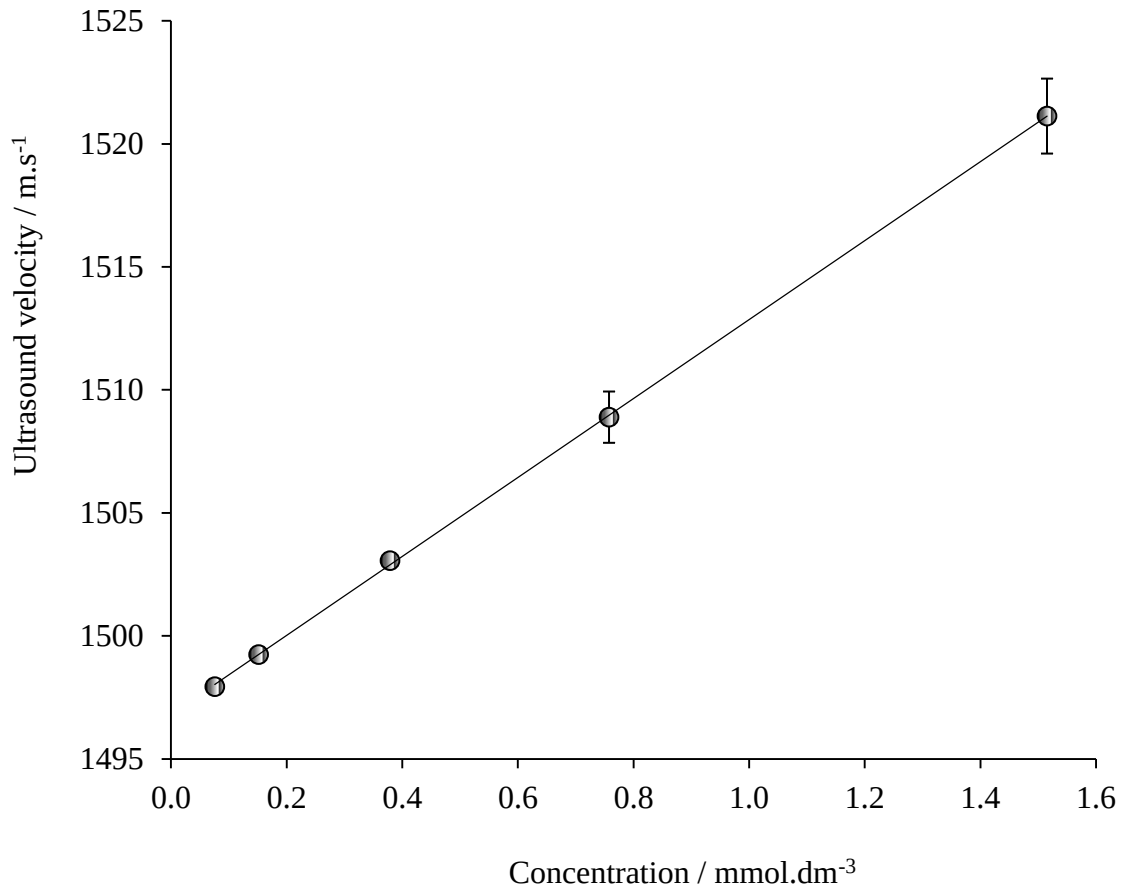

Figure 4.11. Ultrasound velocity of aqueous BSA solutions as a function of concentration (the gradient symbol represents the results of Beneddif, 2010)

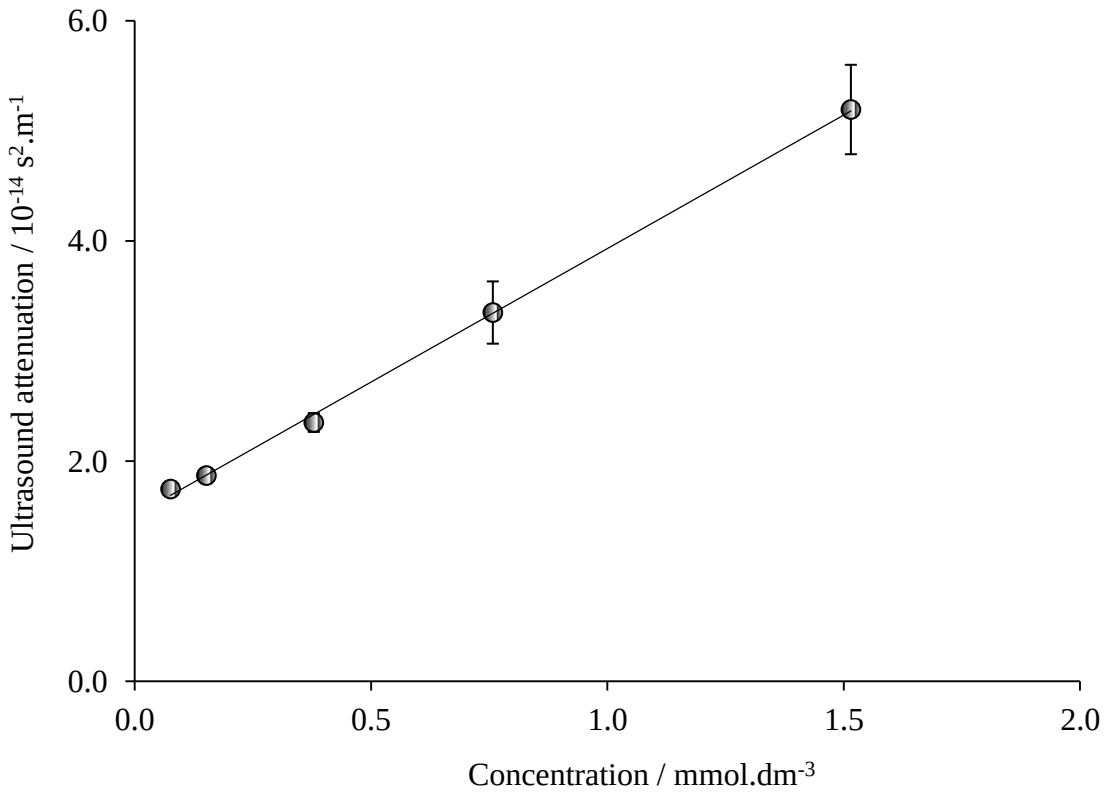

Figure 4.12. Ultrasound attenuation of aqueous BSA solutions as a function of concentration (the gradient symbol represents the results of Beneddif, 2010)

Calculation of density of aqueous BSA solution:

The density of aqueous BSA solutions (0.15, 0.3. 0.6, 1.2 and 2.4 mmol.dm^{-3}) were measured at a temperature of 25 ^{o}C. The theoretical value of density (empty symbol on **Figure 4.13**) of aqueous BSA solutions was calculated considering the molecular weight of BSA as 66000 (Sigma Aldrich) and the partial specific volume of BSA at 25 ^{o}C as 0.734 cm^{3}.g^{-1} (Dayhoff, Perlmann and MacInnes, 1952). Since proteins cannot be considered as hard spheres like ions, and internal water and protein hydrating water has a role in determining protein architecture in solution, and hydrophobic and hydrophilic effects have a role in determining the molar volume (Gekko and Noguchi, 1979; Otting, Liepinsh and Wuthrich, 1991), the partial specific volume was considered in calculating

the theoretical density and volume fraction. The density calculation of 0.15 mmol.dm^{-3} BSA aqueous solution is given as an example:

The mass of 0.15 mmol.dm^{-3} BSA content in solution = (66000 x 0.15) / 1000

= 9.9 g.dm^{-3}

Volume occupied by 9.9 g BSA = (9.9 x 0.734) cm^3.dm^{-3}

= 7.27 cm^3.dm^{-3}

The volume of free or bulk water = (1000 – 7.27) = 992.73 cm^3.dm^{-3}

Mass of free water = (992.73 x 0.997) g.dm^{-3} where the density of water is 0.997 g.cm^{-3}

= 989.76 g.dm^{-3}

The total mass of the solution = (989.76 + 9.9) = 999.70 g.dm^{-3}

Now the density of 0.15 mmol.dm^{-3} is = 999.70 / 1000 = 0.9997 g.cm^{-3} or 1.0 g.cm^{-3}.

Calculation of volume fraction of BSA:

In order to calculate the theoretical volume fraction occupied by the BSA, the volume occupied by BSA at a specific concentration was divided by the total volume of the solution. For example, the theoretical volume fraction of 0.15 mmol.dm^{-3} = 7.27 / 1000 = 0.0073.

The experimental value of the volume fraction was calculated using the equations:

$\Phi_{BSA} = (1 - \Phi_o)$ and (44)

$$\Phi_o = [(\rho - c)/\rho_o] \quad (45)$$

where Φ_{BSA} is the volume fraction of BSA, Φ_o is the volume fraction of water, ρ is the experimental density of the BSA solution, c is the concentration in $g.cm^{-3}$ and ρ_o is the density of water. Both the calculated and the experimental value of density increased maintaining a linear relationship with the volume fraction increase (**Figure 4.13**). The calculated and experimental values of density do not differ significantly because the calculated value is derived by considering partial specific volume of BSA aqueous solution, and the partial specific volume of a solute in aqueous solution reflects the hydrated volume (Chalikian, 2003; Gekko, Kimoto and Kamiyama, 2003).

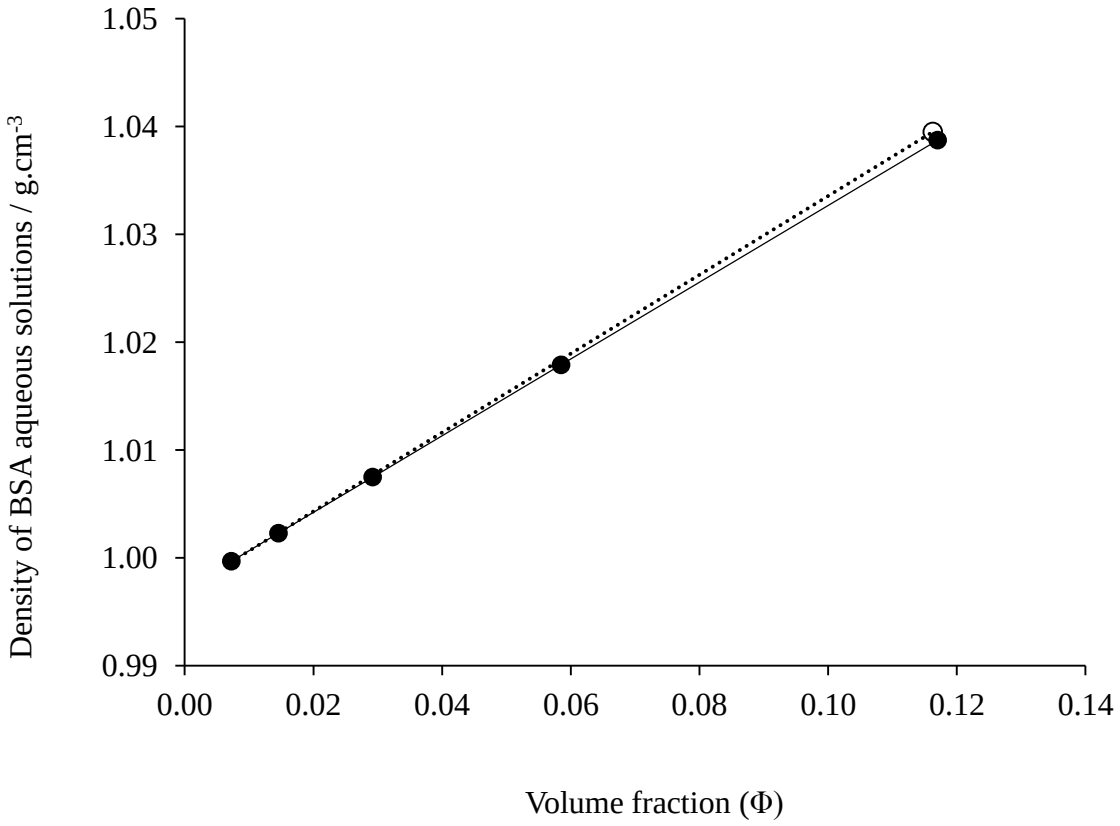

Figure 4.13. Theoretical and experimental values of change in density of BSA aqueous solutions against their volume fraction of hydrated BSA. Solid line with solid symbols represents experimental values whereas dotted line with empty symbols represents theoretical values

Calculation of adiabatic compressibility of aqueous BSA solution:

The theoretical value of the adiabatic compressibility of BSA aqueous solution was calculated considering BSA to be an incompressible hydrated macromolecule using the following equation:

$$K_T = K_{BSA} \times \Phi_{BSA} + K_o \times (1 - \Phi_{BSA}) \quad (46)$$

where K_{BSA} is the compressibility of hydrated BSA, and Φ_{BSA} is the volume fraction of BSA. The experimental adiabatic compressibility of aqueous BSA solutions was estimated following a similar procedure to the potassium halide solutions where the density values were taken from experiment and the velocity values were taken from other research (Beneddif, 2010). Then, the experimental and calculated values of the adiabatic compressibility of BSA solutions were plotted as a function of volume fraction in **Figure 4.14**. A reduction of adiabatic compressibility of BSA aqueous solutions with increment in volume fraction was observed in the case of both experimental and calculated values **(Figure 4.14)**.

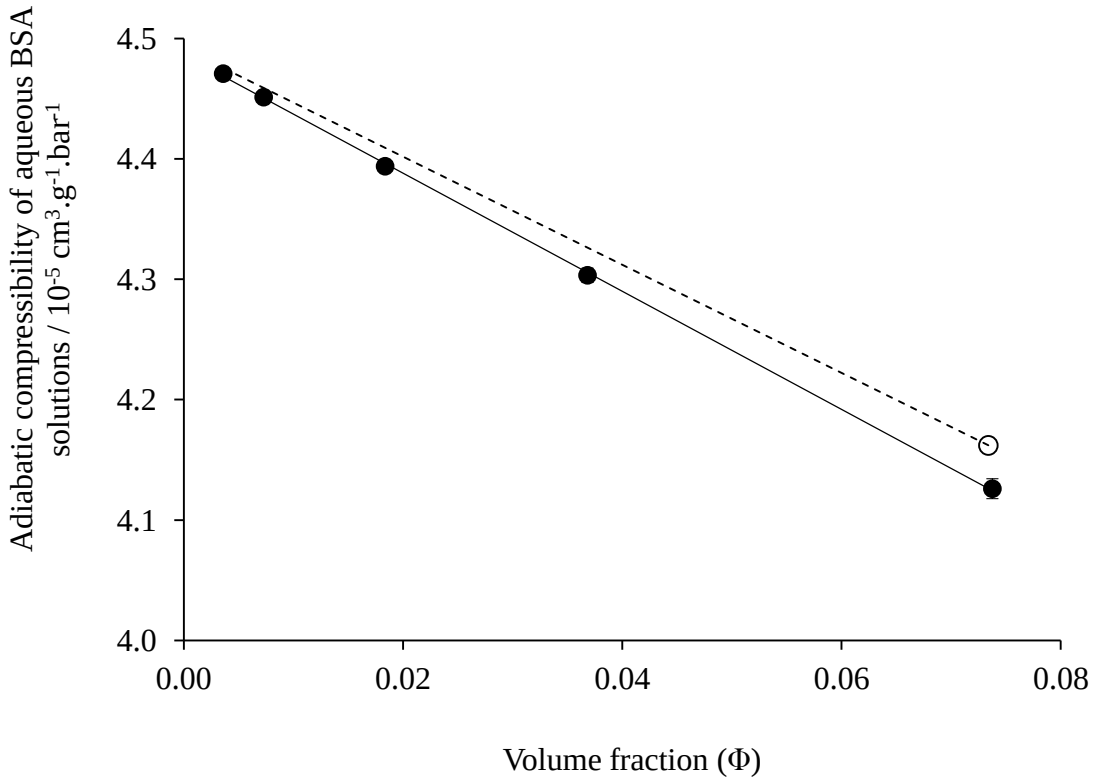

Figure 4.14. Adiabatic compressibility of aqueous BSA solutions as a function of volume fraction of hydrated BSA. Solid symbol (•) is for experimental adiabatic compressibility and hollow symbol (o) is for theoretical adiabatic compressibility

The slope of adiabatic compressibility as a function of volume fraction was -4.91 x 10^{-5} $cm^3.g^{-1}.bar^{-1}$ for the experimental value and -4.49 x 10^{-5} $cm^3.g^{-1}.bar^{-1}$ for the theoretical value. Disparity between the experimental and theoretical adiabatic compressibility of BSA aqueous solution was observed as the theoretical value considers the hydrated BSA in the aqueous environment to be an incompressible molecule. However, the BSA is compressible, and the adiabatic compressibility of protein molecules in aqueous solution is dependent on the intrinsic compressibility of protein molecules and the difference in the compressibility of the hydration shell relative to bulk water (Gekko & Hasegawa, 1986) Principally three kinds of hydration occur in the case of protein molecules in aqueous solution: electrostriction around the charged groups, hydrogen bonded

hydration around the polar groups, and hydrophobic hydration (Gekko and Hasegawa, 1986). Differences in compressibility of protein solutions arise due to the competition between protein-solvent attractive forces and the preferable intramolecular interactions within the protein interior (Dadarlat and Post, 2003). The difference between the experimental and theoretical adiabatic compressibility lines implies that the finite compressibility of the BSA molecules contribute to the total compressibility of solutions.

4.5. Analysis of Bovine Serum Albumin (BSA) and four potassium halide mixed aqueous solutions

The density, ultrasound velocity and attenuation of BSA and potassium halide mixed aqueous solutions were measured at 25 ^{o}C for the composite concentrations including (0.12 + 20), (0.24 + 40), (0.48 + 80) and (0.96 + 160) mmol.dm^{-3}, where the former number is for BSA concentration in a mixed solution and the latter number is for potassium halide concentration in the mixed solution. The result of ultrasound velocity and attenuation of BSA-potassium salt mixed solution as a function of salt concentration (although solutions are made up with both BSA and salt) are presented in **Figure 4.15** and **Figure 4.16**, respectively.

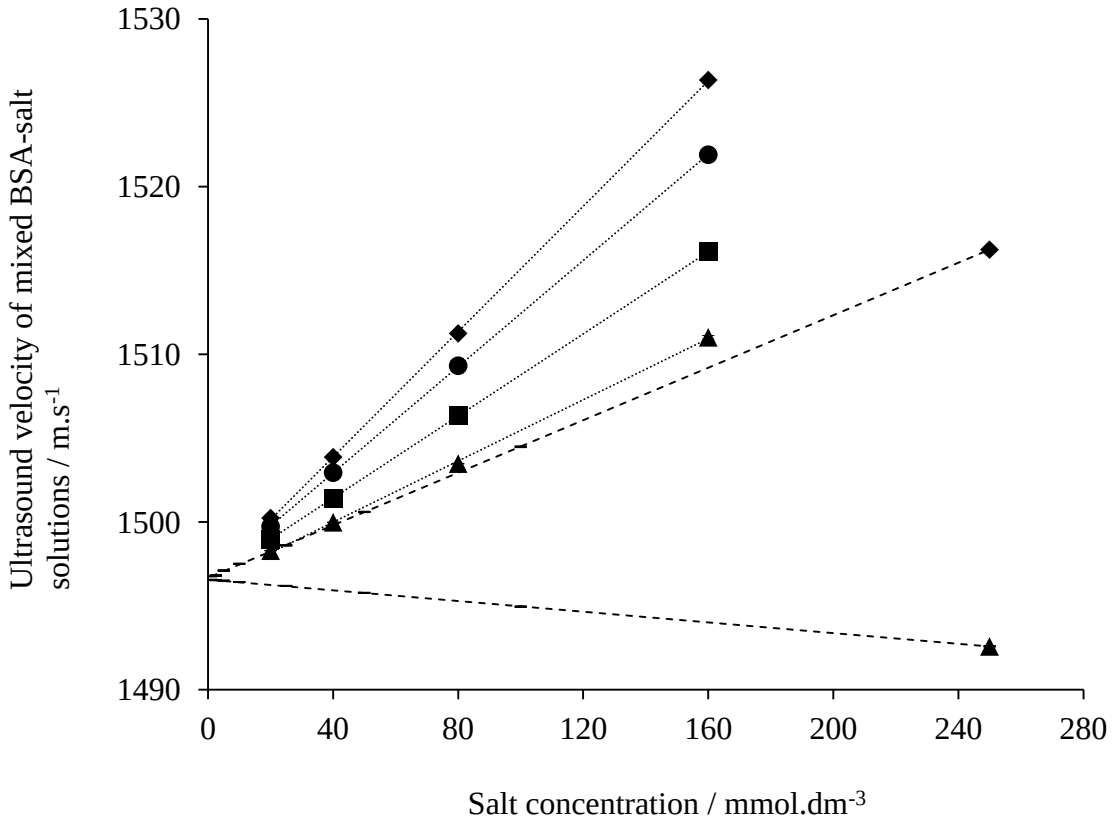

Figure 4.15. Ultrasound velocity of aqueous BSA-salt mixed solutions as a function of salt concentration. BSA-KF (diamond), BSA-KCl (circle), BSA-KBr (square) and BSA-KI (triangle). The dashed line with solid diamond at the end represents ultrasound velocity of KF aqueous solutions, and the dashed line with solid triangle at the end represents ultrasound velocity of KI aqueous solutions

According to **Figure 4.15**, ultrasound velocity increases with the concentration of BSA-salt mixed solutions for all the halides. The order of increment of ultrasound velocity follows the order of BSA-KF> BSA-KCl> BSA-KBr> BSA-KI. The contribution of the polymer dominates for the BSA-KI solution, because in **Figure 4.6**, it can be seen that the ultrasound velocity of KI solutions decreases with increasing concentration, but the ultrasound velocity of BSA-KI mixed solution increases with increasing concentration. For comparison the dashed lines, are for KF and KI alone.

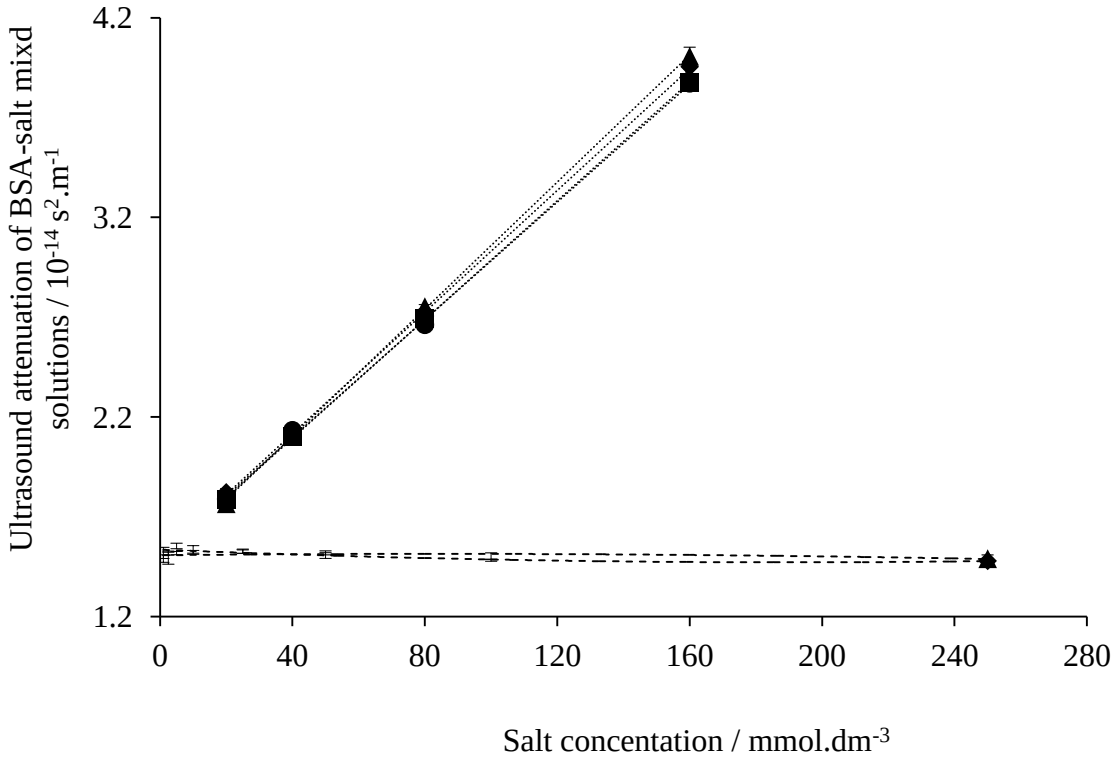

Figure 4.16. Ultrasound attenuation of aqueous BSA-salt mixed solutions as a function of salt concentration. BSA-KF (diamond), BSA-KCl (circle), BSA-KBr (square) and BSA-KI (triangle). The dashed line with solid diamond at the end represents ultrasound attenuation of KF aqueous solutions, and the dashed line with solid triangle at the end represents ultrasound attenuation of KI aqueous solutions

Regardless of contribution of salt, there is substantial effect with the addition of BSA on the combined ultrasound velocity of BSA-salt mixed solutions. By observing **Figure 4.6** and **Figure 4.15**, it can be said that potassium halides also show their impact on the ultrasound velocity change of mixed solutions since the velocity change follows the same sequence in the case of both potassium halides alone and the BSA-potassium halides mixed solutions.

In the case of ultrasound attenuation of BSA-potassium halides mixed solutions, likewise BSA solutions, ultrasound attenuation increased linearly with concentration, and using a post hoc t-test (Tukey HSD test) it has been found that there is no significant

difference in the case of ultrasound attenuation increment among BSA-KI, BSA-KF, BSA-KBr and BSA-KCl mixed solutions. In the BSA-potassium halide mixed solution, it can be assumed that the reorientation of water occurs not only around the ions but also around the BSA polyelectrolyte and around the BSA-ion complex if interaction between ion and protein occurs (Otting, Liepinsh and Wuthrich, 1991; Svergun, Richard, Koch, Sayers, Kuprin and Zaccai, 1998). Ions have impact on the structuring of water around the exposed groups of protein by altering the surrounding water structure (von Hippel and Schleich, 1969). Moreover, at low salt concentrations, electrostatic interaction between salt ions and the dipole moment of the peptide group occurs, and the binding of specific ions with macromolecules depends on the surface property of the macromolecules (Lund, Va´cha & Jungwirth, 2008; Nandi & Robinson, 1972; von Hippel & Schleich, 1969; Vrbka, Jungwirth, Bauduin, Touraud & Kunz, 2006). Following ion interaction with protein molecules, water reorganization occurs around the ion-protein complex.

Calculation of experimental and theoretical volume fraction and density of BSA + potassium halide mixed solution:

The calculation of experimental and theoretical volume fraction and density of BSA + potassium halide mixed solution was similar to the calculation of volume fraction and density of potassium chloride aqueous solution and BSA aqueous solution.

The experimentally and theoretically derived densities of BSA-salt mixed solutions were plotted against their volume fraction in **Figure 4.17**. Experimental values are presented with standard deviation (from two replicate solutions) as error bars which are smaller than the symbol in **Figure 4.17**. This is also the case in **Figure 4.18**.

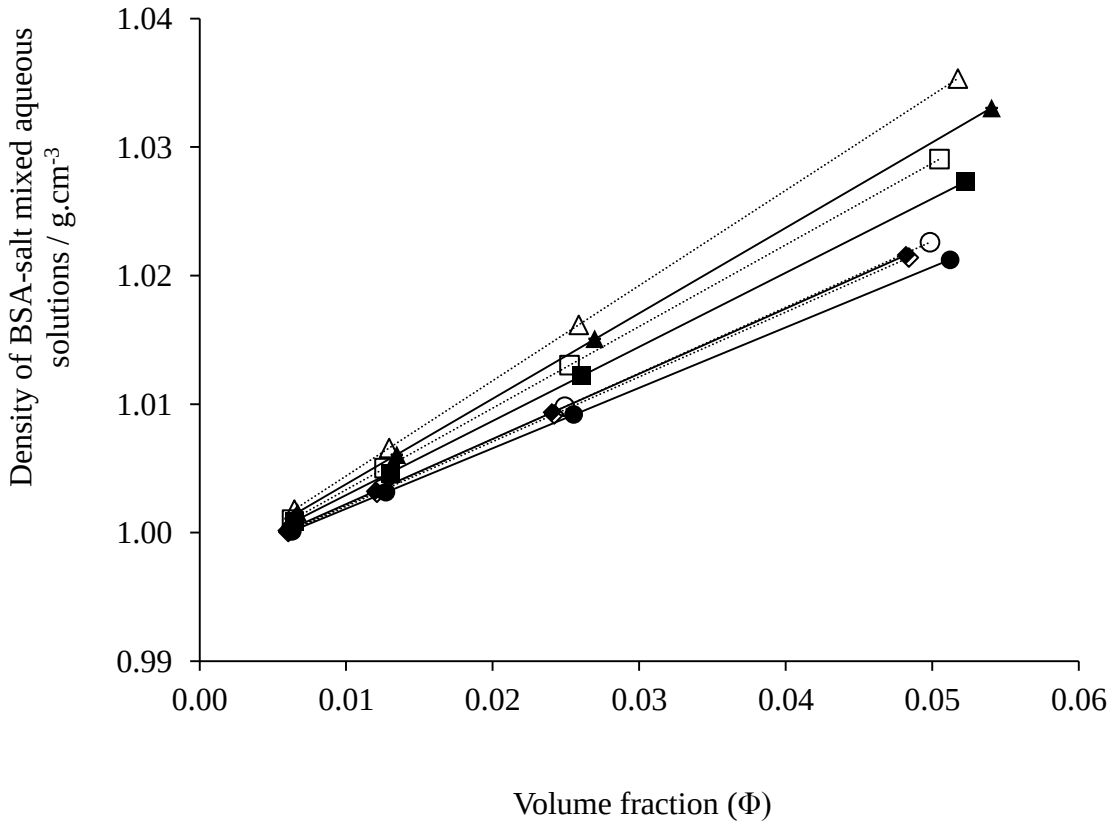

Figure 4.17. Theoretical and experimental values of change in density of BSA and four potassium halide mixed aqueous solutions against their volume fraction. Solid line with solid symbols represents experimental values whereas dotted line with hollow symbols represents theoretical values. BSA-KF (♦, ◊), BSA-KCl (●, o), BSA-KBr (■, □), and BSA-KI (▲, Δ)

Both the experimental and theoretical densities of the mixed solutions increased with increasing volume fraction although the theoretical values differ from the experimental densities. Since the experimental densities of BSA solutions do not vary much from the theoretical densities (calculated by considering hydrated BSA) of BSA solutions (**Figure 4.13**) (Chalikian, 2003; Gekko, Kimoto and Kamiyama, 2003), the variation between theoretical and experimental density values in the case of BSA-salt mixed solutions must be due to consideration of ions as nonhydrated solutes in solution during calculation of the theoretical value, and the theoretical value does not consider any

specific interaction between BSA and ions. The order of experimental density increase with volume fraction increase follows the order of BSA-KI> BSA-KBr> BSA-KF> BSA-KCl (**Figure 4.17**). Comparing the densities as a function of volume fraction for four potassium halides (**Figure 4.9**), it was found that the change in density follows the order of KF>KI>KBr>KCl. The difference between the density results of potassium halide solutions alone and that of BSA-potassium halide mixed solutions can be again attributed to the structuring of water around the ions, around the protein and around the ion-protein complex in BSA-potassium halide mixed solutions under experimental conditions. Therefore, the density of BSA and potassium halide mixed solution cannot be predicted from the density of potassium halide and that of BSA since individual density does not consider any possible interaction between the BSA and the ion, and restructuring of water due to the interaction.

Comparing the experimental density of BSA-KI mixed solutions with the corresponding theoretical density which considers nonhydrated hard I^- and hydrated BSA (**Figure 4.17**), it can be said that loosening of structure of mixed solutions occur. As a result, a less dense structure of solution is formed. Likewise, Br^- and Cl^- also make the structure of solutions less dense. On the other hand, in the case of BSA-KF mixed solutions, slightly more dense structure of solution was observed. The disparity of impact of F^- on density of BSA-salt mixed solutions compared to the effect of three other halide ions can be attributable to the small atomic number of F^- with its high charge density.

Calculation of experimental and theoretical adiabatic compressibility of BSA + potassium halide mixed solution:

The calculation of experimental adiabatic compressibility of BSA + potassium halide mixed solution was similar to the calculation of adiabatic compressibility of potassium chloride aqueous solution and BSA aqueous solution.

The theoretical value of adiabatic compressibility of BSA + potassium halide aqueous solution was calculated considering BSA as an incompressible hydrated macromolecule and potassium halides as incompressible hard spheres using the following equation:

$$K_T = K_{BSA} \times \Phi_{BSA} + K_K \times \Phi_K + K_{halide} \times \Phi_{halide} +$$

$$K_o \times [1 - (\Phi_{BSA} + \Phi_{K\,halide})] \quad (47)$$

Experimental adiabatic compressibility values and theoretically calculated adiabatic compressibility values of BSA-salt mixed solutions were plotted against volume fraction in **Figure 4.18**.

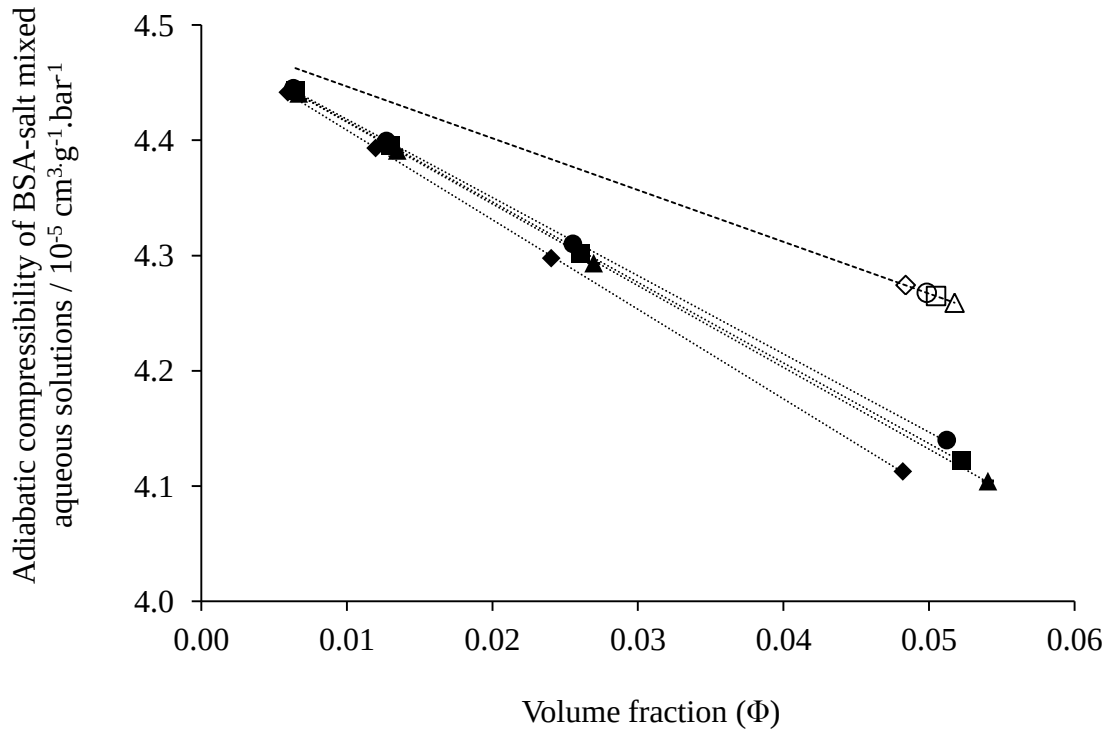

Figure 4.18. Theoretical and experimental values of adiabatic compressibility of BSA and four potassium halides mixed aqueous solutions against their volume fraction. Solid line with solid symbols represents experimental values whereas dotted line with hollow symbols represents theoretical values. BSA-KF (♦, ◊), BSA-KCl (●, o), BSA-KBr (■, □), and BSA-KI (▲, Δ)

The theoretical and experimental adiabatic compressibility values of BSA-salt mixed solutions became smaller with increase in volume fraction. The order of protein-salt mixed solutions in reducing compressibility was BSA-KF> BSA-KI> BSA-KBr> BSA-KCl. The variation of the experimental values of adiabatic compressibilities from the theoretical values might be due to consideration of the incompressibility of the hydrated BSA, potassium ion and halide ions, the presence of ions as nonhydrated entities and ignoring protein-ion interaction phenomena for calculation of the theoretical values. Thus, compressibility of BSA and ions, hydration of ions and protein-ion interactions are expected to play a role in the experimental values of compressibility. It is noted that F^- is a weak kosmotrope and Cl^-, Br^- and I^- are chaotropes, and according to the

Hofmeister series, the order of the halides is $F^- > Cl^- > Br^- > I^-$ (Zhang and Cremer, 2006). Protein stability and conformation are affected by the presence of the neutral salts of the series. Kosmotropes increase the hydrophobicity of protein-water interfaces while chaotropes increase the hydrophilicity of protein-water interfaces (Der, 2008). Depending on the surface property of the protein, specific ions bind to the proteins (Lund, Va'cha and Jungwirth, 2008). The weakly hydrated iodide ion preferably binds to hydrophobic surfaces whereas the highly hydrated fluoride ion preferably binds to charge-dense surfaces through specific anion-cation interactions (Lund, Va'cha and Jungwirth, 2008). In BSA the major anion binding sites are the arginine residues, and BSA has 23 arginine residues. Through binding with BSA, the halides were found to increase the thermostability following the order of $I^- > Br^- > Cl^-$ at ionic strengths of 0.01 and 0.1 (Yamasaki and coworkers, 1991). For comparison, in this study, the iodide, bromide and chloride ions have ionic strengths of 0.02 to 0.16 and follow the same order in reducing BSA-salt mixed solution adiabatic compressibility (**Figure 4.18**). Although a similar trend is observed in the case of the adiabatic compressibility of KF solutions in **Figure 4.10** and that of the BSA-KF mixed solutions (**Figure 4.18**), that is in reducing compressibility the most with increase in volume fraction, the reduction trend was steeper in the case of KF solutions alone compared to the BSA-KF mixed solutions. Moreover, the sequence in the compressibility reduction trend was not the same among the rest of the potassium halides solutions compared to the mixed BSA-KCl, BSA-KBr and BSA-KI solutions. One possible reason behind these disparities might be the hydration or water structuring phenomenon. The adiabatic compressibility of BSA and potassium halide mixed solution cannot be predicted from the adiabatic compressibility of potassium halide and that of BSA since individual adiabatic compressibility does not

consider any interaction between BSA and ion, and the effect of consequent restructuring of water due to the interaction.

4.6. Determination of partial specific volume and partial specific adiabatic compressibility

4.6.1. Partial specific volume

Apparent partial specific volume or $(1- \Phi_o)/c$ was calculated for potassium halides in water, BSA in water and BSA-potassium halides in water using density of solutions, solvent and concentration of solute in g cm^{-3}. The apparent partial specific volume of potassium halide, BSA and BSA-potassium halide solutions are plotted against concentration in **Figure 4.19**, **Figure 4.20** and **Figure 4.21,** respectively. The experimental data points are reported in the figures with standard deviation as error bars. A nonlinear relationship between the apparent partial specific volume and concentration was observed. In order to figure out the curve of apparent specific volume change as a function of concentration, a line was drawn using the highest concentrations data points, and another line was using the lowest concentrations data points. Then a tangent line was drawn to the curve where the tangent line passed through a value of apparent specific volume of the curve. Determination of partial quantities using this method is known as the method of intercepts (Mortimer, 2008, p. 192-193). Extrapolation to zero concentration was performed in order to get the partial specific volumes. The partial specific volumes with standard deviations are presented in **Table 4.6**. For clarification, determination of partial specific volume with standard deviation of BSA can be explained. There are 5 apparent specific volume values at 5 different concentrations

which can be marked as 1, 2, 3, 4, and 5 ranking from low to high concentrations (**Figure 4.20**). A linear line was drawn using the highest concentrations data points (4 and 5), and another linear line was drawn using the lowest concentrations data points (1 and 2). As a result, a curve of apparent specific volume change with data points 2, 3 and 4 was found. Now, a tangent line was drawn using data points 2 and 3 considering the tangent point resides in between data points 2 and 3. Again, another tangent line was drawn using data points 3 and 4 considering the tangent point resides in between data points 3 and 4. By extrapolating to zero concentration, from these 2 tangent lines two values of partial specific volume were found, and the average value was considered as actual partial specific volume. The standard deviation was calculated from the values of partial specific volume used to calculate the average value of partial specific volume.

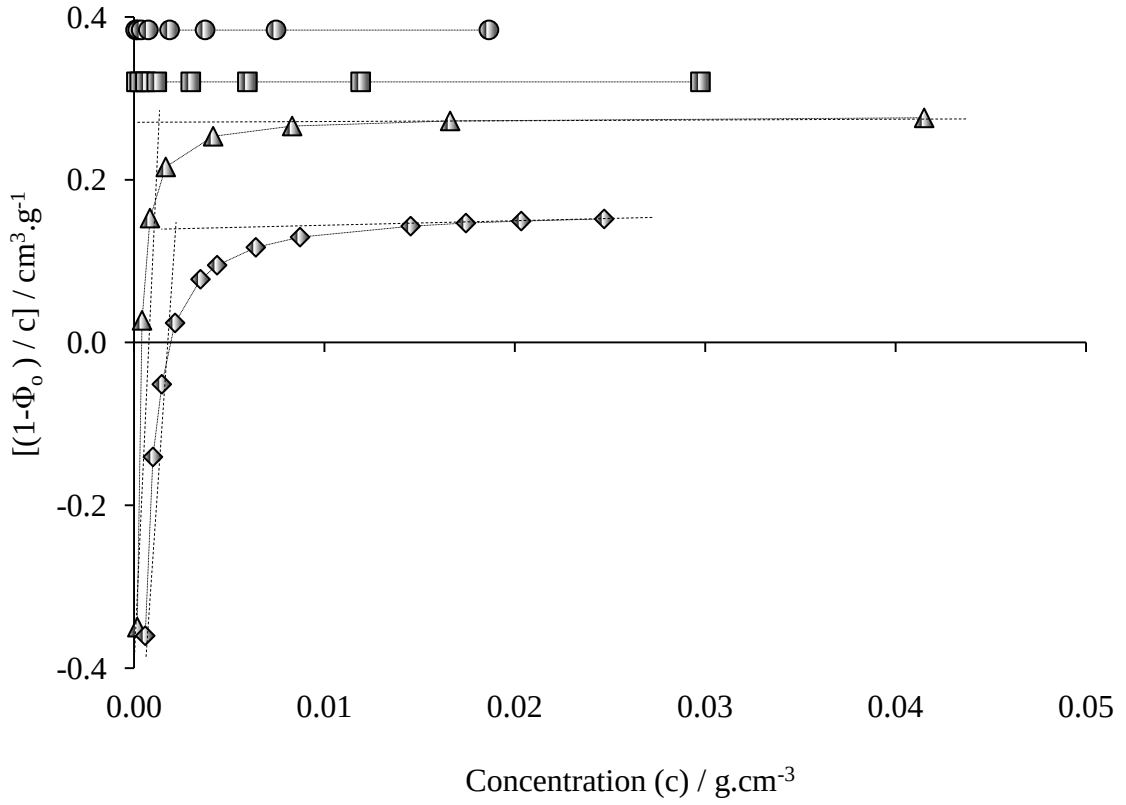

Figure 4.19. [(1 – Φ_o) / c] against concentration for four potassium halide aqueous solutions. Potassium fluoride (diamond), potassium chloride (circle), potassium bromide (square), and potassium iodide (triangle). Gradient symbols represent calculations based on literature values

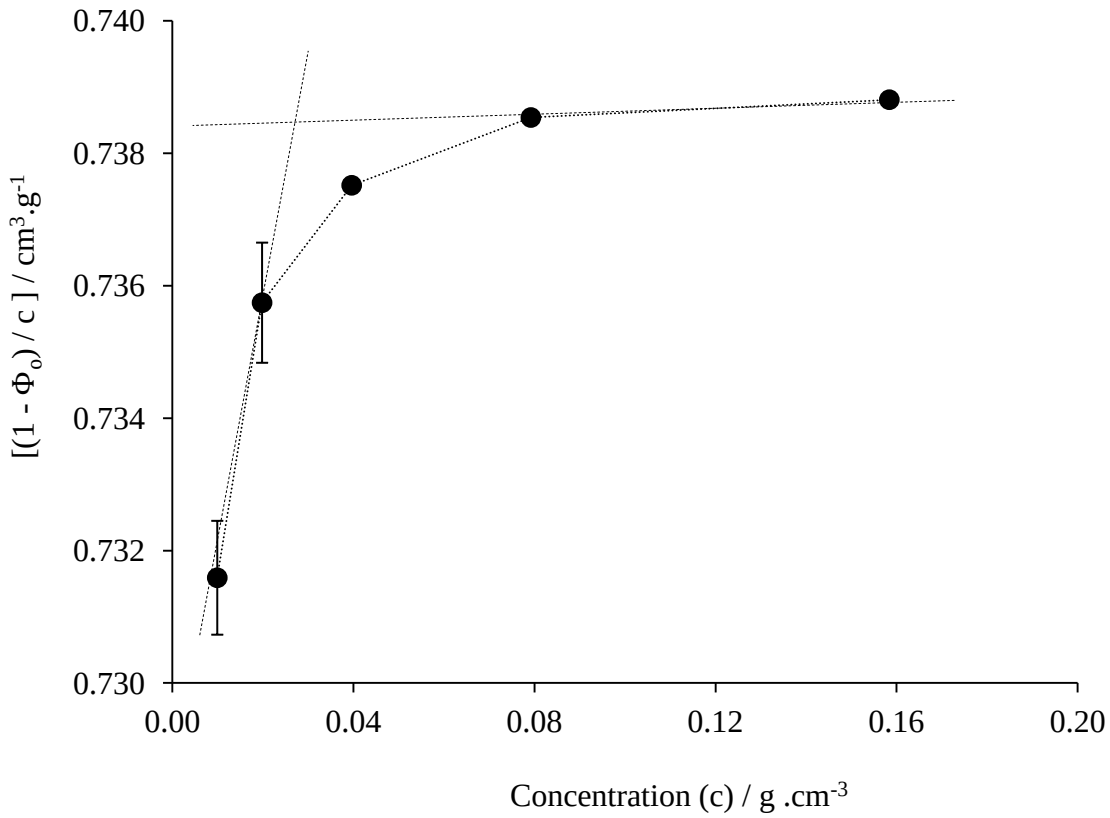

Figure 4.20. **[**$(1 - \Phi_o) / c]$ against concentration for BSA aqueous solutions

Calculation of concentration in g cm^{-3} of BSA + potassium halide mixed solutions:

The concentration calculation in g cm^{-3} of (0.12 mmol.dm^{-3}) BSA + (20 mmol.dm^{-3}) KCl mixed solution (the concentrations of BSA and KCl presented in bracket are the final concentrations in the mixed solution) is given as an example:

0.120 mmol.dm^{-3} BSA solution = 66000 x 0.120 / (1000 x 1000) g.cm^{-3}

$$= 0.008 \text{ g.cm}^{-3}$$

20 mmol.dm^{-3} KCl solution =74.55 x 20 / (1000 x 1000) g.cm^{-3}

$$= 0.002 \text{ g.cm}^{-3}$$

Thus, the ultimate concentration of total solutes (BSA + KCl) in solution = (0.008 + 0.002) $g.cm^{-3}$

= 0.010 $g.cm^{-3}$

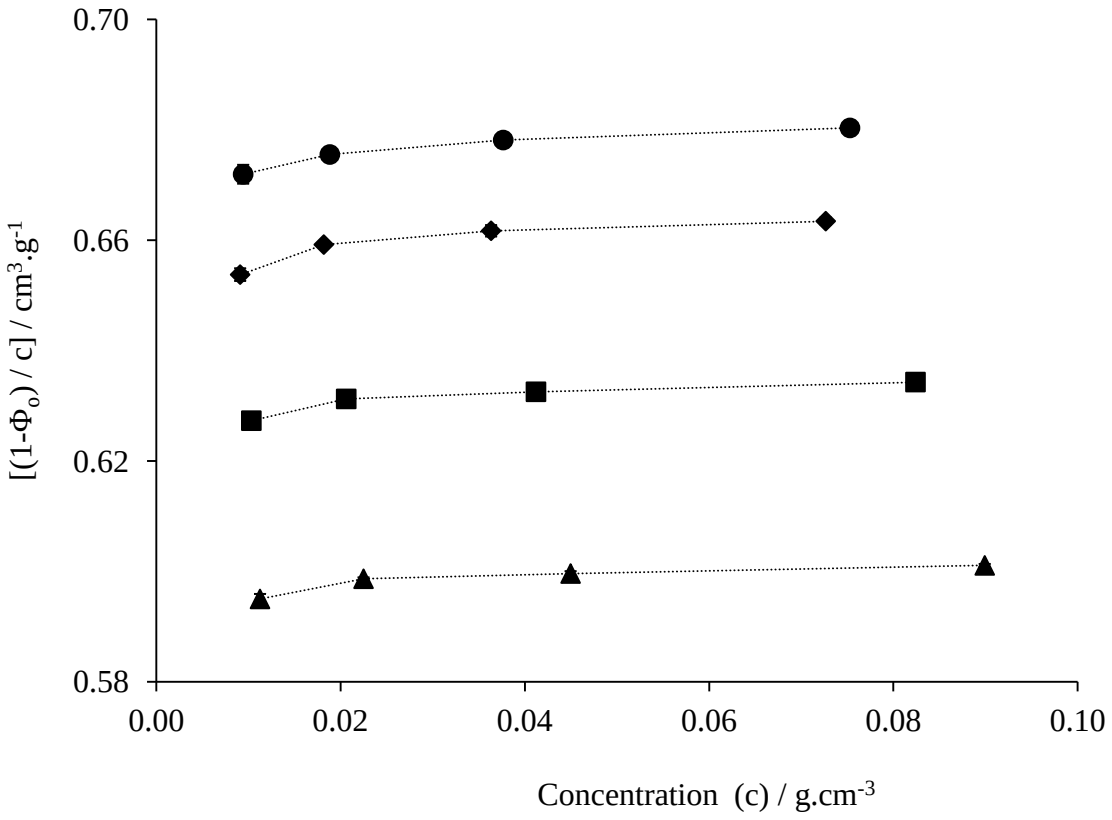

Figure 4.21. $[(1 - \Phi_o) / c]$ against concentration for BSA-salt aqueous solutions. BSA-potassium fluoride (diamond), BSA-potassium chloride (circle), BSA-potassium bromide (square), and BSA-potassium iodide (triangle)

Table 4.6. Partial specific volumes of protein and salt component individually and protein-salt in aqueous solutions at 25 ^{o}C

Solute component	Experimental partial specific volume, v^{o} ($cm^{3}.g^{-1}$)
BSA	0.735 ± 0.002
KCl	0.384 ± 0.000
KBr	0.320 ± 0.000
KI	0.174 ± 0.077
KF	0.019 ± 0.062
BSA + KCl	0.671 ± 0.003
BSA + KBr	0.627 ± 0.005
BSA + KI	0.595 ± 0.005
BSA+ KF	0.653 ± 0.006

The experimentally derived partial specific volume of BSA agrees with the literature values (**Table 4.7**) (Chalikian, Totrov, Abagyan and Breslauer, 1996; Dayhoff, Perlmann and MacInnes, 1952; Gekko and Hasegawa, 1986) which gives confidence in the values obtained for the partial specific volume of potassium halides and the BSA-potassium halides compositions.

Table 4.7. Comparison of experimental value and literature values for partial specific volume of BSA at 25 ^{o}C

Reference	Partial specific volume, v^o ($cm^3.g^{-1}$)
Experimental value	0.735 ± 0.002
Chalikian, Totrov, Abagyan and Breslauer, 1996	0.735 ± 0.003
Dayhoff, Perlmann and MacInnes, 1952	0.734 ± 0.001
Gekko and Hasegawa, 1986	0.735 ± 0.001

4.6.2. Partial specific adiabatic compressibility

The partial specific adiabatic compressibility coefficient can be calculated using the equation:

$$\beta_s^o = -\left(\frac{1}{v^o}\right)\frac{\delta v^o}{\delta P} = \left(\frac{\beta_o}{v^o}\right)\lim_{c\to 0}\left[\frac{(\beta/\beta_o - \Phi_o)}{c}\right] \quad (48)$$

and the partial specific adiabatic compressibility can be calculated using equation:

$$k_s^o = \beta_s^o\, v^o \quad (49)$$

Thus,

$$k_s^o = \beta_o \lim_{c\to 0}\left[\frac{(\beta/\beta_o - \Phi_o)}{c}\right] \quad (50)$$

In order to determine $\lim_{c\to 0}[(\beta / \beta_o - \Phi_o) / c]$ for potassium halides in water, BSA in water and BSA-potassium halides in water, $[(\beta / \beta_o - \Phi_o) / c]$ was determined. The graphs of $[(\beta / \beta_o - \Phi_o) / c]$ against concentration for potassium halides in water, BSA in water and

BSA-potassium halides in water were drawn in **Figure 4.22**, **Figure 4.23** and **Figure 4.24** respectively. The experimental data points are reported in the figures with standard deviation as error bars. A nonlinear relationship between $[(\beta / \beta_o - \Phi_o) / c]$ and concentration was observed. In order to get the values of $\lim_{c \to 0} [(\beta / \beta_o - \Phi_o) / c]$, the same method was followed which was used to determine the partial specific volume of potassium halides, BSA and BSA-potassium halides. The values of $\lim_{c \to 0} [(\beta / \beta_o - \Phi_o) / c]$ are presented in **Table 4.8**. The compressibility coefficient of the solvent water, or β_o, is 4.48×10^{-5} bar^{-1}. Thus, using the value of β_o, v^o (partial specific volume in **Table 4.6**) and $\lim_{c \to 0} [(\beta / \beta_o - \Phi_o) / c]$, the partial specific adiabatic compressibility coefficient (β_s^o) and the partial specific adiabatic compressibility (k_s^o) of solutes were determined, and the values are presented in **Table 4.8**.

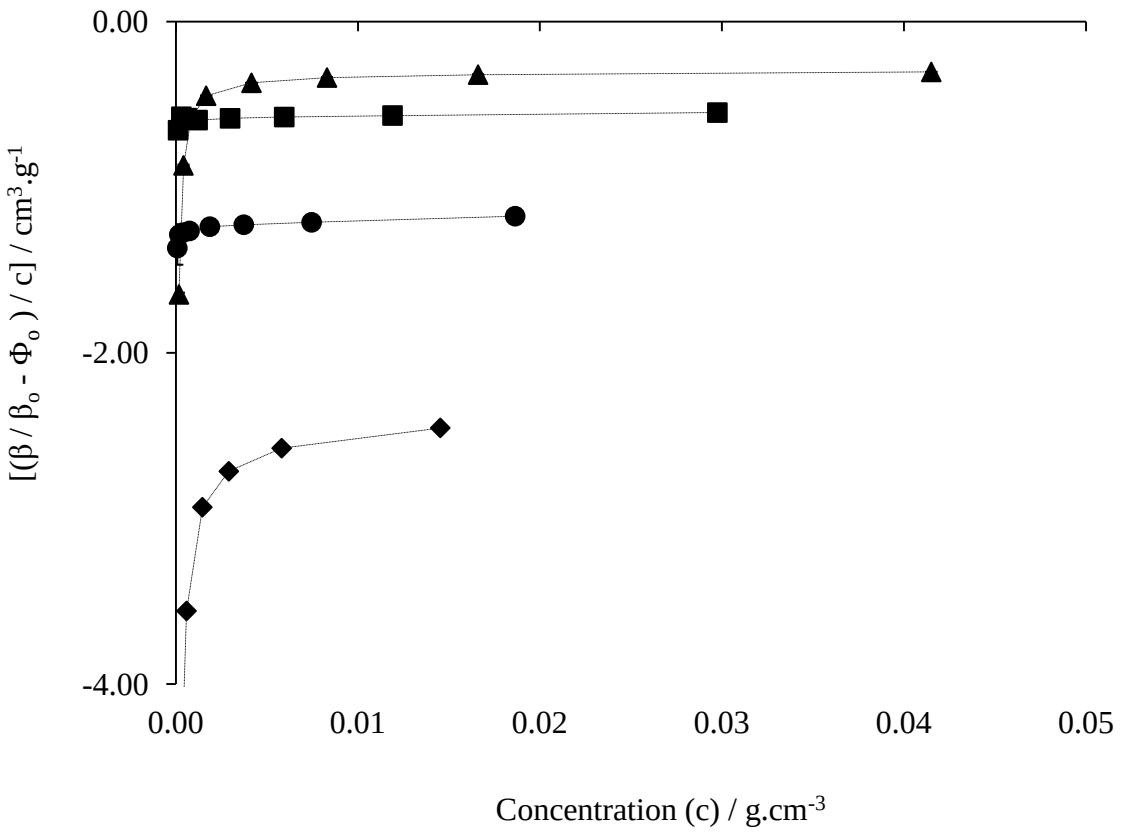

Figure 4.22. $[(\beta / \beta_o - \Phi_o) / c]$ against concentration for four potassium halide aqueous solutions. Potassium fluoride (diamond), potassium chloride (circle), potassium bromide (square), and potassium iodide (triangle)

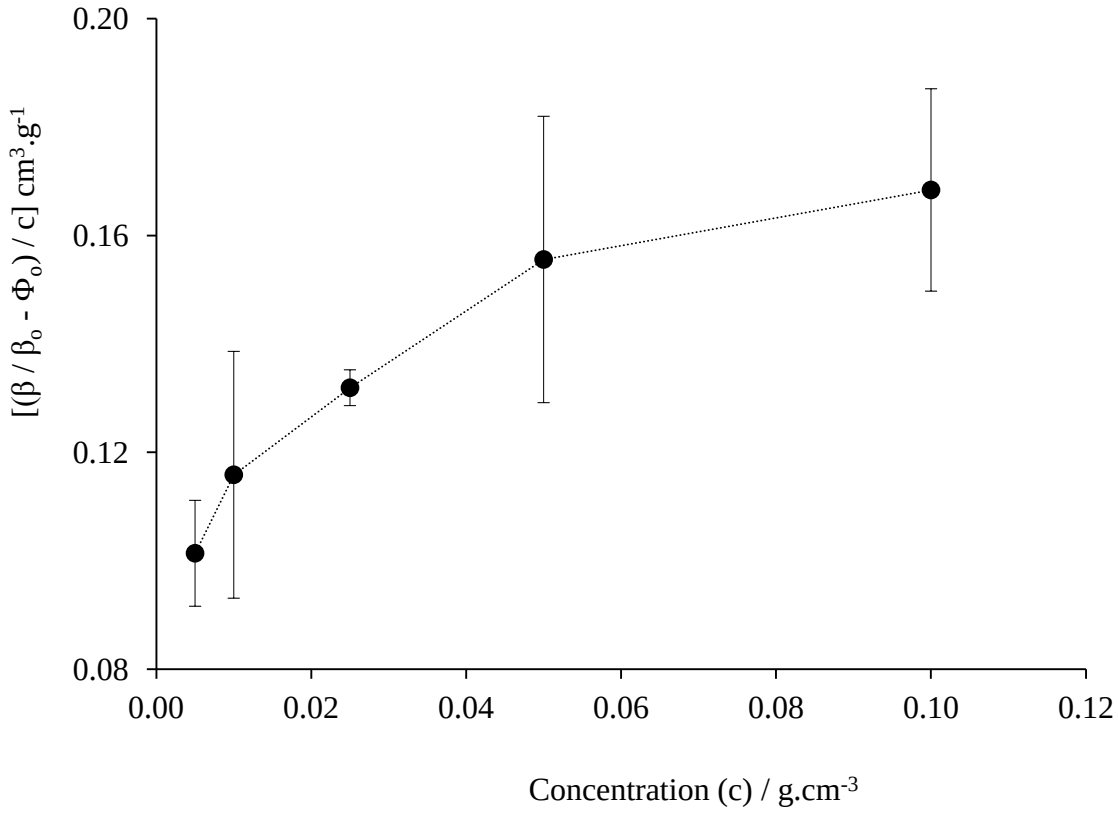

Figure 4.23. **[**(β / β_o – Φ_o) / c)] against concentration for BSA aqueous solutions

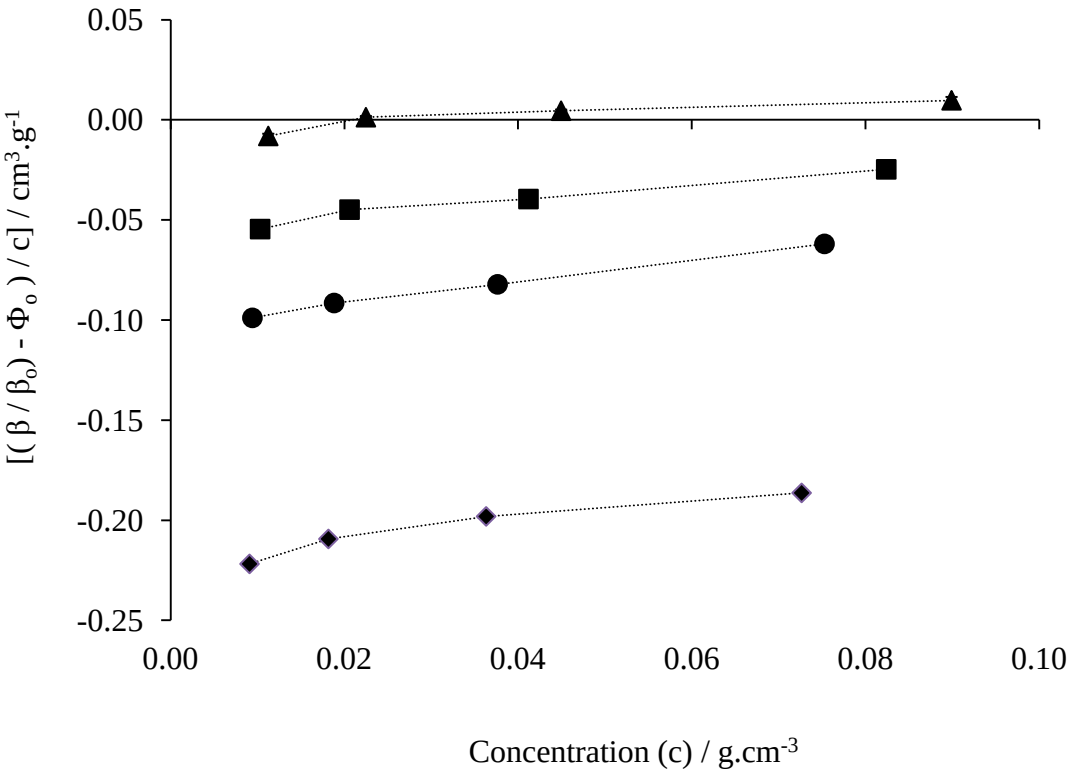

Figure 4.24. $[(\beta / \beta_o - \Phi_o) / c)]$ against concentration for BSA-salt aqueous solutions. BSA-potassium fluoride (diamond), BSA-potassium chloride (circle), BSA-potassium bromide (square) and BSA-potassium iodide (triangle)

Table 4.8. $\lim_{c\to 0}[(\beta / \beta_o - \Phi_o) / c]$, β_s^o and k_s^o of protein and salt components individually and protein-salt in aqueous solutions at 25 ^oC

Solute component	$\lim_{c\to 0}[(\beta / \beta_o - \Phi_o) / c]$ ($cm^3.g^{-1}$)	β_s^o (x 10^{-6} bar^{-1})	k_s^o (x 10^{-6} $cm^3.g^{-1}.bar^{-1}$)
BSA	0.11 ± 0.00	6.50 ± 0.10	4.78 ± 0.10
KCl	-1.27 ± 0.02	-148.47 ± 2.23	-57.01 ± 0.86
KBr	-0.59 ± 0.01	-83.09 ± 1.15	-26.59 ± 0.37
KI	-0.54 ± 0.16	-139.52 ± 42.45	-24.28 ± 7.39
KF	-3.00 ± 0.21	-7024.71 ± 0.00	-134.52 ± 9.31
BSA + KCl	-0.10 ± 0.00	-6.89 ± 0.19	-4.62 ± 0.13
BSA + KBr	-0.06 ± 0.01	-4.02 ± 0.52	-2.52 ± 0.32
BSA + KI	-0.01 ± 0.01	-0.50 ± 0.70	-0.30 ± 0.42
BSA+ KF	-0.22 ± 0.01	-15.20 ± 0.84	-9.93 ± 0.55

Table 4.9. Comparison of experimental value and literature values for partial specific adiabatic compressibility of BSA at 25 ^{o}C

Reference	Partial specific adiabatic compressibility, k_s^o (x 10^{-6} $cm^3.g^{-1}.bar^{-1}$)
Experimental value	4.8 ± 0.10
Chalikian, Totrov, Abagyan and Breslauer, 1996	6.6 ± 0.5
Gekko and Hasegawa, 1986	7.7 ± 0.12
Iqball and Verrall, 1987	5.5

Gekko and Hasegawa (1986) established a linear regression relationship between partial specific compressibility coefficient of globular proteins and partial specific volume with a correlation coefficient of 0.85:

$$\beta_s^o = (185.0\, v^o - 129.3)\, 10^{-6} \text{ bar}^{-1} \quad (51)$$

Using the above relationship the calculated partial specific adiabatic compressibility coefficient of BSA is 6.49 x 10^{-6} bar^{-1} which matches with the experimental value (**Table 4.8**). The researchers (Gekko and Hasegawa, 1986) also established a linear regression relationship between partial specific compressibility coefficient of globular proteins and hydrophobicity with a correlation coefficient of 0.70:

$$\beta_s^o = \left(0.0293\, H_\phi - 22.37\right) 10^{-6} \text{ bar}^{-1} \quad (52)$$

Where H_ϕ is the total hydrophobicity divided by the number of residues, that is, 990 for BSA (Gekko and Hasegawa, 1986). Using the above relationship the calculated partial specific adiabatic compressibility coefficient of BSA is 6.64 x 10^{-6} bar^{-1} which also

matches with the experimental value (**Table 4.8**). Therefore, although the experimental adiabatic compressibility shows variation from the literature values, I have confidence in the experimental values.

Considering partial specific compressibility, it can be said that BSA is much more compressible than the potassium halides. The order of rigidity of potassium halides is KF > KCl > KBr > KI. Moreover, the order of rigidity of BSA+ K halides is (BSA+KF) > (BSA+KCl) > (BSA+KBr) > (BSA+KI). Both of the rigidity orders are similar to the Hofmeister series order (Zhang and Cremer, 2006).

4.7. Investigation of interaction between BSA and potassium halides in aqueous solution

4.7.1 Consideration of density of BSA-potassium halides mixed aqueous solution

The partial specific volumes of BSA and potassium halides (**Table 4.6**) were considered in calculating the density values of BSA-potassium halides mixed solutions; the calculation was similar to the calculation of theoretical density value of BSA using the partial specific volume of BSA. The partial specific volume of BSA in **Table 4.6** was derived using the experimentally measured density values whereas the partial specific volumes of potassium halides in **Table 4.6** were derived using density values from the literature. The calculated density values only consider the structuring of water around ions and protein molecules and do not reflect the ion-protein interaction phenomenon. Again, the partial specific volumes of BSA and potassium halides (**Table 4.6**) were considered in calculating the calculated values of volume fraction of BSA-potassium

halides mixed solutions, and the calculation was similar to the calculation of theoretical volume fraction value of BSA using the literature derived partial specific volume of BSA. The calculation of experimental volume fraction of BSA and potassium halide mixed solutions was similar to the calculation of experimental volume fraction values of BSA aqueous solutions. The calculated density values of BSA-KCl, BSA-KBr, BSA-KI and BSA-KF mixed aqueous solutions were compared against the experimental density values of the solutions against volume fraction in **Figure 4.25, Figure 4.26, Figure 4.27** and **Figure 4.28,** respectively. Since the calculated values do not consider solute-solute interactions, if the experimental density points nicely overlaid the calculated density values, it can be said that no interaction took place between BSA and the potassium and halide ions in the BSA-potassium mixed solution. Deviation of the experimental density line from the calculated density line would reflect interactions between BSA and the potassium halide used in the mixed aqueous solution.

In **Figure 4.25** the experimentally derived densities of BSA-KCl mixed aqueous solutions nicely overlaid the calculated density values. Therefore, it can be said that there is no interaction between BSA and KCl within the used concentration range and experimental condition.

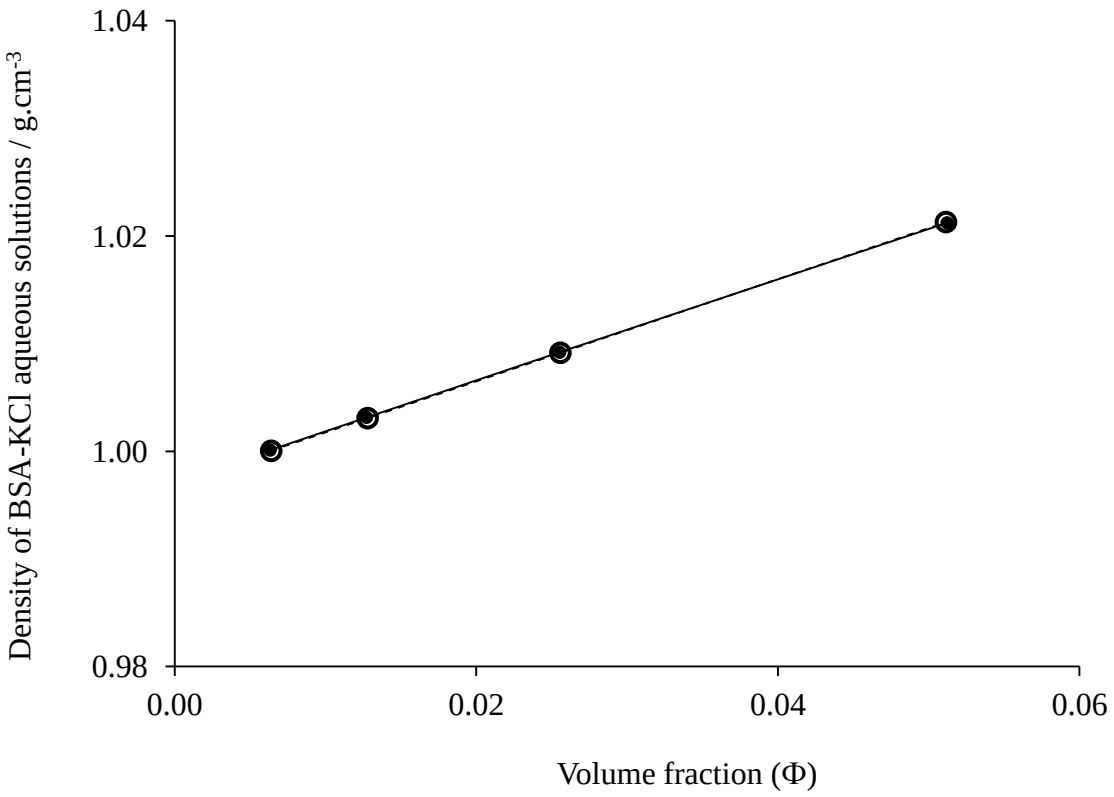

Figure 4.25. Comparison of density against volume fraction for BSA-KCl aqueous solutions. Solid (circle) symbols with solid line represent experimentally derived density values and hollow (circle with dark line) symbols with dashed line represent density values calculated using partial specific volume (**Table 4.6**)

In **Figure 4.26,** the experimentally derived density values of BSA-KBr mixed aqueous solutions deviate slightly from the calculated density values derived from partial specific volume of BSA and KBr. Thus, there might be some interaction between BSA and KBr within the used concentration range.

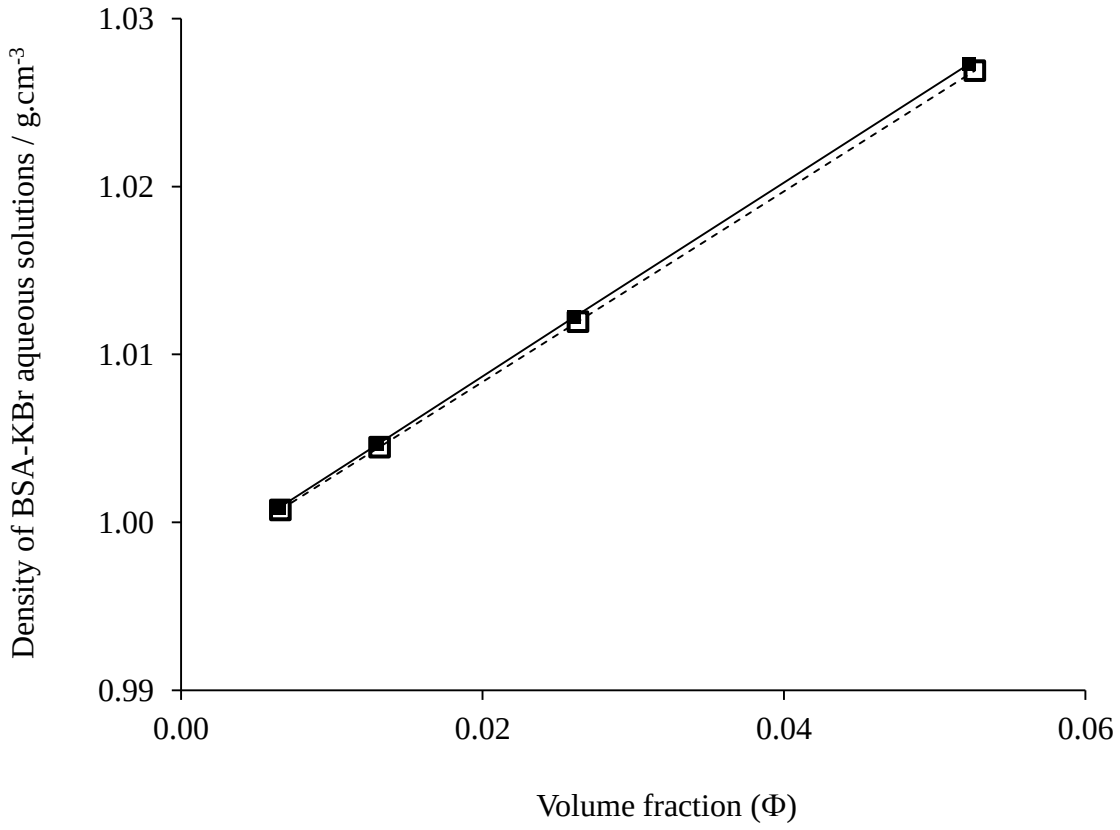

Figure 4.26. Comparison of density against volume fraction for BSA-KBr aqueous solutions. Solid (square) symbols with solid line represent experimentally derived density values and hollow (square with dark line) symbols with dashed line represent density values calculated using partial specific volume (**Table 4.6**)

In **Figure 4.27,** it can be seen that the experimentally derived density values of BSA-KI mixed aqueous solutions deviate distinctively from the calculated density line. Accordingly, there must be interaction between BSA and I^- ions in BSA-KI mixed aqueous solution.

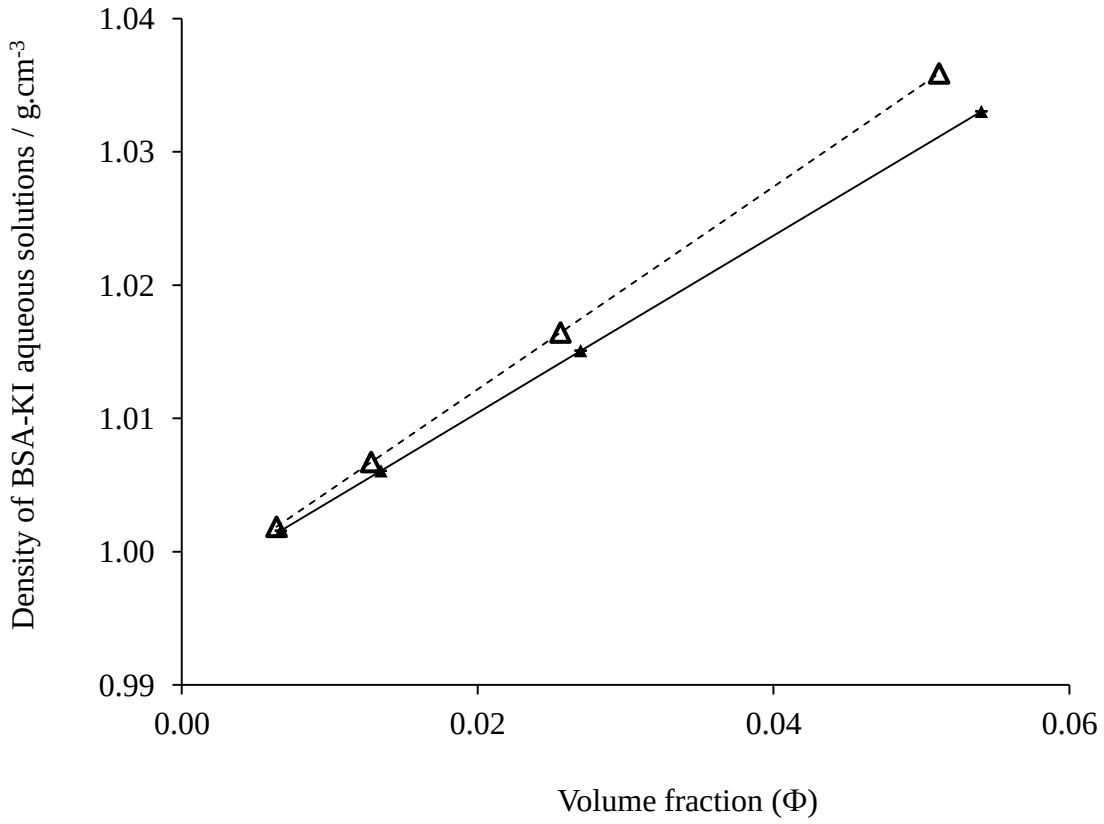

Figure 4.27. Comparison of density against volume fraction for BSA-KI aqueous solutions. Solid (triangle) symbols with solid line represent experimentally derived density values and hollow (triangle with dark line) symbols with dashed line represent density values calculated using partial specific volume (**Table 4.6**)

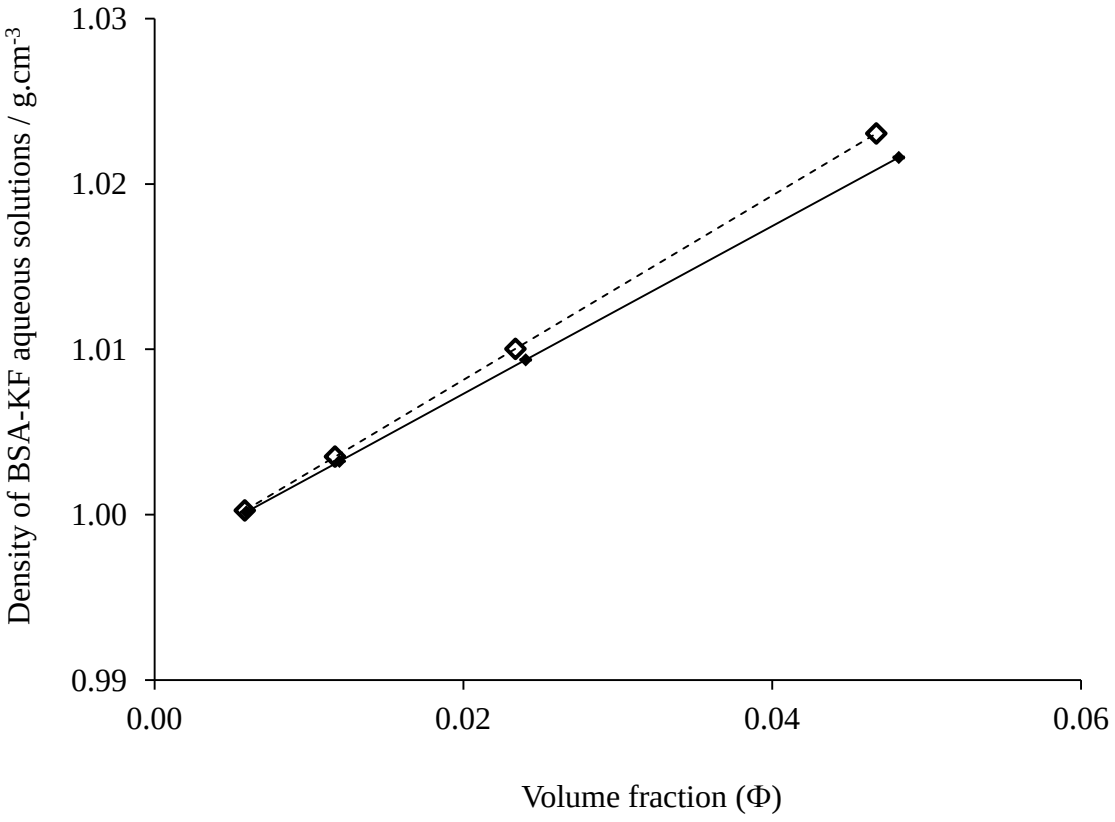

Figure 4.28. Comparison of density against volume fraction for BSA-KF aqueous solutions. Solid (diamond) symbols with solid line represent experimentally derived density values and hollow (diamond with dark line) symbols with dashed line represent density values calculated using partial specific volume (**Table 4.6**)

Just as for the BSA-KI mixed aqueous solutions, in **Figure 4.28,** the experimentally derived density line of the BSA-KF mixed aqueous solutions departs from the calculated density line of BSA-KF mixed aqueous solutions. Hence, F^- ion interacts with BSA within the used experimental condition.

Table 4.10. Comparison of the experimental density value and the density value calculated from partial specific volume (**Table 4.6**) of BSA-salt mixed aqueous solutions for **Figure 4.25** to **Figure 4.28** when both experimental and calculated density lines extrapolate to zero volume fraction

	Experimental density value ($g.cm^{-3}$)	Density value calculated using partial specific volume ($g.cm^{-3}$)	Density of water at 25 ^{o}C ($g.cm^{-3}$)
BSA-KCl mixed aqueous solution	0.997	0.997	0.997
BSA-KBr mixed aqueous solution	0.997	0.997	-
BSA-KI mixed aqueous solution	0.997	0.997	-
BSA-KF mixed aqueous solution	0.997	0.997	-

According to **Table 4.10**, for all the BSA-potassium halide mixed aqueous solutions, the experimental density values and the density values calculated from the partial specific volume (**Table 4.6**) at zero volume fraction extrapolation resemble the density value of water at 25 ^{o}C. Thus, at zero volume fraction, the density of all the BSA-potassium halide mixed solutions behaves like the density of water.

4.7.2 Consideration of adiabatic compressibility of BSA-potassium halides mixed aqueous solution

In order to deduce information on the interaction between BSA and halide ions from adiabatic compressibility measurements, the adiabatic compressibility of BSA-potassium halide mixed solutions was calculated from the individual measurements of

BSA and the potassium halide. Partial specific volumes of the individual BSA and potassium halides were used to determine the volume fraction. Finally, the adiabatic compressibility of BSA-potassium halides mixed aqueous solutions ($K_{(BSA + K\ halide)}$) was calculated using the following equation:

$$K_{(BSA + K\ halide)} = K_{BSA} \times \Phi_{BSA} + K_{K\ halide} \times \Phi_{K\ halide} +$$

$$K_o \times [1 - (\Phi_{BSA} + \Phi_{K\ halide})] \quad (53)$$

The experimentally derived adiabatic compressibility of BSA- KCl, BSA-KBr, BSA-KI and BSA-KF mixed aqueous solutions were compared against the theoretically calculated adiabatic compressibility values as a function of volume fraction in **Figure 4.29, Figure 4.30, Figure 4.31 and Figure 4.32** respectively.

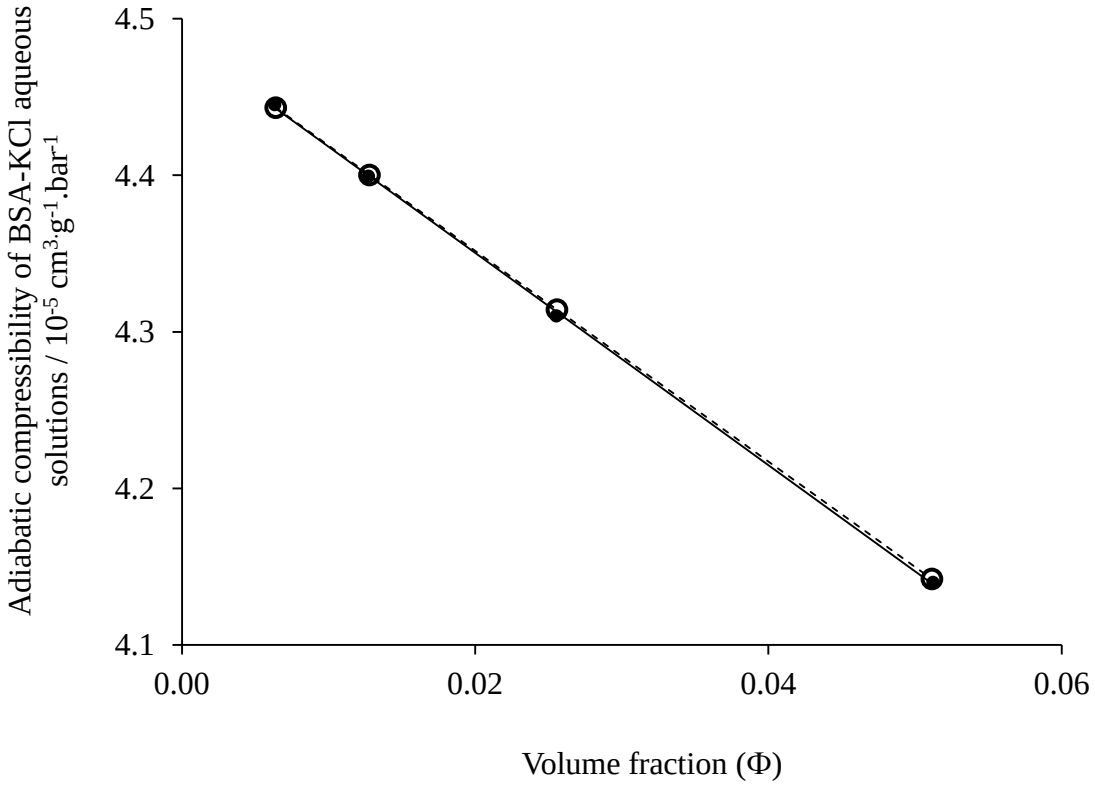

Figure 4.29. Comparison of adiabatic compressibility against volume fraction for BSA-KCl aqueous solutions. Solid (circle) symbols with solid line represent experimentally derived compressibility values and hollow (circle with dark line) symbols with dashed line represent calculated compressibility values

In **Figure 4.29,** similarly to density observations, the experimentally derived adiabatic compressibility of BSA-KCl mixed aqueous solutions nicely overlaid on the calculated adiabatic compressibility values. Therefore, it can be said that there is no interaction between BSA and KCl within the used concentration range and experimental conditions.

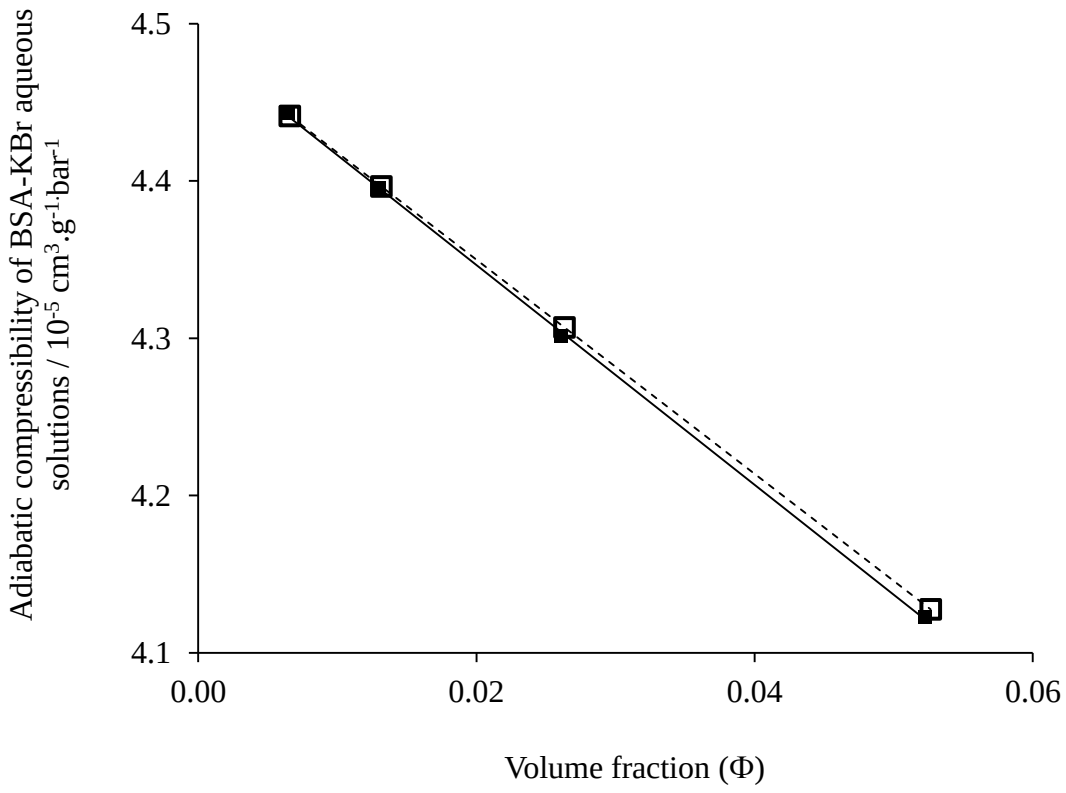

Figure 4.30. Comparison of adiabatic compressibility against volume fraction for BSA-KBr aqueous solutions. Solid (square) symbols with solid line represent experimentally derived compressibility values and hollow (square with dark line) symbols with dashed line represent calculated compressibility values

In **Figure 4.30,** the experimentally derived adiabatic compressibility values of BSA-KBr mixed aqueous solutions slightly deviate from the calculated adiabatic compressibility values derived from partial specific volume of BSA and KBr and from adiabatic compressibility of BSA and KBr. Thus, there might be interaction between BSA and Br^- ions within the used concentration range.

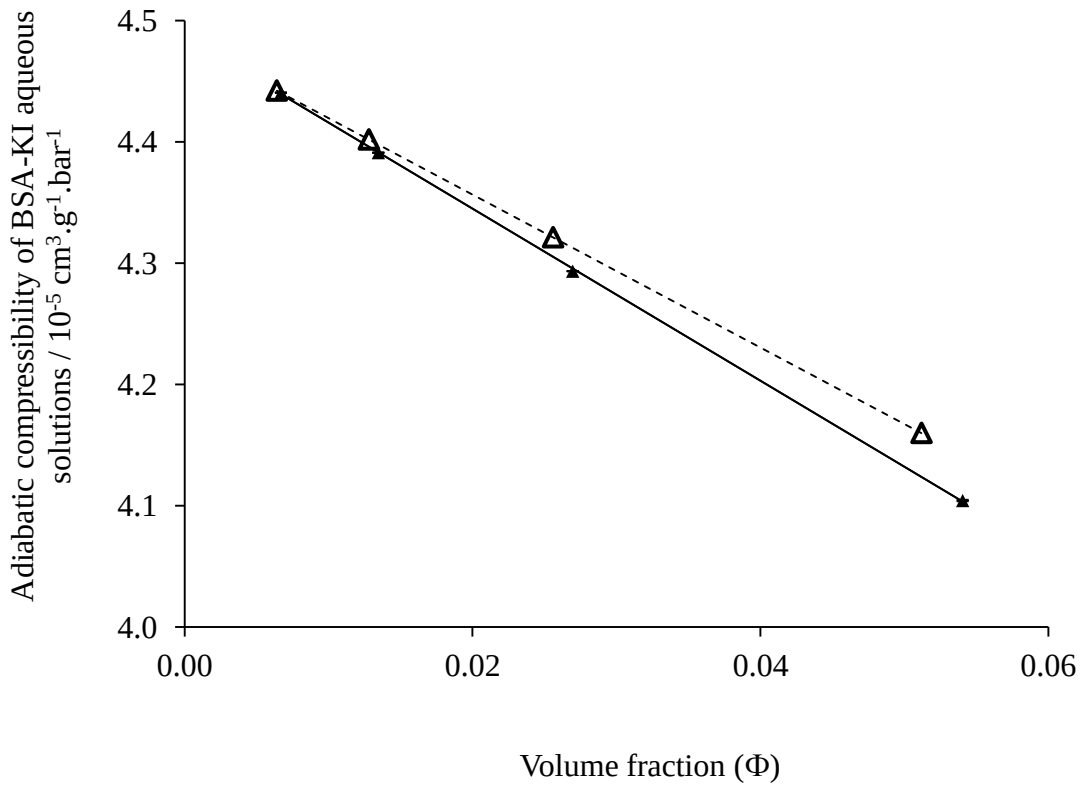

Figure 4.31. Comparison of adiabatic compressibility against volume fraction for BSA-KI aqueous solutions. Solid (triangle) symbols with solid line represent experimentally derived compressibility values and hollow (triangle with dark line) symbols with dashed line represent calculated compressibility values

In **Figure 4.31,** the experimentally derived adiabatic compressibility values of BSA-KI mixed aqueous solution distinctively deviate from the calculated adiabatic compressibility line. Accordingly, there must be interaction between BSA and I^- ions in BSA-KI mixed aqueous solution.

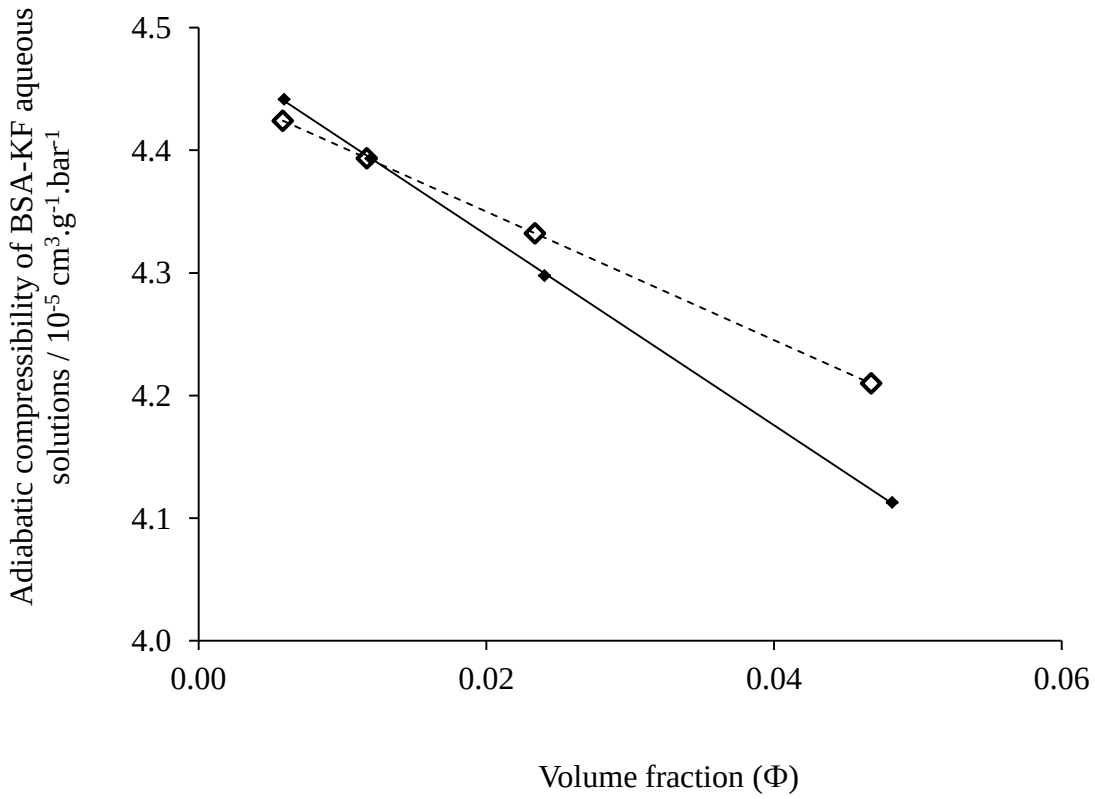

Figure 4.32. Comparison of adiabatic compressibility against volume fraction for BSA-KF aqueous solutions. Solid (diamond) symbols with solid line represent experimentally derived compressibility values and hollow (diamond with dark line) symbols with dashed line represent calculated compressibility values

Just as for the BSA-KI mixed aqueous solution, in **Figure 4.32,** the experimentally derived adiabatic compressibility line of the BSA-KF mixed aqueous solutions departs from the calculated adiabatic compressibility line of BSA-KF mixed aqueous solutions. Hence, F^- ion interacts with BSA within the used experimental condition.

Table 4.11. Comparison of the experimental adiabatic compressibility value and the calculated adiabatic compressibility value of BSA-salt mixed aqueous solutions for **Figure 4.29** to **Figure 4.32** when both experimental and calculated compressibility lines extrapolate to zero volume fraction

	Experimental adiabatic compressibility value ($\times 10^{-5}$ $cm^3.g^{-1}.bar^{-1}$)	Calculated adiabatic compressibility value ($\times 10^{-5}$ $cm^3.g^{-1}.bar^{-1}$)	Adiabatic compressibility of water at 25 ^oC ($\times 10^{-5}$ $cm^3.g^{-1}.bar^{-1}$)
BSA-KCl mixed aqueous solution	4.49	4.49	4.49
BSA-KBr mixed aqueous solution	4.49	4.49	-
BSA-KI mixed aqueous solution	4.49	4.48	-
BSA-KF mixed aqueous solution	4.49	4.46	-

According to **Table 4.11**, the experimental adiabatic compressibility values for all the BSA-potassium halide mixed aqueous solutions, and the calculated adiabatic compressibility values for BSA-KCl mixed aqueous solution and BSA- KBr mixed aqueous solution at zero volume fraction extrapolation resemble those of the adiabatic compressibility value of water at 25 ^oC, but the calculated adiabatic compressibility values for BSA-KI mixed aqueous solution and for BSA- KF mixed aqueous solution at zero volume fraction extrapolation were lower compared to the adiabatic compressibility value of water at 25 ^oC.

Thus, according to both density and adiabatic compressibility results, interaction occurs between BSA and Br^-, I^- and F^- in aqueous solution of BSA-KBr, BSA-KI and BSA-KF.

Ayranci and Duman (2004) reported that, at pH = 7.1, BSA interacts with the halide ions F^-, Br^- and I^- in aqueous solution. Considering the density and compressibility of BSA-potassium halides mixed aqueous solutions, it is observed that high interaction occurs between the BSA and the halide ions I^- and F^- as the experimental line distinctively deviates from the calculated line in the case of both BSA-KI mixed aqueous solutions and BSA-KF mixed aqueous solutions whereas low interaction occurs between the BSA and the Br^- as the experimental line slightly deviates from the calculated line in the case of BSA-KBr mixed aqueous solutions and no interaction occurs between the BSA and the Cl^- as the experimental line does not deviate from the calculated line in the case of BSA-KCl mixed aqueous solutions. In this study, the binding sequence of the halide ions to the BSA does not follow the sequence of ions in the Hofmeister series. According to Nandi and Robinson (1972), salting in of the peptide group is an ion-specific reaction where the sequence of the salting-in constant follows the sequence of the Hofmeister series. Therefore, it can be said that within the used concentration range the binding of the halide ions to the BSA is ion non-specific. The poorly hydrated halide ions such as iodide and bromide might bind to the hydrophobic groups and residues of BSA surface, and the highly hydrated halide ion, fluoride, might bind to BSA by specific anion-cation interactions (Heyda, Vincent, Tobias, Dzubiella and Jungwirth, 2010; Lund, Va´cha, and Jungwirth, 2008).

5. Conclusions

The Hofmeister salts effect on the aqueous solution of protein bovine serum albumin considering adiabatic compressibility and density was studied in this thesis. With the aid of density and compressibility, the binding of the halides to BSA in aqueous solution was examined. The validity of hard sphere model in analyzing density and compressibility of aqueous solutions was also considered.

In the initial stage of research, in order to confirm the reliability of Millipore water, viscosity of Millipore water from two different sources at 25 ^{o}C was determined, and the values of viscosity of water from the two sources was similar which gave trustworthiness of the used Millipore water. Again the experimental relative viscosity of aqueous solutions (a concentration range of 1 mmol.dm^{-3} to 250 mmol.dm^{-3}) of KCl and that of KBr were compared with the theoretically derived relative viscosity; in the case of both potassium halide solutions, the curve pattern of the experimental and the theoretical relative viscosity values were comparable to each other. Since accurate measurement of relative viscosity of electrolyte solutions need precision from the experimentalist in sample solution preparation (Jenkins and Marcus, 1995), the comparable experimental and theoretical relative viscosity of aqueous KCl and KBr solutions gave confidence in the procedures of sample preparation as well as in the experimental results.

Again, comparing the specific viscosities of six potassium salts including potassium acetate, potassium fluoride, potassium formate, potassium chloride, potassium bromide, and potassium iodide against concentration, it was found that potassium acetate has the

highest capacity to increase the viscosity of a solution with increase in concentration and potassium iodide shows the highest capacity in decreasing the specific viscosity with increase in concentration. Considering specific viscosity, the kosmotropic nature of potassium acetate, potassium fluoride and potassium formate and the chaotropic nature of potassium iodide, potassium bromide and potassium chloride were apparent (Collins, 1997).

The ultrasound velocity and attenuation of Milli Q water and aqueous solution of seven potassium salts in the Hofmeister series including KCl, KBr, KI, KF, HCOOK, CH_3COOK and KSCN at 25 ^oC were measured using the ultrasound resonator method. The ultrasound resonator was very precise in measuring temperature, ultrasound velocity and attenuation as the standard deviations for the formerly mentioned parameters were very small. The experimentally measured sound velocity in water was identical to the literature value while the experimentally measured ultrasound attenuation in pure water was 40% lower than the sound attenuation in water calculated from a literature derived equation (Fisher and Simmons, 1977). Considering coefficient of variation, although it was observed that the ultrasonic resonator technique was less precise in measuring ultrasound attenuation than velocity measurement, the accuracy was comparable in terms of velocity and attenuation from other researchers to my measurements of the acoustic properties of salt solutions. The ultrasound velocity increases linearly with the increase in concentration (1 $mmol.dm^{-3}$ to 250 $mmol.dm^{-3}$) for potassium acetate, potassium fluoride, potassium chloride, potassium formate, potassium thiocyanate and potassium bromide solutions, but ultrasound velocity decreases with increasing concentration for potassium iodide solution. The order of salt in increasing sound

velocity was CH3COOK > KF > KCl > KCOOH > KSCN > KBr. According to Freyer (1931), the increase or decrease of sound velocity of a solution is controlled by the dominating impact of either the density or the adiabatic compressibility of the solution.

The analysis of potassium halide aqueous solution was performed. Considering the ions reside as hard sphere in aqueous solution, density and adiabatic compressibility of the aqueous solution was calculated and the calculated values were compared with the literature derived density values and the experimental adiabatic compressibility. As the calculated values show discrepancy from the literature density values and the experimental compressibility values of potassium halide solutions, it can be concluded that the presence of ions in the aqueous solution is not as hard spheres but rather the ions are responsible for the restructuring of water. Freyer (1931) stated that highly hydrated ions are responsible for a large reduction in compressibility. The sequence of potassium halides in reducing adiabatic compressibility of aqueous solution is KF > KCl > KBr > KI and the sequence is similar to the Hofmeister series.

The ultrasound velocity and attenuation in BSA aqueous solution was found to be increased linearly with concentration increase (higher limit of concentration was 1.5 $mmol.dm^{-3}$) (Beneddif, 2010) which implies no intermolecular interaction occurs between BSA molecules within the concentration range used, and the only existing interaction is between water and BSA molecules. In order to analyze the aqueous BSA solutions (0.15, 0.3. 0.6, 1.2 and 2.4 $mmol.dm^{-3}$), the experimental densities were compared with the calculated values which were calculated using the partial specific volume of BSA. Similarity in the experimental and the calculated density values also indicate the interaction of water with BSA in aqueous solution. Again adiabatic

compressibility of aqueous BSA solution was calculated considering BSA as hydrated but incompressible molecule in aqueous solution. The difference between the experimental and the calculated compressibility values of aqueous BSA solution indicates that BSA exists in solution as compressible molecule, and the finite compressibility of BSA molecules have contribution to the total compressibility of solutions.

Observing ultrasound velocity of potassium halide, BSA and BSA-salt mixed solutions, it can be said that regardless of contribution of salt, there is substantial effect with the addition of BSA on the combined ultrasound velocity of BSA-salt mixed solutions. In addition, as the velocity change follows same sequence in the case of both potassium halides solutions alone and BSA-potassium halides mixed solutions, potassium halides also has their impact on the ultrasound velocity change of the mixed solutions. The ultrasound attenuation increased lineally with concentration in the case of BSA-salt mixed solutions and there was no significant difference in attenuation increment with the variation of potassium halides. Analyzing the density and the adiabatic compressibility of BSA-salt mixed solutions, it was found that the calculated density and adiabatic compressibility values are not similar to the experimental values of these parameters. The order of experimental density increase with volume fraction increase follows the order of BSA-KI> BSA-KBr> BSA-KF> BSA-KCl. The theoretical and experimental density variation in the case of BSA-salt mixed solutions must be due to consideration of ions as nonhydrated solutes in solution during calculation of the theoretical value, and the theoretical value does not consider any interaction between BSA and ions. Again, comparing the experimental density of mixed solutions with the corresponding

theoretical density, it can be said that I^-, Br^- and Cl^- cause loosening of the solution structure and make the solution less dense whereas F^- makes the solution slightly denser. The disparity of impact of F^- on density of BSA-salt mixed solutions compared to the effect of three other halide ions can be attributable to the small atomic number of F^- with its high charge density. The order of protein-salt mixed solutions in reducing compressibility was BSA-KF> BSA-KI> BSA-KBr> BSA-KCl. The variation of the experimental values of adiabatic compressibility from the theoretical values might be due to consideration of incompressibility of BSA, potassium ion and halide ions, the presence of ions as nonhydrated entities and ignorance of protein-ion interaction phenomenon for calculation of theoretical values. Thus, the density and the adiabatic compressibility of BSA-potassium halide mixed solutions cannot be predicted from the density and the adiabatic compressibility of potassium halide and that of BSA since individual components density and adiabatic compressibility does not consider any interaction between the BSA and the ion, and restructuring of water due to the interaction.

Using method of intercept, the partial specific volume of potassium halides, BSA and BSA-salt in water was determined. The partial specific adiabatic compressibility of potassium halides, BSA and BSA-salt in water was also determined. Comparing the partial specific compressibility, it was found that BSA is much more compressible than potassium halides. The rigidity of potassium halides follows the order of KF > KCl > KBr > KI. Again, the rigidity of BSA+ K halides follows the order of (BSA+KF) > (BSA+KCl) > (BSA+KBr) > (BSA+KI). The rigidity orders of both the individual

potassium halides and the BSA-K halides are similar to the Hofmeister series order (Zhang and Cremer, 2006).

In order to figure out what density and adiabatic compressibility entails about the interaction between the BSA and the halide ion, density and adiabatic compressibility of BSA-potassium halide mixed solutions were calculated using the determined partial specific volume of BSA and potassium halides, the calculated values ignore the interaction between the BSA and the potassium halides. The comparison between the calculated and the experimental values of density and of adiabatic compressibility entails that, interaction occurs between BSA and Br-, I- and F- ions in aqueous solution of BSA-KBr, BSA-KI and BSA-KF, but there is no interaction between BSA and Cl^- ion in BSA-KCl mixed aqueous solution. Within the concentration range used the binding of halide ions to BSA do not follow the sequence of the Hofmeister series; otherwise it can be said that the binding of ion to BSA is ion non-specific to the Hofmeister series.

References

Andrews, M. E., Moses, J. R., Sendhil, S., Rakkappan, C., & Jayakumar, R. (2002). Adiabatic compressibility and intrinsic viscosity studies of peptide aggregates. *Letters in peptide science, 9*, 167-172.

Apenten, R. K.O., Buttner, B., Mignot, B., Pascal, D., & Povey, M. J. W. (2000). Determination of the adiabatic compressibility of bovine serum albumin in concentrated solution by a new ultrasonic method. *Food Hydrocolloids , 14*, 83-91.

Ayranci, E., & Duman, O. (2004). Binding of fluoride, bromide and iodide to bovine serum albumin, studied with ion selective electrodes. *Food Chemistry, 84*, 539-543.

Baldwin, R. L. (1996). How Hofmeister ion interactions affect protein stability. *Biophysical Journal, 71*, 2056-2063.

Banipal, T. S., Singh, K., Banipal, P. K., Sood, A. K., Singh, P., Singh, G., Patyar, P. (2008). Volumetric and viscometric studies of some metal acetates in aqueous solutions at T = (288.15 to 318.15) K. *Journal of Chemical and Engineering Data, 53,* 2758-2765.

Barlow, A. J., & Yazgan, E. (1966). Phase change method for the measurement of ultrasonic wave velocity and a determination of the speed of sound in water. *British Journal of Applied Physics, 17,* 807-819.

Barnes, H. A. (2000). *A handbook of elementary rheology.* Aberystwyth: University of Wales.

Beneddif, F. (2010). Etude de l'interaction de la serum albumine bovine et de la vanilline par la methode des ultrasons. University of Manitoba.

Bermúdez-Salguero, C., & Gracia-Fadrique, J. (2011). Densities, refractive indices, speeds of sound, and surface tensions for dilute aqueous solutions of 2-methyl-1-propanol, cyclopentanone, cyclohexanone, cyclohexanol, and ethyl acetoacetate at 298.15 K. *Journal of Chemical and Engineering Data, 56,* 3823-3829.

Bigelow, C. C. (1967). On the average hydrophobicity of proteins and the relation between it and protein structure. *Journal of Theoretical Biology , 16*, 187-211.

Blandamer, M. J., Davis, M. I., Douheret, G., & Reis, J. C. (2001). Apparent molar isentropic compressions and expansions of solutions. *Chemical Society Reviews, 30*, 8-15.

Bockris, J. O'M & Saluja, P. P. S. (1972). Ionic solvation numbers from compressibilities and ionic vibration potentials measurements. *The Journal of Physical Chemistry, 76,* 2140-2151.

Bridgman, P.W. (1970). *The physics of high pressure.* New York: Dover Publications.

Brooks, R. (1960). Determination of the velocity of sound in distilled water. *The Journal of the Acoustical Society of America, 32,* 1422-1425.

Bull, H. B. (1940). Viscosity of solutions of denatured and of native egg albumin. *Journal of Biological Chemistry, 133,* 39-49.

Cacace, M. G., Landau, E. M., & Ramsden, J. J. (1997). The Hofmeister series: salt and solvent effects on interfacial phenomena. *Quarterly Reviews of Biophysics, 30,* 241-277.

Chalikian, T. V. (2003). Volumetric properties of proteins. *Annual Review of Biophysics and Biomolecular Structure, 32, 207-235.*

Chalikian, T. V., & Breslauer, K. J. (1996). Compressibility as a means to detect and characterize globular protein states. *Biochemistry, 93,* 1012-1014.

Chalikian, T. V., Sarvazyan, A. P., & Breslauer, K. J. (1994). Hydration and partial compressibility of biological compounds. *Biophysical Chemistry, 51,* 89-109.

Chalikian, T. V., Totrov, M., Abagyan, R., & Breslauer, K. J. (1996). The hydration of globular proteins as derived from volume and compressibility measurements: Cross correlating thermodynamic and structural data. *Journal of Molecular Biology, 260,* 588–603.

Chmielewska, A., Stasiewicz, A. W., & Bald, A. (2005). Viscosimetric studies of aqueous solutions of salts of carboxylic acids. *Journal of Molecular Liquids, 122,* 110-115.

Collins, K. D. (1997). Charge density-dependent strength of hydration and biological structure. *Biophysical Journal, 72,* 65-76.

Collins, K. D. (2004). Ions from the Hofmeister series and osmolytes: effects on proteins in solution and in the crystallization process. *Methods, 34,* 300-11.

Collins, K. D., & Washabaugh, M. W. (1985). The Hofmeister effect and the behavior of water at interfaces. *Quarterly Reviews of Biophysics, 18,* 323.

Cooper, A. (1976). Thermodynamic fluctuations in protein molecules. *Proceedings of the National Academy of Sciences USA, 73,* 2740-2741.

Cooper, A. (2000). Heat capacity of hydrogen-bonded networks: An alternative view of protein folding thermodynamics. *Biophysical Chemistry, 85,* 25-39.

Coupland, J. N. (2004). Low intensity ultrasound. *Food Research International, 37,* 537-543.

Curtis, R. A., & Lue, L. (2006). A molecular approach to bioseparations: Protein-protein and protein-salt interactions. *Chemical Engineering Science, 61,* 907-923.

Dadarlat, V. M., & Post, C. B. (2001). Insights into protein compressibility from molecular dynamics simulations. *The Journal of Physical Chemistry B, 105*, 715-724.

Dadarlat, V. M., & Post, C. B. (2003). Adhesive-cohesive model for protein compressibility: An alternative perspective on stability. *Proceedings of the National Academy of Sciences, 100,* 14778-14783.

Dadarlat, V. M., & Post, C. B. (2006). Decomposition of protein experimental compressibility into intrinsic and hydration shell contributions. *Biophysical Journal, 91*, 4544-4554.

Damodaran, S. (1989). Influence of protein conformation on its adaptability under chaotropic conditions. *International Journal of Biological Macromolecules, 11,* 2-8.

Dayhoff, M. O., Perlmann, G.E., MacInnes, D. A. (1952). The partial specific volumes, in aqueous solution, of three proteins. *Journal of the American Chemical Society, 74,* 2515-2517.

Der, A. (2008). Salts, interfacial water and protein conformation. *Biotechnology and Biotechnological Equipment, 22,* 629-633.

Desnoyers, J. E., & Perron, G. (1972). The viscosity of aqueous solutions of alkali and tetraammonium halides at 25 ^{0}C. *Journal of Solution Chemistry, 1,* 199-212.

Dill, K. A. (1990). Dominant forces in protein folding. *Biochemistry, 29,* 7133-7155.

Dill, K. A., Truskett, T. M., Vlachy, V., & Lee, B. H. (2005). Modeling water, the hydrophobic effect, and ion salvation. *Annual Review of Biophysics and Bimolecular Structure, 34,* 173-199.

Dougherty, R. C. (2001). Density of salt solutions: Effect of ions on the apparent density of water. *Journal of Physical Chemistry B, 105,* 4514-4519.

Dukhin, A. S., & Goetz, P. J. (2009). Bulk viscosity and compressibility measurement using acoustic spectroscopy. *The Journal of Chemical Physics, 130,* 1-13.

Eden, D., Matthew, J. B., Rosa, J. J., & Richards, F. M. (1982). Increase in apparent compressibility of cytochrome c upon oxidation. *Proceedings of the National Academy of Sciences USA, 79,* 815-819.

Eggers, F. & Funck, T. (1973). Ultrasonic measurements with milliliter liquid samples in the 0.5-100 MHz range. *Review of Scientific Instruments, 44,* 969-977.

Engel, T., Drobney, G., & Reid, P. (2008). *Physical chemistry for the life sciences.* London: Pearson Education, Inc.

Fennema, O. R. (Ed.) (1993). *Food chemistry*. New York: Marcel Dekker Inc.

Finet, S., Skouri-Panet, F., Casselyn, M., Bonnete, F., & Tardieu, A. (2004). The Hofmeister effect as seen by SAXSs in protein solutions. *Current Opinion in Colloid and Interface Science, 9*, 112-116.

Fisher, F. H., & Simmons, V. P. (1977). Sound absorption in sea water. *The Journal of the Acoustical Society of America, 62*, 558-564.

Fox, P. F., & McSweeney, P. L. H, (2003). *Advance dairy chemistry volume 1 proteins.* New York: Kluwer Academic plenum Publishers.

Franks, F. (Ed.). (1972). *Water: A comprehensive treatise.* New York: Plenum Press.

Franks, F. (Ed.). (1988). *Characterization of proteins.* New Jersey: Humana Press.

Frauenfelder, H., Hartmann, H., Karplus, M., Kuntz, I. D., Kuriyan, J., Parak, F., Petsko, G. A., Ringe, D., Tilton Jr., R. F. (1987). Thermal expansion of a protein. *Biochemistry, 26*, 254-261.

Frederick, K. K., Marlow, M. S., Valentine, K. G., & Wand, A. J. (2007). Conformational entropy in molecular recognition by proteins. *Nature, 448*, 325-329.

Fredriksson, H., & Åkerlind, U. (2008). *Physics of functional materials.* Chichester: John Wiley & Sons Ltd.

Frye, K. J., & Royer, C. A. (1998). Probing the contribution of internal cavities to the volume change of protein unfolding under pressure. *Protein Science, 7*, 2217-2222.

Freyer, E. B. (1931). Sonic studies of the physical properties of liquids. II. The velocity of sound in solutions of certain alkali halides and their compressibilities. *Journal of the American Chemical Society, 53*, 1313-1320.

Gavish, B., Gratton, E., & Hardy, C. J. (1983). Adiabatic compressibility of globular proteins. *Proceedings of the National Academy of Sciences USA, 80*, 750-754.

Gekko, K., & Hasegawa, Y. (1986). Compressibility-structure relationship of globular proteins. *Biochemistry, 25*, 6563-6571.

Gekko, K., & Noguchi, H. (1979). Compressibility of globular proteins in water at 25 degree C. *The Journal of Physical Chemistry, 83*, 2706-2714.

Gekko, K., & Yamagami, K. (1991). Flexibility of food proteins as revealed by compressibility. *Journal of Agricultural and Food Chemistry, 39*, 57-62.

Gekko, K., Kimoto, A., & Kamiyama, T. (2003). Effects of disulfide bonds on compactness of protein molecules revealed by volume, compressibility, expansibility changes during reduction. *Biochemistry, 42*, 13746-13753.

Ghelis, C., & Yon, J. (1982). *Protein folding.* New York: Academic Press, Inc.

Gotto, S., & Isemura, I. (1964). Studies of hydration and the structure of water and their role in protein structure. *Bulletin of the Chemical Society of Japan, 37*, 1697.

Goss, S. A., & Dunn, F. (1974). Concentration dependence of ultrasonic absorption in aqueous solutions of bovine serum albumin. *Ultrasonics Symposium Proceedings, IEEE,* 65-68.

Gunton, J. D., Shiryayev, A., & Pagan, D. L. (2007). *Protein condensation.* New York: Cambridge University Press.

Guo, G. J., & Zhang, Y. G. (2001). Equilibrium molecular dynamics calculation of the bulk viscosity of liquid water. *Molecular Physics, 99,* 283-289.

Hai-Lang, Z., & Shi-Jun, H. (1996). Viscosity and density of water + sodium chloride + potassium chloride solutions at 298.15 K. *Journal of Chemical and Engineering Data, 41*, 516-520.

Hamabata, A., & Hippel, P. H. (1973). Model studies on the effects of neutral salts on the conformational stability of biological macromolecules. II. Effects of vicinal hydrophobic groups on the specificity of binding of ions to amide groups. *Biochemistry, 12*, 1264-1271.

Haque, Z., & Kinsella, J. E. (1989). Relative emulsifying activity of bovine serum albumin and casein as assessed by three different methods. *Journal of Food Science, 54*, 1341-1344.

Haynes, W. M. (Ed.). (2010). *CRC Handbook of chemistry and physics.* New York: CRC Press.

Heintz, A., Klasen, D., & Lehmann, J. K. (2002). Excess molar volumes and viscosities of binary mixtures of methanol and the ionic liquid 4-methyl-N-butylpyridinium tetrafluoroborate at 25, 40, and 50 ^{o}C. *Journal of Solution Chemistry, 31*, 467-476.

Heyda, J., Vincent, J. C., Tobias, D. J., Dzubiella, J., & Jungwirth, P. (2010). Ion specificity at the peptide bond: Molecular dynamics simulations of N-methylacetamide in aqueous salt solutions. *The Journal of Physical Chemistry B, 114,* 1213-1220.

Heyrovska, R. (2007). Dependences of molar volumes in solids, partial molal and hydrated ionic volumes of alkali halides on covalent and ionic radii and the golden ratio. *Chemical Physics Letters, 436,* 287–293.

Hill, S. E., Ledward, D. A., & Mitchell, J. R (Eds). (1998). *Functional properties of food macromolecules.* Maryland: Aspen Publishers, Inc.

Hippel, P. H., & Wong, K. Y. (1964). Neutral salts: the generality of their effects on the stability of macromolecular conformations. *Science, 145*, 577-580.

Hinton, J. F., & Amis, E. S. (1971). Solvation numbers of ions. *Chemical Reviews, 71,*627-674.

Hirose, M., Nishizawa, Y., & Lee, J. Y. (1990). Gelation of bovine serum albumin by glutathione. *Journal of Food Science, 55,* 915-917.

Hosoda, M., Takagi, K., Ogawa, H., Nomura, H., & Sakai, K. (2005). Rapid and precise measurement system for ultrasonic velocity by pulse correlation method designed for chemical analysis. *Japanese Journal of Applied Physics, 44,* 3268-71.

Hribar, B., Southall, N. T., Vlachy, V., & Dill, K. A. (2002). How ions affect the structure of water. *Journal of the American Chemical Society, 124,* 12302-12311.

Imai, T., Nomura, H., Kinoshita, M., & Hirata, F. (2002). Partial Molar Volume and compressibility of alkali-halide ions in aqueous solution: Hydration shell analysis with an integral equation theory of molecular liquids. *The Journal of Physical Chemistry B, 106,* 7308-7314.

Iqball, M., & Verrall, R. E. (1987). Volumetric properties of aqueous solutions of bovine serum albumin, human serum albumin, and human hemoglobin. *Journal of Physical Chemistry, 91,* 1935-1941.

Isaacs, N. (1981). *Liquid phase high pressure chemistry.* UK: John Wiley and Sons.

James, C. J., Mulcahy, D. E., & Steel, B.J. (1984). Viscometer calibration standards: viscosities of water between 0 and 60 ^{0}C and of selected aqueous sucrose solutions at 25 ^{o}C from measurements with a flared capillary viscometer. *Journal of Physics D: Applied Physics, 17,* 225-230.

Jencks, W. P. (1987). *Catalysis in chemistry and enzymology.* New York: Dover.

Jenkins, H. D. B., & Marcus, Y. (1995). Viscosity B-coefficients of ions in solution. *Chemical Reviews, 95,* 2695-2724.

Kaatze, U., Eggers, F., & Lautscham, K. (2008). Ultrasonic velocity measurements in liquids with high resolution-techniques, selected applications and perspectives. *Measurement Science and Technology, 19,* 1-21.

Kamiyama, T., & Gekko, K. (1997). Compressibility and volume changes of lysozyme due to guanidine hydrochloride denaturation. *Chemistry Letters, 26,* 1063.

Kaun, N., Baena, J. R., Newnham, D., & Lendl, B. (2005). Terahertz pulsed spectroscopy as a new tool for measuring the structuring effect of solutes on water. *Applied Spectroscopy, 59,* 505-510.

Kauzmann, W. (1959). *Advances in protein chemistry.* (C. B. Anfinsen, Ed.) New York: Academic Press Inc.

Kirino, Y., Yokoyama, T., Hirono, T., Nakajima, T., & Nakashima, S. (2009). Effect of density-driven flow on the through-diffusion experiment. *Journal of Contaminant Hydrology, 106,* 166-172.

Koneshan, S., Rasaiah, J. C., Lynden-Bell, R. M., & Lee, S. H. (1998). Solvent structure, dynamics, and ion mobility in aqueous solutions at 25 °C. *The Journal of. Physical Chemistry B, 102,* 4193-4204.

Kunitz, M., Anson, M. L., Northrop, J. H. (1934). Molecular weight, molecular volume, and hydration of proteins in solution. *The Journal of General Physiology, 17,* 365-373.

Lakshmanan, M., Dhathathreyan, A., & Miller, R. (2008). Synergy between Hofmeister effect and coupled water in proteins: Unusual dilational moduli of BSA at air/solution interface. *Colloids and Surfaces A: physiochemical and Engineering Aspects, 324,* 194-201.

Lee, C., Allen, M. D., Bycroft, M., & Wong, K. (2005). Electrostatic interactions contribute to reduced heat capacity change of unfolding in a thermiphilic ribosomal protein L30e. *Journal of Molecular Biology, 348,* 419-431.

Lee, S., Tikhomirova, A., Shalvardjian, N., and Chalikian, T. V. (2008). Partial molar volumes and adiabatic compressibilities of unfolded protein states. *Biophysical Chemistry, 134,* 185-199.

Lewis, M. J. (1987). *Physical properties of foods and food processing systems.* Horwood: Ellis Horwood Ltd.

Lewin, S. (1974). *Displacement of water and its control of biochemical interactions.* (S. Lewin, Ed.) New York: Academic Press.

Li, H., Yamada, H., & Akasaka, K. (1999). Effect of pressure on the tertiary structure and dynamics of folded basic pancreatic trypsin inhibitor. *Biophysical Journal, 77,* 2801–2812.

Litovitz, T. A., & Davis, C.M. (1964). *Physical acoustics.* (W. P. Manson, Ed.). New York: Academic Press.

Lladze, V. V., Ermolenko, D., & Makhayadze, G. I. (2001). Heat capacity changes upon burial of polar and nonpolar groups in proteins. *Protein Science, 10,* 1343-1352.

Lund, M., Va´cha, R., & Jungwirth, P. (2008). Specific ion binding to macromolecules: Effects of hydrophobicity and ion pairing. *Langmuir, 24,* 3387-3391.

Machado, F. F., Coimbra, J. S., Rojas, E. E., Minim, L. A., Oliveira, F. C., & Sousa, R. C. (2007). Solubility and density of egg white proteins: Effect of pH and saline concentration. *LWT- Food Science and Technology, 40,* 1304-1307.

Manciu, M., & Ruckenstein, E. (2003). Specific ion effects via ion hydration: I Surface tension. *Advances in Colloid and Interface Science, 105,* 63-101.

Malkin, A. Y., & Isayev, A. I. (2006). *Rheology: Concepts, methods, and applications.* Toronto: Chemtec Publishing.

Marcus, Y. (2009a). Effect of ions on the structure of water: structure making and breaking. *Chemical Reviews, 109,* 1346-1370.

Marcus, Y. (2009b). The standard partial molar volumes of ions in solutions. Part 4. Ionic volumes in water at 0-100 ^{o}C. *The Journal of Physical Chemistry B, 113,* 10285-10291.

Mathieson, J. G., & Conway, B. E. (1974). Partial molal compressibilities of salts in aqueous solution and assignment of ionic contributions. *Journal of Solution Chemistry, 3,*455-477.

McClements, D. J. (1991). Ultrasonic characterization of emulsions and suspensions. *Advances in Colloid and Interface Science, 37,* 33-72.

McSkimin, H. J. (1965). Velocity of sound in distilled water for the temperature range 20 ^{o} – 75 ^{o}C. *The Journal of the Acoustical Society of America, 37,* 325-328.

Millero, F. J., Ward, G. K., & Chetirkin, P. (1976). Partial specific volume, expansibility, compressibility, and heat capacity of aqueous lysozyme solutions. *The Journal of Biological Chemistry, 251,* 4001-4004.

Mohanty, A., & Swain, S. K. (2010). Ultrasonic and viscometric investigation of albumin protein in aqueous solution. *Journal of the Indian Chemical Society, 87,* 461-464.

Mori, K., Seki, Y., Yamada, Y., & Matsumoto, H. (2006). Evaluation of intrinsic compressibility of proteins by molecular dynamic simulation. *The Journal of Chemical Physics, 125,* 1-13.

Mortimer, R. G. (2008). *Physical chemistry.* Burlington: Elsevier Academic Press.

Mott, R. L. (1990). *Applied fluid mechanics.* Toronto: Merril Publishing Company.

Nakai, S., & Li-Chan, E. (1988). *Hydrophobic interactions in food systems.* Florida: CRC Press, Inc.

Nandi, P. K., & Robinson, D. R. (1972). Effects of salts on the free energy of the peptide group. *Journal of the American Chemical Society, 94,* 1299-1308.

Narasimham, A. V. (1993). Ultrasonic dispersion and relaxation and the bulk viscosity coefficient of a liquid. *Acustica, 79,* 73-81.

Nikam, P. S., & Sawant, A. B. (1997). Viscosity of potassium halides and symmetrical tetraalkylammonium bromides in acetonitrile + water mixtures at 298.15 K. *Journal of Chemical & Engineering Data, 42,* 1151-1156.

Nostrand, V. (2005). *Encyclopedia of chemistry*. New Jersey: John Wiley & Sons, Inc.

Ohtaki, H. (2001). Ionic solvation in aqueous and nonaqueous solutions. *Monatshefte fur Chemie 132,* 1237-1268.

Otting, G., Liepinsh, E., & Wuthrich, K. (1991). Protein hydration in aqueous solution. *Science, 254,* 974-980.

Out, D. J. P. & Los, J. M. (1980).Viscosity of aqueous solutions of univalent electrolytes from 5 to 95 ^{o}C. *Journal of Solution Chemistry, 9,* 19-35.

Pan, X., & Glatz, C. E. (2003). Solvent effects on the second virial coefficient of subtilisin and solubility. *Crystal Growth & Design, 3,* 203-207.

Papadakis, E. P. (1967). Ultrasonic phase velocity by the pulse-echo-overlap method. Incorporating diffraction phase corrections. *Journal of the Acoustical Society of America, 42,* 1045-51.

Papadakis, E. P. (1973). The measurement of small changes in ultrasonic velocity and attenuation. *Critical Reviews in Solid State and Materials Sciences, 3,* 373-418.

Penkova, R. K., Koynova, R., Kostov, G., & Tenchov, B. G. (1996). Thermal stability of calf skin collagen type I in salt solutions. *Biochemica et Biophysica Acta, 1297,* 171-181.

Pfeiffer, H., Heremans, K., & Wevers, M. (2008). The influence of correlated protein-water volume fluctuations on the apparent compressibility of proteins determined by ultrasonic velocimetry. *Biochimica et Biophysica Acta, 1784,* 1546-1551.

Photchanachai, S. & Kitabatake, N. (2001). Heating of β-lactoglobulin A solution in a closed system at high temperatures. *Journal of Food Science, 66,* 647- 652.

Pinkerton, J. M. M. (1947). A pulse method for the measurement of ultrasonic absorption in liquids: Results for water. *Nature, 160,* 128-129.

Povey, M. J. (1997). *Ultrasonic techniques for fluids characterization.* San Diego: Academic Press.

Pradipasena, P., & Rha, C. (1977). Effect of concentration on apparent viscosity of a globular protein solution. *Polymer Engineering and Science, 17,* 861-864.

Rayleigh, J. W. (1945). *The theory of sound*. New York: Dover.

Rao, N.P., & Verrall, R.E. (1987). Ultrasonic velocity, excess adiabatic compressibility, apparent molar volume, and apparent molar compressibility properties of binary liquid

mixtures containing 2-butoxyethanol. *The Canadian Journal of Chemical Engineering, 65,* 810-816.

Reis, J. C. R. (1998). New thermodynamic relations concerning apparent molar isentropic compression and apparent and partial isentropic compressibilities. *Journal of the Chemical Society, Faraday Transactions, 94,* 2385-2388.

Rieskautt, M. M., & Ducruix, A. F. (1989). Relative effectiveness of various ions on the solubility and crystal growth of lysozyme. *The Journal of Biological Chemistry, 264,* 745-748.

Robinson, D. R., & Jencks, W. P. (1965). The Effect of concentrated salt solutions on the activity coefficient of acetyltetraglycine ethyl ester. *Journal of the American Chemical Society, 87,* 2470-2479.

Sarvazyan, A. P. (1982). Development of methods of precise ultrasonic measurements in small volumes of liquids. *Ultrasonics, 20,* 151-154.

Sarvazyan, A. P. (1991). Ultrasonic velocimetry of biological compounds. *Annual Review of Biophysics and Biophysical Chemistry, 20,* 321-342.

Sarvazyan, A. P. & Chalikian, T. V. (1991). Theoretical analysis of an ultrasonic interferometer for precise measurements at high pressures. *Ultrasonics, 29,* 119-124.

Saeed, R., Uddin, F., Masood, S., & Asif, N. (2009). Viscosities of ammonium salts in water and ethanol + water systems at different temperatures. *Journal of Molecular Liquids, 146,* 112-115.

Schrier, E. E., & Schrier, E. B. (1967). The salting-out behavior of amides and its relation to the denaturation of protein by salts. *The Journal of Physical Chemistry, 71,* 1851-1860.

Shimizu, S., & McLaren, W. M. (2006). The Hofmeister series and protein-salt interactions. *The Journal of Chemical Physics, 124,* 234905-1-234905-4.

Sikorski, Z. E. (2001). *Chemical and functional properties of food proteins.* Pennsylvania: Technomic Publishing Company, Inc.

Sochava, I. V., & Smirnova, O. I. (1993). Heat capacity of hydrated and dehydrated globular proteins. Denaturation increment of heat capacity. *Food Hydrocolloids, 6,* 513-524.

S*ö*hnel, O. & Novotny, P. (1985). *Densities of aqueous solutions of inorganic substances.* New York: ELSEVIER.

Soper, A. K., & Weckström, K. (2006). Ion solvation and water structure in potassium halide aqueous solutions. *Biophysical Chemistry, 124,* 180-191.

Stokes, R. H., & Mills, R. (1965). *Viscosity of electrolytes and related properties.* New York: Pergamon Press.

Strobl, G. (2007). *The physics of polymers.* Berlin: Springer.

Svergun, D. I., Richard, S., Koch,M. H. J., Sayers, Z., Kuprin, S., and Zaccai, G. (1998). Protein hydration in solution: Experimental observation by x-ray and neutron scattering. *Proceedings of the National Academy of Sciences of the United States of America, 95,* 2267-2272.

Tamura, Y., & Gekko, K. (1995). Compactness of thermally and chemically denatured ribonuclease A as revealed by volume and compressibility. *Biochemistry, 34,* 1878-1884.

Tanford, C. (1968). Protein denaturation. *Advances in Protein Chemistry, 23,* 121-182.

Tanford, C. (1980). *The hydrophobic effect: Formation of micells and biological membranes.* (C. Tanford, Ed.) New York: John Wiley & Sons.

Taulier, N., Beletskaya, I. V., & Chalikian, T. V. (2005). Compressibility changes accompanying conformational transitions of apomyoglobin. *Biopolymers, 79,* 218-229.

von Hippel, P. H., & Schleich, T. (1969). Ion effects on the solution structure of biological macromolecules. *Accounts of Chemical Research, 2,* 257-265.

Vrbka, L., Jungwirth, P., Bauduin, P, Touraud, D., & Kunz, W. (2006). Specific ion effects at protein surfaces: A molecular dynamics study of bovine pancreatic trypsin inhibitor and horseradish peroxidase in selected salt solutions. *Journal of Physical Chemistry B, 110,* 7036-7043.

Weast, R. C. (Ed.). (1988-1989). *CRC handbook of chemistry and physics.* Florida: CRC Press Inc.

Weight, M. R. (2007). *An introduction to aqueous electrolyte solutions.* Chichester: John Wiley.

Williamson, R. C. (1969). Echo-phase comparison technique and measurement of sound velocity in water. *The Journal of the Acoustical Society of America, 45,* 1251-1257.

Yamasaki, M., Yano, H., & Aoki, K. (1991). Differential scanning calorimetric studies on bovine serum albumin: II. Effects of neutral salts and urea. *International Journal of Biological Macromolecules, 13,* 322-328.

Zaytsev, I. D. & Aseyev, G. G. (Eds.) (1992). *Properties of aqueous solutions of electrolytes.* Florida: CRC Press.

Zhang, Y., & Cremer, P.S. (2006). Interactions between macromolecules and ions: the Hofmeister series. *Current Opinion in Chemical Biology, 10,* 658–663.